# Holocene Paleoenvironmental History from Stable Isotopes in Lake Sediment, North-Central Washington State

by

Daniel B. Nelson

B.A., Hampshire College, 2001

Submitted to the Graduate Faculty of

Arts and Sciences in partial fulfillment

of the requirements for the degree of

Master of Science

University of Pittsburgh

2004

UNIVERSITY OF PITTSBURGH

FACULTY OF ARTS AND SCIENCES

This dissertation was presented

by

Daniel B. Nelson

It was defended on

November 16, 2004

and approved by

Michael Rosenmeier

Brian Stewart

Mark B. Abbott
(Thesis Director)

**Holocene Paleoenvironmental History from Stable Isotopes in Lake Sediment, North-Central Washington State**

Daniel B. Nelson, M.S.

University of Pittsburgh, 2004

Population growth in the Pacific Northwest has led to increased demand for water resources. Current understanding of the natural cycle of moisture availability is limited, however, by the short duration for which instrumental climate data are available. Here, a detailed paleoenvironmental study from Castor Lake in north-central Washington State is presented to examine the frequency, duration, and magnitude of droughts, lake system dynamics, and other climate events during the past ~16,000 years. The combined use of stable isotope measurements of endogenic carbonate and organic sediment with trace element analysis and standard sedimentological methodologies provides a more coherent basis for understanding environmental change through this period than would be possible through the application of a single technique. Results show that the region was significantly affected by the Younger Dryas cold reversal between approximately 12,500 cal yr BP and 11,500 cal yr BP. The period from approximately 8,200 cal yr BP to 5,900 cal yr BP contains evidence for prolonged aridity, as lake-levels declined and water column stratification broke down. The period spanning the last ~6,000 years is characterized by relative climate stability, but the highly resolved sediment proxy data for this interval reveal several drought events larger than anything experienced in the historic record,

with some episodes persisting well over a century. Furthermore, the past fifty-years appear to be anomalously wet in the context of the long-term record obtained from Castor Lake. Preparation for large drought events may therefore be inadequate because water resource allocation laws were written during this interval. Future large-scale drought events are inevitable, however, given the frequency with which they are observed to occur in the past, and the increasing influence of anthropogenic warming.

## TABLE OF CONTENTS

PREFACE ..... xi
1. INTRODUCTION ..... 1
1.1. Pacific Northwest ..... 2
1.2. General Paleoclimate Background ..... 5
1.2.1. Early Holocene ..... 6
1.2.2. Middle Holocene ..... 8
1.2.3. Late Holocene ..... 10
1.3. Project Objectives ..... 12
2. PALEOENVIRONMENTAL INVESTIGATION AT CASTOR LAKE, NORTH-CENTRAL WASHINGTON STATE USING LAKE SEDIMENT ORGANIC MATTER ..... 13
2.1. Introduction ..... 14
2.2. Study Area ..... 21
2.3. Methods ..... 23
2.4. Results ..... 27
2.5. Discussion ..... 32
2.6. Conclusion ..... 38
3. LATE-QUATERNARY ENVIRONMENTAL HISTORY FROM STABLE ISOTOPES AND TRACE ELEMENT GEOCHEMISTRY AT CASTOR LAKE, NORTH-CENTRAL WASHINGTON STATE ..... 40
3.1. Introduction ..... 41
3.2. Study Area ..... 44
3.3. Methods ..... 48
3.3.1. Sediment Recovery, Field Methods, and Sampling ..... 48
3.3.2. Chronology ..... 49
3.3.3. Carbonate Sample Preparation ..... 52
3.3.4. XRD & SEM ..... 52
3.3.5. Stable Isotopes ..... 53
3.3.6. Trace Elements ..... 53
3.4. Results ..... 54
3.4.1. Lithology, Bulk Density & LOI ..... 54
3.4.2. XRD ..... 58
3.4.3. SEM ..... 60
3.4.4. Stable Isotopes ..... 61
3.4.5. Trace Elements ..... 63
3.5. Discussion ..... 65
3.5.1. Model for Interpretation ..... 65
3.5.2. Paleoenvironmental Interpretation ..... 70
3.5.3. Comparison with Other Paleoenvironmental Records ..... 75
3.6. Conclusion ..... 76

4. A DROUGHT RECORD OF THE PAST 6,000-YEARS FROM OXYGEN ISOTOPES IN ENDOGENIC ARAGONITE AT CASTOR LAKE, NORTH-CENTRAL WASHINGTON STATE ..... 78
4.1. Introduction ..... 79
4.2. Study Area ..... 80
4.3. Methods ..... 84
4.3.1. Coring and Field Measurements ..... 84
4.3.2. Chronology ..... 85
4.3.3. Stable Isotopes ..... 88
4.3.4. Palmer Drought Severity Index Correlation ..... 89
4.4. Results ..... 90
4.5. Discussion ..... 97
4.5.1. Drought in the Pacific Northwest ..... 97
4.5.2. Proxy record of Drought in the Pacific Northwest ..... 100
4.5.3. Lake Sediment Stable Isotopes as a Proxy for Drought ..... 102
4.5.4. Oxygen Isotopes ..... 102
4.5.5. Carbon Isotopes ..... 105
4.5.6. Castor Lake Record ..... 106
4.6. Conclusion ..... 109
5. CONCLUSION ..... 111
5.1. Future Work at Castor Lake ..... 111
5.2. Future Work in the Greater Region ..... 114
APPENDIX A ..... 116
Modern Surface Water Isotope Data ..... 116
APPENDIX B ..... 119
Trace Element Data ..... 119
APPENDIX C ..... 121
Lead-210 and Cesium-137 Data ..... 121
BIBLIOGRAPHY ..... 123

## LIST OF TABLES

Table 2.1 Radiocarbon dates from Castor Lake................................................................ 24
Table 3.1 Radiocarbon dates from Castor Lake................................................................ 49
Table 4.1 Radiocarbon dates from Castor Lake................................................................ 85

## LIST OF FIGURES

Figure 1.1 General location map of Washington State. Field area indicated by star.................... 3

Figure 2.1 Base map showing Castor Lake, Mud Lake, and Conconully, WA. Bonaparte Meadows is located approximately 46 km northeast of Mud Lake. Weather station data is from Conconully. Regional pollen data are from Mud Lake and Bonaparte Meadows (Mack et al., 1979). Contour interval = 400 feet............................................................................ 20

Figure 2.2 Age vs. depth plot for Castor Lake radiocarbon and tephra dates. Radiocarbon ages used in age model shown as closed circles, radiocarbon ages shown as closed squares were not used in age model. Tephra ages shown as gray triangles. ............................................ 25

Figure 2.3 Lithology, bulk density, and loss on ignition (LOI) data from Castor Lake plotted vs. age. Pollen data are from Mud Lake and Bonaparte Meadows (Mack et al., 1979). LOI data expressed as weight percent of total sediment mass. 'Residue' from LOI is composed of biogenic silica and clastic sediment. Thick line on LOI plots represents a 5-point running average of the data. ................................................................................................................ 27

Figure 2.4 Lithology, total organic carbon (TOC), total nitrogen (TN), TOC/TN ratio, and stable isotope data from Castor Lake organic sediment. Pollen zones are from Mud Lake and Bonaparte Meadows (Mack et al., 1979). TOC and TN values have been corrected for carbonate sediment removal, and are expressed as a percent of total dry sediment mass.... 28

Figure 3.1 Base map showing Castor Lake, Mud Lake, and Conconully, WA. Bonaparte Meadows is located approximately 46 km northeast of Mud Lake. Weather station data is from Conconully. Regional pollen data are from Mud Lake and Bonaparte Meadows (Mack et al., 1979). Contour interval = 400 feet............................................................................ 43

Figure 3.2 Temperature, dissolved oxygen, conductivity, and pH data from Castor Lake water column in the primary coring location from summer 2003 (open squares) and winter 2004 (open circles).................................................................................................................. 46

Figure 3.3 Age vs. depth plot for Castor Lake radiocarbon and tephra dates. Radiocarbon ages used in age model shown as closed circles, radiocarbon ages shown as closed squares were not used in age model. Tephra ages shown as gray triangles. ............................................ 51

Figure 3.4 Lithological, bulk density, and magnetic susceptibility data from Castor Lake. Pollen data are from Mud Lake and Bonaparte Meadows (Mack et al., 1979). .............................. 54

Figure 3.5 Lithological, and loss on ignition (LOI) data from Castor Lake. LOI data expressed as a weight percent of total sediment mass. LOI 'residue' is composed of biogenic silica and clastic sediment. Thick line on LOI plots represents a 5-point running average of the data. Pollen data are from Mud Lake and Bonaparte Meadows (Mack et al., 1979). ......... 55

Figure 3.6 X-ray diffraction (XRD) data from Castor Lake carbonate sediment. Expected location of aragonite peaks indicated by multiple letter 'A' markings on top plot. ............. 58

Figure 3.7 Example scanning electron microscopy (SEM) image of Castor Lake treated carbonate sediment samples. Rice-shaped grains are indicative of endogenic aragonite.

Lack of large rounded grains suggests that no terrigenous carbonate is present. Biogenic carbonate is also absent in all samples. .... 60
Figure 3.8 Stable isotope data from Castor Lake carbonate sediment shown with core lithology and regional pollen data (Mack et al., 1979). .... 62
Figure 3.9 Trace element ratio data from Castor Lake shown with core lithology, oxygen isotope data, and regional pollen record (Mack et al., 1979). Trace element ratios have been multiplied by an integer value in some cases in order to produce more convenient numbers, as absolute values are not important. .... 64
Figure 4.1 Base map showing Castor Lake, Mud Lake, and Conconully, WA. Bonaparte Meadows is located approximately 46 km northeast of Mud Lake. Weather station data is from Conconully. Regional pollen data are from Mud Lake and Bonaparte Meadows (Mack et al., 1979). Contour interval = 400 feet. .... 80
Figure 4.2 Modern surface water isotope data from vicinity of Castor Lake. Samples collected between 2000 and 2004, over an area from 48° N to 49° N latitude, and 119° W to 121° W longitude. Open system lakes and rivers plot near the Global Meteoric Water Line (GMWL) due to limited atmospheric interaction. Closed system lakes plot far from the GMWL along the Relative Evaporation Line (REL) due to increased influence by evaporation. .... 82
Figure 4.3 Stable isotope data from carbonate sediment in the entire Castor Lake sediment core. Core lithological units shown at right next to regional pollen record (Mack et al., 1979). Dashed lines indicate lithological unit boundaries. .... 91
Figure 4.4 High resolution stable isotope data from the past ~2,000 years at Castor Lake. Data are plotted to show sample thickness, as the core was sampled continuously every 3.7 mm (~7 years) on average. Note high degree of covariance between records on decadal time scales ($r^2$=0.60). .... 92
Figure 4.5 Castor Lake oxygen isotope data compared to 20th-century records of precipitation at Conconully, WA, the Pacific Decadal Oscillation (PDO) index, and 20-year low-pass filter of Palmer Drought Severity Index (PDSI) data. Precipitation and PDSI axes are reversed to show drier conditions increasing to the right, PDO axis is not reversed, but also shows increasing aridity to the right. Note correlation between Castor Lake isotope and PDSI data ($r^2$=0.43) despite difference in sampling resolution. Conconully precipitation data are incomplete after the 1980's. Precipitation data were obtained from the National Climatic Data Center (NCDC). PDO data were obtained from the Joint Institute for the Study of the Ocean and Atmosphere (JISAO) via the World Wide Web (http://tao.washington.edu/main.html). PDSI data were obtained at the NOAA World Data Center for Paleoclimatology website (http://www.ncdc.noaa.gov/paleo/). .... 93
Figure 4.6 Chronology changes from adjusting the 1,500-year oxygen isotope record from Castor Lake to the Palmer Drought Severity Index (PDSI) reconstruction from 47.5° N, 120° W. Data normalized to unit variance. Thin line represents isotope record plotted using the original chronology based on radiocarbon dates. Thick line represents adjusted chronology. Gray zones indicate radiocarbon dates, with thickness representative of error range. .... 94
Figure 4.7 Adjusted Castor Lake oxygen isotope record shown with Palmer Drought Severity Index (PDSI) reconstruction from 47.5° N, 120° W ($r^2$=0.45). Castor Lake data have been normalized to unit variance. PDSI data have been smoothed with a 20-year low-pass filter.

PDSI data were obtained from the NOAA World Data Center for Paleoclimatology website (http://www.ncdc.noaa.gov/paleo/)........................................................................................ 95
Figure 4.8 Composite oxygen isotope record from Castor Lake. Data show 1,500-year tuned sequence with 6,000 cal yr BP to 1,500 cal yr BP sequence plotted using radiocarbon chronology. Data normalized to unit variance. Dry periods designated by gray bars. ....... 96

# PREFACE

I would like to thank the National Science Foundation and the University of Pittsburgh for funding to support this research. I also thank the following people and lab groups for sample processing and lab access: Jason Curtis, Bruce Finney, Paul Wilkinson, Brian Stewart, Rosemary Capo, Brian Games, Jean Blachére, Al Stewart, Lawrence Livermore National Laboratory, and the University of California at Irvine. Additional thanks to Mark Abbott, Mike Rosenmeier, Brian Stewart, and Mike Ramsey for advising on some or all phases of the project. Lastly, I thank Nathan Stansell and Mark Besonen for assistance in the field.

# 1. INTRODUCTION

Lake sediment archives are powerful tools for examining environmental change beyond the limiting confines of the instrumental and historical record. Lakes are unique among proxy recorders in that perhaps no other continental archive can be found under as wide a variety of geographic distribution and environmental setting. This diversity makes them highly valuable, but also renders them complicated to interpret, as it requires that each system be approached on an individual basis with no single standard model for interpretation applicable to all settings. Additionally, this means lakes vary in the types of environmental changes recorded in their sediment records. The focus of this investigation is to examine environmental change in north-central Washington State over the period between the last major advance of continental glaciation and the present. This interval covers the past ~15,000 years and encompasses the very latest portion of the Pleistocene, and the entire Holocene epoch. A central focus of this research is to examine drought variability on millennial, centennial, and multi-decadal time scales, with particular effort towards investigations of centennial to multi-decadal drought variability over the past ~6,000 years. Additional attention is focused on identifying major regional-scale changes common among proxy records such as the Younger Dryas and major middle Holocene drought events, as well as understanding how climatic changes influence aquatic productivity, and on investigating evidence for other environmentally driven changes preserved in sediment records. These goals are accomplished through applications of sedimentology, stable isotope composition of carbonate and organic sediment, trace element geochemistry, and various other tools commonly applied in paleolimnological research.

## 1.1. Pacific Northwest

Rapidly increasing human population in the Pacific Northwest is placing high demands on the limited available water resources. With few naturally occurring major fresh-water reservoirs, a large percentage of the total water used for both urban and industrial applications must ultimately come from seasonal snow-pack from the Cascade Mountain Range. This near total reliance on annually replenished water resources makes the region inherently susceptible to changes in moisture availability, as severe multi-year drought episodes may exceed the limit of system's ability to cope with such events. Observational data for moisture availability and other climate parameters is limited to approximately the last 100 years. This interval is too short to fully comprehend the cyclical changes present in the climate system or the range of natural variability, yet it is the period on which all water resource legislation is based. In order to increase the understanding of natural variability in the climate system of the Pacific Northwest so that efforts may be made to prepare for the full range and recurrence interval of possible future climate events, efforts must be made to extract climatic information from the geologic and biotic record that extend beyond the short period for which instrumental data are available.

The focus area of this study lies between 48°30' N and 48°40' N (Fig.1.1), and the Pacific westerlies are, on average, strongest between ~45° N and 50° N (Bryson and Hare, 1974).

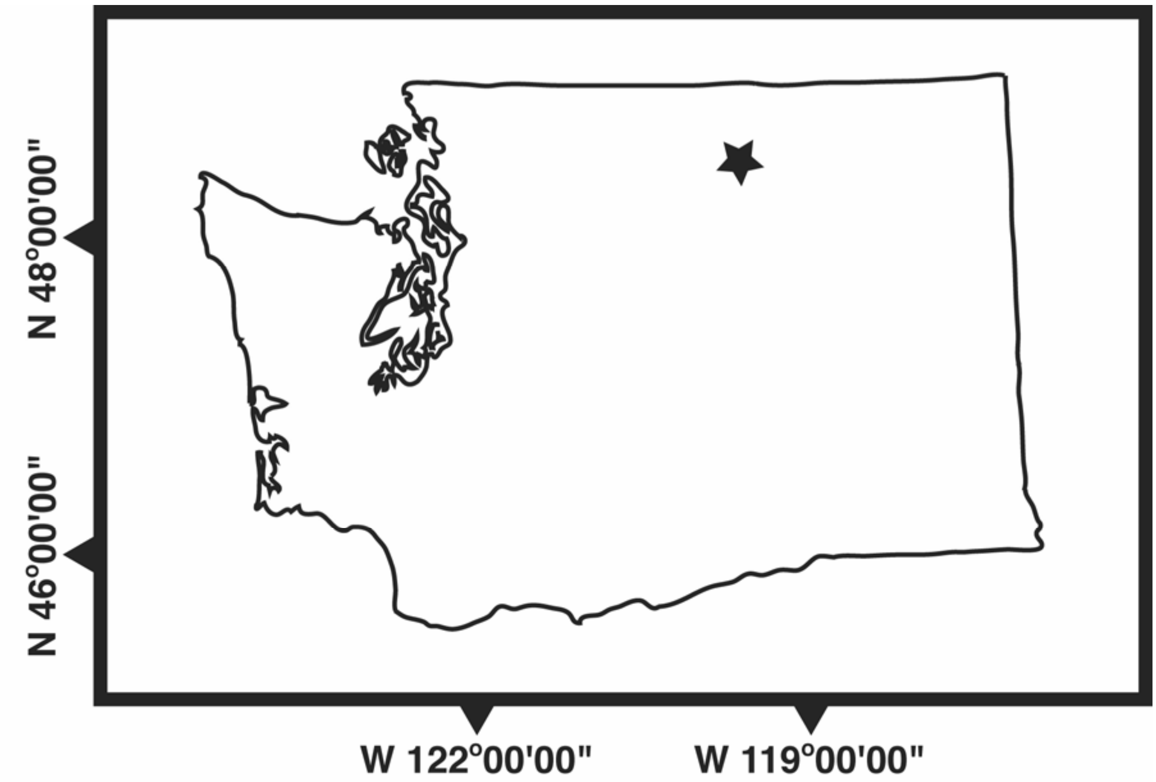


**Figure 1.1 General location map of Washington State. Field area indicated by star.**

Because the field area exists near the latitudinal center of this region of maximum Pacific westerly wind strength it is in the direct path one of the main routes where these winds can cross the western cordillera (Bryson and Hare, 1974). Local climate is thus dominated by Pacific airflow in the winter months, although occasional short-lived events may deliver northern or eastern air masses. In the summer months, the climate tends to be controlled by hot, dry air masses due to the position of the Pacific High-Pressure system in the ocean at these latitudes (Bryson and Hare, 1974). This dominance of the Pacific Ocean on local climate creates an environment characterized by dry summers and wetter winters and springs. Data obtained from the National Climatic Data Center (NCDC) for the closest weather station at Conconully, WA show that average adjusted monthly precipitation values from July to October are only 15 mm/month, while November to February monthly averages are 27 mm/month, and March to June monthly averages are 24 mm/month. Average summer temperature is approximately 18°C and average winter temperature is approximately 3.6°C. Low summer precipitation values and high summer temperatures demonstrate the climate system described by observations of changes in the position of atmospheric pressure centers over Pacific, and outline the need for winter snow pack to provide the necessary water resources for the region.

This research is largely based in Okanogan County in north-central Washington State in the Okanogan and Methow River Valleys near the towns of Omak, Winthrop, and Twisp. Specific lake sites from which sediment cores were collected include Castor, Davis, Little Twin, Big Twin, Alta, Campbell, Lime Belt Blue, Round, Duck, Long, Bonaparte, Wannacut Blue, and Sinlahekin Blue Lakes. Various sedimentological and geochemical analyses were performed on all of the core samples that were collected in order to understand the broad pattern of regional change. Numerous other sites were also visited, but not cored, and water samples were collected at every location as well as at several lakes within North Cascades National Park and at several river locations. Based on this background field and laboratory work, Castor Lake was selected as the best lake to focus on as a regionally representative site for a variety of reasons. First, the local catchment has largely escaped anthropogenic land-use changes, permitting calibration of the paleoenvironmental signal with the instrumental climate record. Castor Lake is also relatively protected from wind, and is relatively deep relative to its surface area. These conditions promoted the preservation of laminated sediments throughout most of the Holocene sequence, thus limiting sediment mixing through wind action, bioturbation, and other processes and allowing for the extraction of the highest resolution climate signal possible given the sedimentation rates. Third, and perhaps most important, the small volume of Castor Lake causes it to respond rapidly to environmental change, limiting the lag in response time observed in larger systems and maximizing the magnitude of changes in proxy data.

## 1.2. General Paleoclimate Background

The majority of information regarding paleoenvironmental conditions in the Pacific Northwest over the last ~15,000 years comes from a combination of glacial, paleolimnological/palynological, and climate modeling studies. Each of these types of proxy record contribute information on different aspects of the environmental history. Additional information regarding variability over the past ~1000 years is available from studies of tree-rings, which offer some of the highest resolution paleoenvironmental data available. Consequentially, aspects of the more recent periods of environmental history are better understood than those that are older. The increasing difficulty in dating sediments and applying modern analogs with increasing age contribute to this effect as well.

Changes in solar insolation probably exerted the greatest influence on post-glacial climate fluctuations in the Pacific Northwest on millennial time-scales, and although this influence ultimately drove glacial retreat, and was therefore highly important during the glacial period as well, changes in the position and size of the Laurentide ice sheet may have played a more direct role in millennial-scale climate forcing during deglaciation (COHMAP, 1988; Whitlock, 1992). Maximum summertime solar insolation occurred just after widespread deglaciation at ~9,000 cal yr BP, when summer values were ~8% higher, and winter values ~8-10% lower than today. The retreat of the Laurentide ice sheet probably led to complex reorganization of atmospheric and oceanic circulation patterns as well. This included a major transition from glacial conditions where surface winds were dominated by easterlies due to the presence of an anticyclonic zone centered over the Laurentide ice sheet, to conditions more akin to the modern system where surface westerlies exert a dominant influence (COHMAP, 1988). However, such large-scale changes do not entirely explain the variability observed in proxy records. Understanding additional factors such as associated shifts in ocean dynamics, regional vegetation, hydrologic drainage, and other localized effects is necessary to elucidate the exact nature of these events.

### 1.2.1. Early Holocene

Evidence exists throughout the Pacific Northwest for early Holocene glacial advances, and inferred cool and moist conditions following Pleistocene deglaciation (Beget, 1981; Heine, 1998a; Heine, 1998b; Luckman and Osborn, 1979; Thomas et al., 2000; Waitt et al., 1982), although chronological control for glacial studies is often poor. Luckman and Osborn (1979) cited moraine stratigraphic evidence for an early Holocene glacial advance in the Banff-Jasper-Yoho area of the middle Canadian Rocky Mountains, but the age of this advance could only be constrained as being between deglaciation (locally 10,850 to 10,950 cal yr BP) and the deposition of the Mazama tephra, ca. 7,585 cal yr BP (Hallett et al., 1997). Waitt et al. (1982) reported similar evidence for an early Holocene glacial advance in the Enchantment Lakes Basin of the North Cascade Range in Washington, and also bracketed the advance between deglaciation and the deposition of the Mazama tephra. Beget (1981) observed a similar glacial advance near Glacier Peak in Washington bracketed between deglaciation and the Mazama tephra, but was also able to obtain a radiocarbon date from charcoal within the till at 9,330 to 9,430 cal yr BP. This interpretation was questioned, however, when the till containing the charcoal fragments was re-interpreted as a debris flow (Davis and Osborn, 1987).

Recent work on moraine-dammed lakes on Mount Rainier used radiocarbon dates from sediment cores to constrain the time of early Holocene glacial advance in the Pacific Northwest to between 10,900 and 10,000 cal yr BP (Heine, 1998b). Early Holocene glacial advances between 9,450 and 8,400 cal yr BP were also identified at nearby Mt. Baker (Thomas et al., 2000). Glacial studies to the south of the North Cascades, however, show no evidence of Holocene glacial advances with the exception of those of the Little Ice Age, which spanned the period from approximately the mid-14th to the mid-19th centuries (Clark and Gillespie, 1997). In contrast to evidence from the North Cascades region in the USA, radiocarbon dates from the north at Castle Peak in southern British Columbia identified an elevated paleo-timberline, and inferred warmer mean growing season temperatures between 9,700 and 9,200 cal yr BP (Clague and Mathewes, 1989), further indicating the complex regional nature of climate change in the Pacific Northwest.

A composite study of regional pollen records suggest that during the latest Pleistocene and early Holocene, temperate forest communities invaded the Pacific Northwest, and continued warming in the early Holocene allowed temperate conifers to expand in the un-glaciated region of the southern Puget Trough (Whitlock, 1992). Pollen data also indicate that the un-glaciated region of the southwestern Columbia Basin experienced little change in vegetation throughout the course of deglaciation, although areas to the north affected by the retreat of glacial ice and the recurring catastrophic drainage of glacial Lake Missoula in the Scabland floods were invaded by open parkland vegetation. Nearly all pollen records cite evidence for the onset of major drought conditions in the early to middle Holocene (Whitlock, 1992).

Lake-level changes inferred from the sedimentary record of Mahoney Lake in southern British Columbia indicate that before ~5,500 cal yr BP, environmental conditions were characterized by periods of low effective precipitation (Lowe et al., 1997). Effective precipitation can be defined as the fraction of total precipitation that is stored in the soil and is available for plant growth, or contributes to ground water and increases lake-levels. However, the few high water stands that did occur in this otherwise dry period tended to be of longer duration than those that occurred during periods characterized by higher effective precipitation (Lowe et al., 1997). Late Quaternary vegetation and climate change data from McCall Fen in Long Valley, Idaho suggest a cool, moist climate similar to the present from 14,300 to 11,500 cal yr BP, followed by a significantly warmer and drier regional climate from 11,500 to 3,400 cal yr BP, with maximum aridity occurring just after the deposition of the Mazama tephra (Doerner and Carrara, 2001). The early Holocene sediment record from Big Lake, south-central British Columbia suggests a similar climatic history, with fresh and relatively deep water conditions from deglaciation to ~8,400 cal yr BP, followed by a period of lower lake stands and more saline waters until ~6,600 cal yr BP (Bennett et al., 2001).

### 1.2.2. Middle Holocene

Most lacustrine and glacial records from the middle Holocene in the Pacific Northwest suggest the existence of drier conditions, although the exact timing of these events do not always agree completely (Bennett et al., 2001; Clague and Mathewes, 1989; Doerner and Carrara, 2001; Lowe et al., 1997; Whitlock, 1992). The absence of any well documented glacial advances in the region during the middle Holocene lends support to the notion of low effective moisture during this interval (Luckman and Osborn, 1979; Ryder and Thomson, 1986; Waitt et al., 1982), and the onset of the well-documented xerothermic (hot & dry) interval (Lowe et al., 1997; Ryder and Thomson, 1986; Whitlock, 1992).

The timing of return to relatively cool and moist conditions after the xerothermic interval varies depending on location throughout the Pacific Northwest (Bennett et al., 2001; Doerner and Carrara, 2001; Lowe et al., 1997). Glacial studies contribute little information regarding this transition, as the larger late Holocene or little ice age advances of the last ~1,000 years would have eradicated any smaller scale advances that might have occurred at this time. A known exception occurs in the southern Coast Mountains of British Columbia, where the Garibaldi phase of glacier expansion (6,800 to 5,700 cal yr BP) is preserved, although it less extensive than that of the late neo-glacial (Ryder and Thomson, 1986). The Garibaldi advance is thought to correlate with the end of the xerothermic interval in the Coast Range, although it is noted that this transition appears to vary regionally, ranging between 7,800 and 6,800 cal yr BP in coastal southern British Columbia and adjacent Washington, to between 4,450 and 3,200 cal yr BP east of the Coast and Cascade Mountains.

Clague and Mathewes (1989) suggest an end to the generally warmer climate occurred between 6,800 and 5,700 cal yr BP based on their work at Castle Peak, British Columbia, although chronological control for the end of the warm event is not as good as that for the beginning. Pollen data from the Northwest suggest differential timing for vegetation responses to the end of summer drought conditions after 6,800 to 5,700 cal yr BP (Whitlock, 1992). Palynologic evidence from sites in the Okanogan Highland indicate a brief cooling between 3,750 and 1,600 cal yr BP, although in general, modern forests were established in the area after 2,550 to 1,600 cal yr BP (Whitlock, 1992).

The general interpretation offered for lake-level fluctuations in Mahoney Lake in southern British Columbia is that the period after 5,500 cal yr BP is characterized by a lack of episodes of very low effective moisture (Lowe et al., 1997). This transition is interpreted as coinciding with the end of the xerothermic interval in this area. Some correlation exists between this record and evidence from Big Lake, south-central British Columbia, although the changes at Big Lake appear to lag those observed in the Mahoney Lake record. Big Lake data indicate that beginning at 6,600 cal yr BP lake-levels and runoff increased, effective moisture in the region reached its highest point in the Holocene, and diatom species indicative of lake water eutrophy became abundant (Bennett et al., 2001).

The end of the middle Holocene at Big Lake was characterized by changes in diatom assemblage at 3,600 cal yr BP indicative of a transition to slightly more saline, and shallower conditions associated with a period with lower effective moisture (Bennett et al., 2001). This is broadly consistent with the dry interval seen in the Mahoney Lake record between 2,800 and 1,500 cal yr BP (Lowe et al., 1997). Most other pollen records from the Pacific Northwest do not recognize the slight shift to more arid conditions identified in the Big Lake record, but this is probably the result of the insensitivity of pollen records to such small scale changes (Bennett et al., 2001). Conversely, the McCall Fen record from west-central Idaho indicates a transition to cooler and more moist conditions at 3,400 cal yr (Doerner and Carrara, 2001). Additional evidence for late-middle Holocene climate change comes from sediment cores from bogs in the southern Coast Mountains of British Columbia. These data show evidence for a glacial advance (Tiedemann advance) between 3,550 and 1,850 cal yr BP (Ryder and Thomson, 1986).

### 1.2.3. Late Holocene

Most palynological studies in the Pacific Northwest report only minor changes regional climate after the middle Holocene xerothermic interval (Bennett et al., 2001; Clague and Mathewes, 1989; Doerner and Carrara, 2001; Lowe et al., 1997; Mack et al., 1979; Whitlock, 1992). However, this conclusion is not universally supported, as some sediment records based on more sensitive proxies than pollen, such as changes in diatom assemblage, suggest a return to more arid conditions in the late Holocene (Bennett et al., 2001; Lowe et al., 1997). Additional lake sediment records indicate more short-lived periods of centennial to multi-decadal-scale drought. Records from southern British Columbia and Alberta, Canada indicate episodes of drought during the Medieval Warm Period (MWP) (900-1200AD), in the early 1600's, and around 1800 AD (Campbell, 1998; Hallett et al., 2003). Several glacial studies, however, report that the largest advances since the early Holocene and late Pleistocene are late neo-glacial in age (~450 yr old) (Luckman and Osborn, 1979; Ryder and Thomson, 1986; Waitt et al., 1982).

Tree-ring studies become effective tools for examining environmental change in the late-Holocene, as numerous samples may be found that span the last ~500 years, with a few chronologies extending back as far as ~1,500 years into the past. These records generally record drought conditions or changes in temperature. Periods of widespread drought have been identified in the recent past using this approach, most notably during the late 1600's to early 1700's, 1740's to 1760's, the late 1700's to early 1800's, the 1840's, the early 1900's, and the 1930's (Gedalof, 2002; Graumlich, 1987; Knapp et al., 2004). Within these generalized periods of drought, however, there is considerable variation among records with respect to duration and intensity of any one event, as certain local subtleties undoubtedly exert confounding influences.

Although the broad pattern of regional climate change during the late Pleistocene and Holocene epochs in the Pacific Northwest is generally understood at millennial time scales, significant questions persist about the timing of events and the nature of sub-millennial-scale change. Additional questions also remain regarding the spatial response to climate change, and the nature of the forcing factors that ultimately drove the climate system to undergo the transformations that are observed in the proxy record. Only through continued work to develop a more densely distributed geographic network of paleoenvironmental records, and through the application of new and more highly refined analytical methods for generating proxy data and improving chronological control, can we hope to answer these questions in the future. Doing so will not only improve our understanding of the climate system, but it will also allow us to be more properly prepared for changes in climate that will undoubtedly affect us in the future.

### 1.3. Project Objectives

The Castor Lake sediment record is remarkable from the standpoint that the lake system is sensitive enough to record environmental change at multi-decadal time scales, yet is long enough to resolve changes into the late Pleistocene. Locating such a sediment record would not have been likely without significant background research and fieldwork. The goals of this investigation are to attempt to resolve some of the issues regarding the timing of millennial scale events seen in other proxy records in the Pacific Northwest, particularly the Younger Dryas, and major middle Holocene drought events. Additional attention is focused on centennial to multi-decadal scale drought variability over the past ~2,000 and ~6,000 years. The work presented here is divided into three chapters, each intended for stand-alone publication. Minor redundancies exist between the chapters and the introductory text as a result of this structure.

# 2. PALEOENVIRONMENTAL INVESTIGATION AT CASTOR LAKE, NORTH-CENTRAL WASHINGTON STATE USING LAKE SEDIMENT ORGANIC MATTER

Paleoenvironmental investigations based on the organic fraction of lake sediment provide some of the most complex types of lacustrine proxy data to interpret due to the varied and changing makeup of this material. We report such results from a continuous sediment record from Castor Lake in north-central Washington State spanning the late Pleistocene to the present. Changes in regional vegetation and aquatic productivity over this period are documented from variations in the makeup of organic matter. Analyses are not limited to only organic sediment, however, and include general sedimentology, bulk density, total organic matter content, total carbonate content, total organic carbon, total nitrogen, TOC/TN ratios, and $\delta^{13}C$ and $\delta^{15}N$ measurements of bulk organic matter. Chronological control is provided by eleven accelerator mass spectrometry (AMS) radiocarbon dates and tephrochronology. Results show a significant response to the Younger Dryas cold reversal, as well as a clearly resolved middle Holocene arid period. Sedimentary and geochemical changes that are approximately coincident with the deposition of the Mount Mazama and Mount Saint Helens Y tephras raise questions regarding the interaction of volcanic, lacustrine, and climatic processes that are unresolved at this time.

## 2.1. Introduction

The organic fraction of lake sediment is composed largely of a mixture of lipids, carbohydrates, proteins, and other organic matter components derived from organisms that have lived in and around the lake (Meyers and Teranes, 2001). The complexity of this sediment fraction introduces a level of uncertainty into interpretations of proxy data derived from bulk organic material. Recent technological advances have made possible the isolation and analysis of individual compounds from organic sediment for isotopic analysis (Bird et al., 1995). As these practices become more widespread, a wealth of new information will become available regarding paleoenvironmental change. However, analytical complications and costs of compound-specific isotopic analyses of organic matter prohibit widespread implementation of such techniques at present in paleolimnology. Isotopic measurements of bulk organic matter also reveal valuable information, are much easer and less costly to perform, and are therefore more widely utilized at this time. Additional measurements of bulk organic matter, such as total organic matter, total organic carbon (TOC), total nitrogen (TN) and carbon/nitrogen ratios (C/N) can reveal a considerable amount of information, especially when combined with other sediment proxies such as carbonate content, pollen records or $\delta^{18}O$ measurements of carbonate.

Organic carbon and nitrogen concentrations in lake sediments represent the proportion of the total flux of these two elements to the lake water from allochthonous and autochthonous sources that are successfully incorporated into the sediment without recycling by some other process prior to sedimentation (Hodell and Schelske, 1998). Measurements of the relative contribution of these elements can be interpreted as indicators of changes in aquatic productivity, changes in the delivery rate of terrestrial organic matter to the lake, or changes in the rate of recycling of as they are incorporated into the sedimentary record. The lack of a single control on the flux of organic carbon and nitrogen to the sediment record means that interpretations based on these data must be made in tandem with interpretations of other proxy signals.

Combining total organic carbon (TOC) and total nitrogen (TN) data to calculate a TOC/TN ratio is an effective way to examine changes in the relative contribution of terrestrial and aquatic organic matter to the sediment. In lakes where a significant component of the sediment is comprised of carbonate, it is necessary to differentiate between total carbon (TC), and total organic carbon (TOC) when working with ratios of carbon and nitrogen. Nonvascular aquatic plants like diatoms typically have low TOC/TN ratios, between 4 and 10, while vascular land plants, which contain cellulose, have ratios of 20 and higher (Lamb et al., 2004; Meyers and Ishiwatari, 1995). This variation may be used to discern the probable source of organic sediment, or determine if the source is mixed. Furthermore, evidence suggests that the TOC/TN signal is not subject to change through selective diagenesis beyond minor changes that take pace in the sediment water interface, so the proxy is applicable within long-term sediment records (Talbot and Johannessen, 1992).

The large number of isotopic controls and sources of organic carbon in bulk lake sediment introduce significant levels of complexity into interpretations of $\delta^{13}C$ data from organic matter. Organic matter is ultimately derived from photosynthesis, although three main chemical pathways for photosynthesis are observed in nature, each with a unique isotopic fractionation effect with respect to carbon. The most common pathway for terrestrial vegetation and aquatic algae is the $C_3$ Calvin pathway, although some grasses use the $C_4$ Hatch-Slack pathway, while others, mostly succulents, utilize the crassulacean acid metabolism (CAM) pathway (Meyers and Ishiwatari, 1995). The isotopic composition of organic matter that enters the lake from terrestrial sources is typically ~-27‰ for $C_3$ plants, ~-13‰ for $C_4$ plants, and between ~-4 to –20‰ for

CAM plants (Lamb et al., 2004). In systems where the only source of organic matter is terrestrial, $\delta^{13}C$ values can serve as an effective tool for interpreting changes in vegetation through time. Complications arise when the organic matter source is a mix of terrestrial and aquatic vegetation, as diatoms typically have $\delta^{13}C$ values between ~-19‰ and –23‰, and phytoplankton are commonly ~-30‰ (Lamb et al., 2004; McKenzie, 1985). Understanding the overlap in the isotopic signal between aquatic and terrestrial sources of organic matter can be improved by examining $\delta^{13}C$ data in combination with C/N ratios, as terrestrial and aquatic material with the same $\delta^{13}C$ value will have a different C/N value (Meyers and Teranes, 2001).

Additional variability in $\delta^{13}C$ of organic matter occurs as a result of changes in the degree of photosynthetic fractionation by phytoplankton, where the preferential uptake of $^{12}C$ over $^{13}C$ decreases as productivity increases to the point where carbon begins to become limited (McKenzie, 1985). Where terrestrial organic matter is not a significant contributor to the sediment, or its contribution remains constant, changes in $\delta^{13}C$ of bulk organic matter may be interpreted as a proxy for aquatic productivity. However, when productivity increases to the point at which the water column becomes depleted in $CO_2$, which can occur in shallow lakes with high pH, plants will increasingly rely on $HCO_3^-$ as a carbonate source, which is about 8‰ heavier than $CO_2$ (Brenner et al., 1999). In alkaline water where pH is greater than 8.3, more than 99% of dissolved inorganic carbon (DIC), the source of carbon used in photosynthesis, is in the form of $HCO_3^-$ (Hassan et al., 1997). Additional complications can arise in systems where methanogenesis occurs in the sediment, which can release carbon in the form of methane to the lake water with an isotopic composition approaching –70‰ (Quay et al., 1986). Such variations in the $\delta^{13}C$ of the DIC pool will ultimately be incorporated into aquatic organic matter that utilizes this carbon source and can therefore complicate proxy interpretations. Despite the complicating factors involved in interpreting a $\delta^{13}C$ signal from organic matter, diagenetic effects have been shown to be limited (Hodell and Schelske, 1998). Therefore, the signal preserved in the isotope ratio of organic carbon is a record of processes in and around the lake and can be applied to paleoenvironmental investigations.

Nitrogen isotopes have not been used as extensively in paleolimnology because of the even larger number of factors that influence the nitrogen isotopic composition of bulk organic sediment compared to carbon (Talbot, 2001). Any attempt to use such information must be accompanied by a suite of other proxy data, and even then, the response of the $\delta^{15}N$ signal may be ambiguous. Despite the complications, $\delta^{15}N$ may reveal changes that are not apparent from other proxy data. Much of the difficulty with nitrogen isotopes comes from the fact that inorganic nitrogen occurs in a an even wider variety of chemical forms and oxidation states than carbon, which leads to more complex cycling through the various inorganic and organic reservoirs (Talbot, 2001). With respect to aquatic productivity, nitrogen behaves in much the same way that carbon does where organisms preferentially utilize $^{14}N$, thereby enriching the remaining inorganic nitrogen pool with $^{15}N$ (Talbot, 2001). This behavior has been exploited to estimate the trophic state of lakes through analysis of sediment $\delta^{15}N$ in concert with sediment $\delta^{13}C$ (Brenner et al., 1999). This approach can be successful in some settings, with increasing $\delta^{15}N$ indicating increasing trophic state, but when systems become hypereutrophic and nitrogen becomes severely limited, cyanobacteria populations can increase and begin fixing atmospheric nitrogen (~0‰) in significant quantities, which causes the $\delta^{15}N$ of the resulting sediment to decrease (Gu et al., 1996). The non-linear response to changes in productivity requires the use of additional proxies to resolve the changes.

Additional complexities result from the large number of reactions with which nitrogen can be involved in aquatic systems, each with an associated fractionation factor. These include dissolution, ammonia volatilization, fixation, assimilation, ammonium assimilation, remineralization, nitrification, and denitrification (Talbot, 2001). Studies of modern systems also reveal a large knowledge deficit in current understanding of nitrogen cycling. In Lake Superior, for example, contrary to theory and culture experiments, organic matter $\delta^{15}N$ values were found to be *greater* than that of the dissolved inorganic nitrogen substrate from which they formed (Ostrom et al., 1998). Although Lake Superior is not an analogous system to Castor Lake, such results identify the need for greater understanding of nitrogen system dynamics at all scales. Nitrogen isotope data can still play a useful role in paleoenvironmental investigations, however, provided that an attempt is made to understand the likely controls specific to the system in question.

Measurements of sediment proxies that are expressed as a weight-percent of total sediment mass, such as percent total organic carbon (TOC) or percent carbonate, must also be interpreted with caution due to the interfering "dilution" effects that such records can have on one another. Apparent changes in the relative contribution of a particular component may not reflect a real change in the flux of that component to the sediment, but rather a dilution, or concentration effect from changes in the flux of another component. Such ambiguities may be avoided by converting measurements expressed as a weight-percent into an approximation of the flux of that component to the sediment, but doing so requires very accurate chronological control and continuous measurement of dry sediment bulk density. While the latter are relatively easy to obtain, chronological control of the caliber needed for such an exercise is rarely available in sediment records that are not dated through varve counting. Attempts to convert weight-percent data into sediment flux are highly sensitive to slight alterations in the core chronology, and therefore should not be used where chronological error is greater than a few decades. An alternative approach to overcoming the effects of weight-percent based proxy interference is to measure all significant components of the sediment so that all such data may be interpreted simultaneously. Although less desirable than accurate flux data, this alternative approach provides a good way of extracting useful information from a sediment record when chronological control is not sufficient for sediment flux calculations.

The combination of total organic carbon, total nitrogen, TOC/TN ratios, total organic matter, total carbonate, and bulk density measurements from a sediment core from Castor Lake (Fig.2.1) are used here to investigate changes in environmental conditions in north-central Washington State from the late Pleistocene to the present.

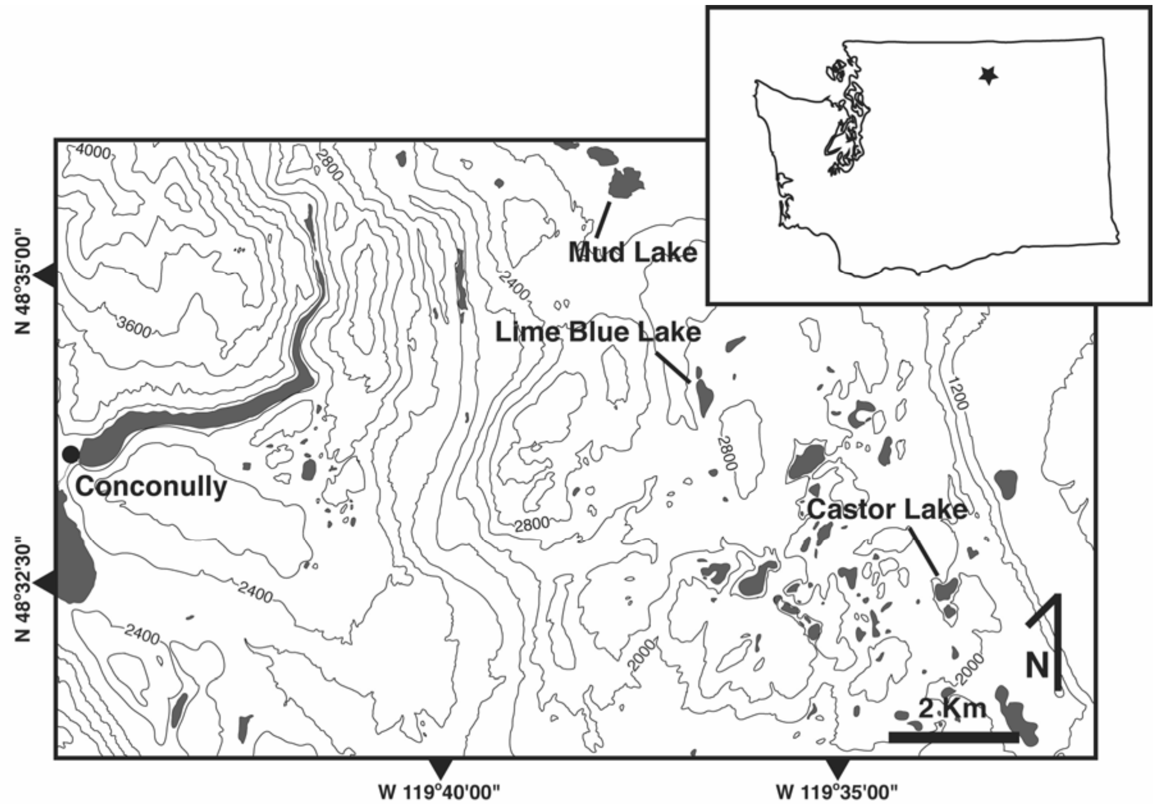


**Figure 2.1 Base map showing Castor Lake, Mud Lake, and Conconully, WA. Bonaparte Meadows is located approximately 46 km northeast of Mud Lake. Weather station data is from Conconully. Regional pollen data are from Mud Lake and Bonaparte Meadows (Mack et al., 1979). Contour interval = 400 feet.**

Additional information comes from core sedimentology, $\delta^{13}C$ and $\delta^{15}N$ measurements of the organic fraction of the sediment. These data are complimented by a regional pollen record from Mud Lake and Bonaparte Meadows, which are approximately 8 and 46 km from Castor Lake, respectively (Mack et al., 1979). This work results in an increased understanding of vegetation changes and aquatic productivity, which can ultimately be related to climate variability in the region over the last ~15,000 years.

## 2.2. Study Area

Castor Lake (48.54° N, 119.56° W) is located in the Lime Belt region of Okanogan County in Washington State on a terrace margin of the Okanogan River. The system is effectively closed–basin, meaning it has no active surface outflow, and is most likely a kettle lake associated with the retreat of the Cordillean ice sheet (Fig.2.1). The lake sits on a relative topographic high, making it unlikely that deep groundwater from distant sources contribute in any significant degree to the lake water. Residence time estimates from lakes in similar environmental settings in central and northern Alberta range from 0.2 to 20 years, depending on whether the hydrology is open, closed, or somewhere in between (Gibson et al., 2002). The closed-basin hydrology of Castor Lake suggests that residence time is probably closer to the upper limits of this range. Surface water pH was 8.5 in late July of 2003 and alkalinity was approximately 565 mg/L. Although the DIC pool was not directly measured, it is likely that the majority of inorganic carbon is in the form of bicarbonate, given the high alkalinity and pH of the lake water. Lake surface elevation is about 591 meters above sea level, maximum water depth is ~11.5 meters, and lake surface area is ~0.07 km$^2$. The catchment is approximately 3.24 km$^2$ and is almost entirely undeveloped. Field-based bathymetric surveys reveal a single large, flat basin with gently sloping sides rising to the shores.

Based on sedimentological analyses and limited modern limnological investigation conducted in July of 2003 and February of 2004, the lake appears to be warm monomictic or meromictic. Winter temperature, conductivity, and pH profiles all show an unstratified water column indicating seasonal water column circulation, but dissolved oxygen profiles show permanent anoxic conditions in the hypolimnion. The reasons for permanent anoxia are unclear, but it may be a result of the topographic protection of the basin. The lake is surrounded by relatively steep, forested hill slopes, which might serve to limit the water surface wind speed on the lake, thus preventing complete seasonal overturn. Hypolimnetic anoxia is unlikely to be the result of lake-water eutrophy, as the lake is currently too alkaline to support fish populations, and water column visibility extends up to several meters. Whatever the cause of the permanent anoxia, the result has been the preservation of finely laminated sediment throughout most of the Holocene, as well as very limited benthic ostracod growth.

Regional climate is primarily dominated by Pacific westerlies, which are at their strongest between 45° and 50° N (Bryson and Hare, 1974). These winds are controlled by the Aleutian low-pressure system, and the North Pacific high-pressure system. During the winter months the Aleutian low strengthens and moves to a more southern position, delivering cool, moist air to the coast of Washington state and resulting in the winter wet season. In the summer months, the Aleutian low weakens, moves northward and is replaced by the North Pacific high. The latter delivers more arid air masses to the state. Arctic air masses occasionally enter the region, but are typically replaced quickly by incoming Pacific westerlies (Bryson and Hare, 1974). Modern climate data from the closest weather station to Castor Lake at Conconully, WA were acquired from the National Climatic Data Center (NCDC). Average annual adjusted precipitation values for the period from 1960 to 1990 were 277 mm/yr, average summer temperatures (Jun-Aug) were 18.0°C, and average winter temperatures (Dec-Feb) were –3.6°C.

## 2.3. Methods

A 4.5 m modified piston core (5 cm diameter) was collected in the summer of 2003 with overlapping sections down to approximately 3.78 m (Wright et al., 1984). The uppermost portions of the sediment sequence were not recovered. Cores were transported to the University of Pittsburgh for analysis, and stored in polyvinyl chloride (PVC) tubes at ~4°C prior to sampling.

Cores were split, photographed, and detailed descriptions of lithological changes were made. Bulk density measurements were conducted at 2 cm intervals throughout the length of the core using a known volume of sediment and a drying oven to remove water. The same samples were subsequently used for loss on ignition (LOI) analysis at 500° and 1000°C in order to determine approximate mass fraction of organic matter and carbonate, respectively (Dean, 1974). Loss on ignition sample residue was comprised of a combination of terrigenous clastic sediment and biogenic silica. Smear slides were also made from samples at selected intervals over the length of the sediment sequence. Additional samples collected from the same location as the samples used for LOI were sent to the University of Alaska at Fairbanks for %C, %N, $\delta^{13}C$, and $\delta^{15}N$ analyses. Isotopic results are presented in standard per-mille notation. Precisions for $\delta^{13}C$ and $\delta^{15}N$ analyses were reported to be within 0.05‰, and 0.25‰, respectively. Measurements of %C and %N in the organic component of the lake sediment were converted to percent total organic carbon (TOC) and total nitrogen (TN) by using the calculated carbonate content data from LOI analyses to correct for the relative mass fraction of carbonate that was removed from the sample prior to analysis. Molar ratios of TOC/TN content were calculated based on these data.

Chronological control is provided by eleven accelerator mass spectrometry (AMS) radiocarbon dates (Table 2.1) and two tephra layers of known age.

**Table 2.1 Radiocarbon dates from Castor Lake.**

| Core | Drive Depth (cm) | $^{14}$C age ($^{14}$C yr B.P.) with error | Median calibrated age (cal yr B.P.) | 2-sigma calibrated age range (cal yr B.P.) | Material | Lab accession number |
|---|---|---|---|---|---|---|
| A-03 D-1 | 23 | 435 ± 40 | 492 | 328-540 | Grass | CAMS# 104906 |
| A-03 D-1 | 75 | 1530 ± 35 | 1416 | 1334-1518 | Charcoal | CAMS# 104907 |
| B-03 D-2 | 9 | 1890 ± 35 | 1833 | 1725-1919 | Pine Needle | CAMS# 104908 |
| B-03 D-2 | 75 | 3385 ± 35 | 3622 | 3479-3715 | Charcoal | CAMS# 104910 |
| B-03 D-3 | 8 | 4095 ± 45 | 4608 | 4442-4816 | Seed | UCI# 7527 |
| B-03 D-3 | 36 | 5160 ± 100 | 5911 | 5661-6173 | Charcoal | CAMS# 104909 |
| B-03 D-3 | 56 | 5815 ± 25 | 6628 | 6502-6721 | Seed | UCI# 7488 |
| B-03 D-4 | 52 | 6720 ± 80 | 7582 | 7432-7682 | Seed | CAMS# 104911 |
| B-03 D4 | 88 | 9425 ± 30 | 10648 | 10557-11035 | Seed | UCI# 7590 |
| B-03 D-5 | 16 | 10025 ± 35 | 11465 | 11259-11908 | Seed | UCI# 7491 |
| B-03 D-5 | 40 | 11020 ± 35 | 13022 | 12675-13169 | Seed | UCI# 7493 |

Radiocarbon measurements were performed on charcoal or identifiable terrestrial macrofossils, including seeds from the *cyperaceae* sedge family in many cases. Possible hard-water effects were avoided by ensuring that only identifiable remains from terrestrial plants were used for dating. Analyses were performed at the Center for Accelerator Mass Spectrometry (CAMS) at Lawrence Livermore National Laboratory, and W.M. Keck Carbon Cycle Accelerator Mass Spectrometry at the University of California, Irvine (UCI). Samples analyzed at the UCI lab were pre-treated at the University of Pittsburgh following standard acid-base-acid procedure (Abbott and Stafford, 1996). All radiocarbon ages were calibrated using the CALIB online software program version 4.4.2 (Stuiver and Reimer, 1993; Stuiver et al., 1998).

Several tephra layers were present in the sediment sequence, although many were very thin and not readily identifiable with the unaided eye. Two tephras of significant thickness were sampled and sent to Washington State University for identification by electron microprobe. The first of these tephras was identified as the Mount Saint Helens (MSH) W tephra which has been dated at 1480 AD (470 BP) by dendrochronology (Mullineaux, 1986). The second identified tephra unit is from the Mazama climactic eruption that formed Crater Lake in Oregon ca. 6,730 ± 40 $^{14}C$ yr BP (7,585 cal yr BP) (Hallett et al., 1997).

An age-depth model was developed for the Castor Lake sediment core using linear interpolation between measured ages on an age-depth plot (Fig.2.2).

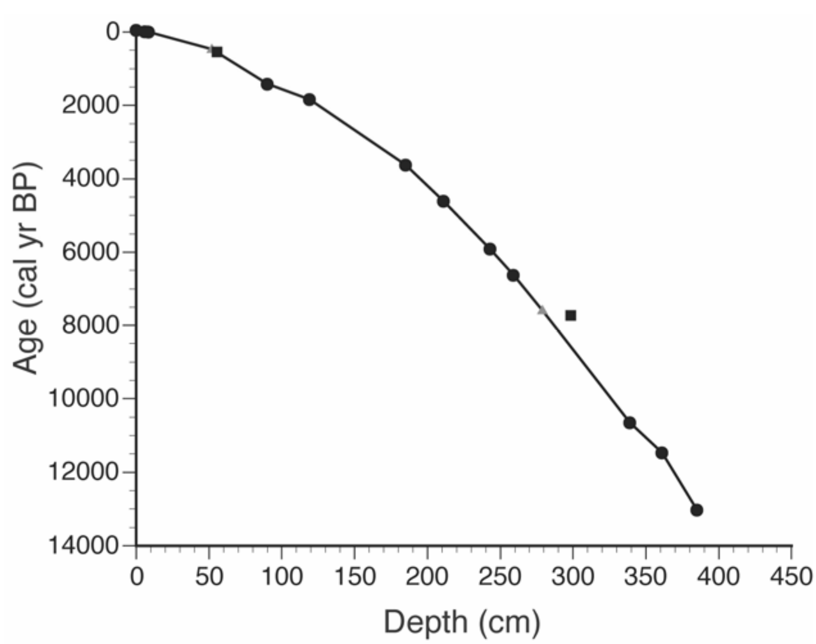


**Figure 2.2 Age vs. depth plot for Castor Lake radiocarbon and tephra dates. Radiocarbon ages used in age model shown as closed circles, radiocarbon ages shown as closed squares were not used in age model. Tephra ages shown as gray triangles.**

Tephra unit thicknesses were subtracted from the age-depth model due to their deposition as instantaneous events. Two radiocarbon dates were excluded from this model: 435 ± 40 $^{14}C$ yr BP, and 6,720 ± 80 $^{14}C$ yr BP (Table 2.1). The first of these dates were excluded due to the close proximity to the very well-dated MSH W tephra. The radiocarbon date does not contradict the age model, given the range of error in the radiocarbon measurement, but accuracy is improved by using only the tephra age. The second excluded age lies approximately 20 cm below the Mazama tephra, but was reported to be slightly younger. Given the very well established age of the Mazama tephra, this age must have been contaminated with a small amount of modern $^{14}C$ during sample preparation. All subsequent discussions of proxy data will be made with regard to age, not depth.

## 2.4. Results

The Castor Lake sediment sequence can be divided into six zones using lithology (Fig.2.3).

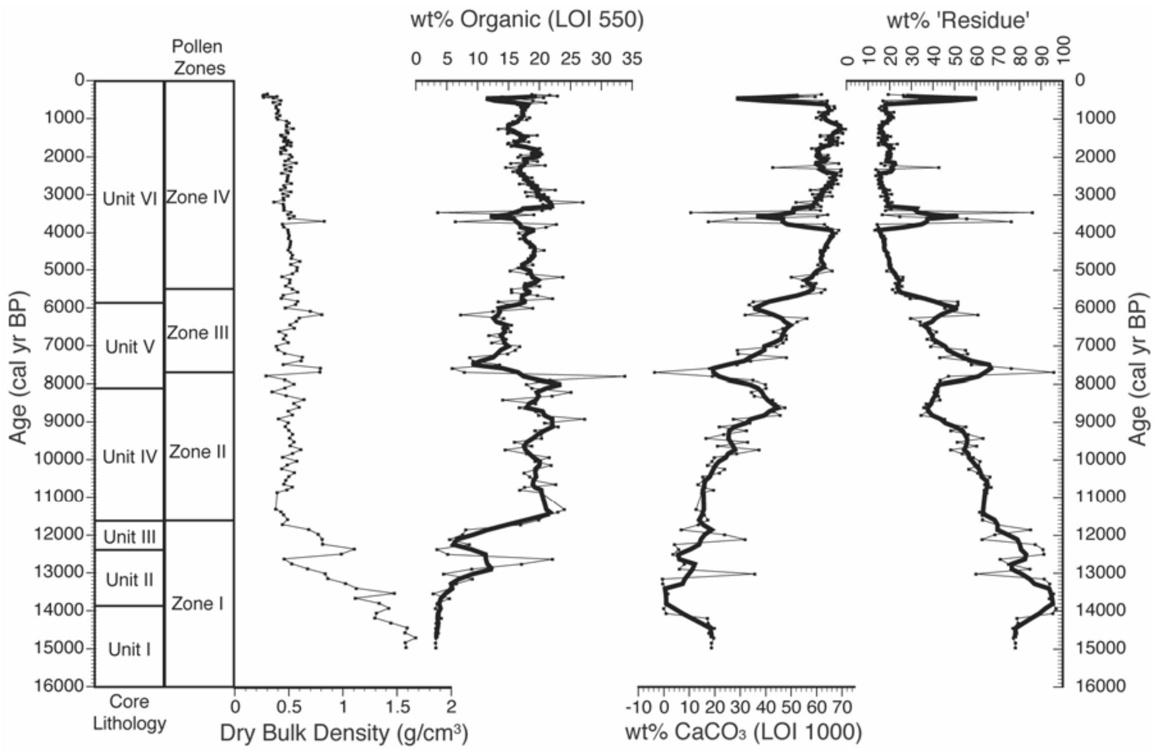


**Figure 2.3 Lithology, bulk density, and loss on ignition (LOI) data from Castor Lake plotted vs. age. Pollen data are from Mud Lake and Bonaparte Meadows (Mack et al., 1979). LOI data expressed as weight percent of total sediment mass. 'Residue' from LOI is composed of biogenic silica and clastic sediment. Thick line on LOI plots represents a 5-point running average of the data.**

Unit I (>~14,000 cal yr BP) is composed of massive and laminated grey silt sequences. Bulk densities reach the highest values in this unit, organic matter is almost entirely absent, and carbonate content is very low (Fig.2.3). Total organic carbon and total nitrogen values are nearly zero, and TOC/TN values show an increasing trend from approximately 11 to 15. Carbon isotope data display a very sharp decrease over this interval, beginning at ~-21‰ and dropping to ~-28‰. Nitrogen isotope data are largely incomplete for this period due to low total nitrogen concentration in the sediment (Fig.2.4). Smear slide analyses of several sample locations reveal an abundance of fine-grained angular quartz clasts. The concentration of non-quartz clasts is greatest near the bottom of Unit I.

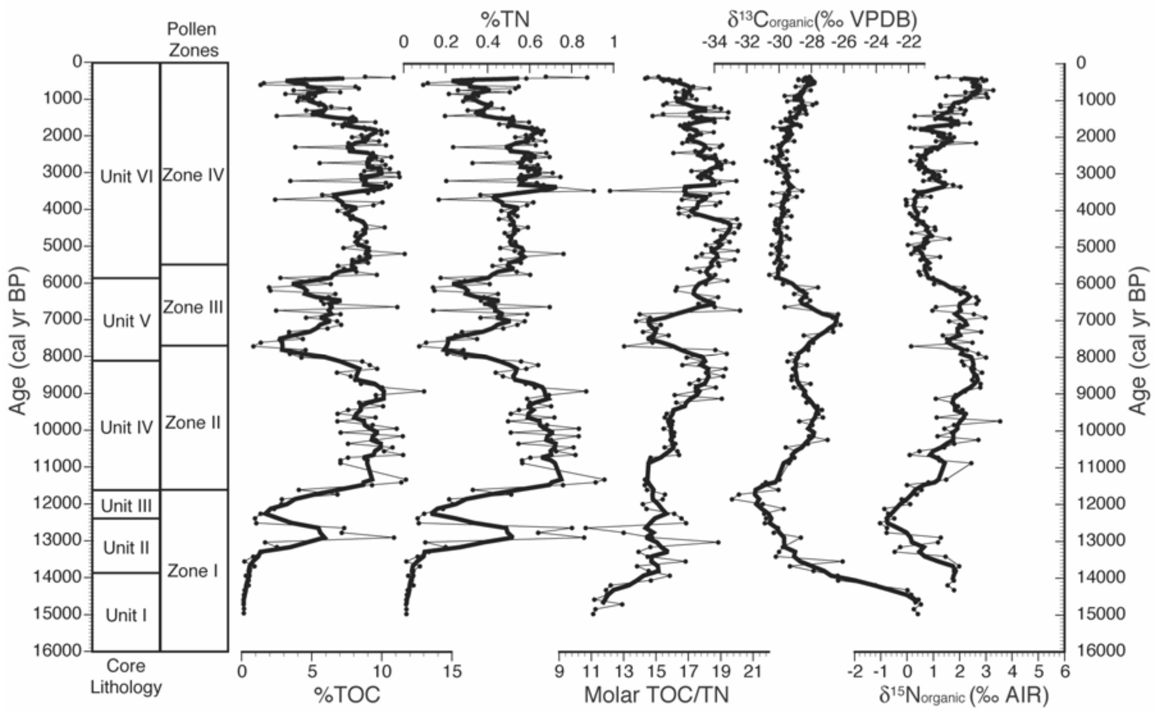


**Figure 2.4 Lithology, total organic carbon (TOC), total nitrogen (TN), TOC/TN ratio, and stable isotope data from Castor Lake organic sediment. Pollen zones are from Mud Lake and Bonaparte Meadows (Mack et al., 1979). TOC and TN values have been corrected for carbonate sediment removal, and are expressed as a percent of total dry sediment mass.**

Unit II (~14,000 – 12,500 cal yr BP) sediment color shifts from grey to dark brown, and some laminated structure is present. Three bands of coarse-grained material most likely represent the Glacier Peak B, M, G tephra sequence, ca. 13,160 cal yr BP (Foit et al., 1993), although the material was not sent for positive identification. Bulk density decreases substantially in this unit, and organic matter and carbonate content both increase (Fig.2.3). Total organic carbon and total nitrogen also increase over this unit before beginning to decline at approximately 12,700 cal yr BP, but TOC/TN values remain rather constant values of ~15. Carbon isotopic composition continues the sharp decline with decreasing age, although the rate of decrease diminishes slightly. Nitrogen isotope values decline from ~2‰ to the lowest values observed in the entire sediment record of ~-1‰ near the top of the sequence (Fig.2.4). Smear slides demonstrate abundant fine-grained angular quartz clasts, but some organic matter is also present.

Unit III (~12,500 – 11,500 cal yr BP) marks a return to sediment properties observed in Unit I with laminated and massive inorganic grey silt. Bulk density increases again to levels approaching those in Unit I. Organic matter decreases to almost zero, and carbonate content also shows a decline (Fig.2.3). The decline in TOC and TN values that began in Unit II reach minimum conditions in the middle of Unit III before beginning an increase to the top of the unit, but TOC/TN values remain relatively constant at ~15. Carbon isotopes continue to decline to the top if Unit III, where the most negative values of the entire sediment sequence are reached at ~-31‰. Nitrogen isotopic composition increases by approximately 2‰ over this unit (Fig.2.4). Smear slides from Unit III look much like Unit I slides, although the minor amount of non-quartz clasts seen in Unit I are mostly absent in Unit III.

Unit IV (~11,500 – 8,200 cal yr BP) consists of a sequence of finely laminated sediments that become lighter in color with decreasing age. Bulk density reaches values of approximately 0.5 $g/cm^3$ at the beginning of this unit, and little change is seen in this proxy after this period throughout the rest of the sediment sequence, excluding minor short-term fluctuations. Organic matter fluctuates around its highest average sustained value in the record of approximately 20% before declining sharply at the top of the unit (Fig.2.3). Carbonate content increases steadily from about 20% at the base of the unit to about 40% at the top before experiencing a sharp decline (Fig.2.3). Calculated residue abundance is greatest at the base of this unit and decreases with decreasing age. Total organic carbon and total nitrogen values remain relatively stable over this interval, with TOC fluctuating around 9% and TN fluctuating around 0.6%. Ratios of TOC/TN increase from ~15 to ~19. Carbon isotopic composition increases until about 9,500 cal yr BP, before beginning a gradual decline to the top of the unit. Nitrogen isotope values show only a steady increase (Fig.2.4). Smear slide analysis indicates an increasingly significant portion of the non-organic/non-carbonate (weight percent residue from LOI) is composed of diatom frustules towards the top of the unit.

Unit V (~8,200 – 5,900 cal yr BP) marks the only portion of the Holocene sediment sequence that does not contain sub-millimeter-scale laminations. Sediments in this unit have an identifiable horizontal orientation, but discrete lamina are not present, and abundant rip up clasts are observed. The Mazama tephra occurs near the beginning of this unit. Bulk density continues to fluctuate around the baseline values attained in Unit IV (Fig.2.3). Organic matter concentrations reach the lowest sustained values observed in the entire Holocene sequence of approximately 10-15%, and carbonate content increases after an initial decline (Fig.2.3). After a sharp initial decline, TOC and TN values increase and remain near 7% and 0.4%, respectively, for most of Unit V before declining again near the top of the unit. Ratios of TOC/TN decrease over this period from values of ~19 to ~14 and then rebound to ~19 near the end of Unit V. Increases in $\delta^{13}C_{organic}$ occur until the middle of the section, followed by a decline towards the end. Nitrogen isotopic composition remains relatively stable before a decline of ~1‰ towards the top (Fig.2.4). Smear slides reveal the most abundant concentrations of diatom frustules in the record, particularly over the interval in which the weight percent residue (clastic + biogenic silica) values show a strong increase (Fig.2.3).

Unit VI (~5,900 cal yr BP – ~400 cal yr BP) is comprised of finely laminated sediments up to the present sediment-water interface, and there is no evidence for major disturbance from the beginning of this unit to modern times. Bulk density continues to fluctuate around the baseline values (Fig.2.3). Average organic matter content increases slightly to the 15-20% range, and the gradual increase in carbonate content that began in the early Holocene stabilizes around 60% by the beginning of the unit (Fig.2.3). Total organic carbon and total nitrogen show no large-scale trends until ~3,500 cal yr BP, at which time both experience a slight decline. After this period, values re-stabilize at a slightly more elevated levels compared to the early part of the unit, before beginning a gradual decline to the top of the sediment sequence at ~2,000 cal yr BP. Ratios of TOC/TN follow the same general pattern as the TOC and TN data, although the decrease near 3,500 cal yr BP occurs slightly sooner, near 4,200 cal yr BP, and the decreasing trend at the top of the unit is more gradual than that of the TOC and TN data. Carbon isotopic changes in Unit VI are marked by minimal variability compared to the rest of the sediment core, although a slight increase can be seen at ~3,500 cal yr BP, followed by a gradual increase toward the top of the section. Nitrogen isotope composition is stable until ~3,500 cal yr BP, where values increase ~1‰, then decrease by almost the same amount, before beginning a gradual increase starting at ~2,500 cal yr BP and continuing to the top of the unit. Some larger-scale oscillations are seen between ~2,000 and ~1,500 cal yr BP though (Fig.2.4). Sediments in Unit VI are composed primarily of carbonaceous mud and biogenic silica, with a sparse clastic component.

## 2.5. Discussion

The low organic matter, carbonate, TOC and TN values, and high percentage of clastic sediment (Figs.2.3&2.4) indicate that the area surrounding Castor Lake was probably a periglacial environment with sparse tundra grasses on the landscape and low levels of aquatic productivity during the period represented by Unit I. Carbon isotopes probably recorded a gradual invasion of $C_3$ forests from the south, as they replaced the $C_4$ tundra grasses of the northwardly migrating periglacial landscape (Fig.2.4). The dominance of the $\delta^{13}C_{organic}$ signal by a $C_4$-$C_3$ vegetation transition precludes the use of these data as a measure of productivity, as any changes resulting from this would be overwhelmed by the vegetation change.

Climate conditions improve in Unit II (~14,000 – 12,500 cal yr BP), as increases in TOC, TON, and organic matter indicates the onset of significant aquatic productivity (Figs.2.3&2.4). Ratios of TOC/TN show that the bulk organic sediment is composed of a mix of aquatic and terrestrial organic matter, and although aquatic productivity is increasing, the change is not recorded in the $\delta^{13}C_{organic}$ record because the $C_4$-$C_3$ transition is still underway (Fig.2.4). The decrease in $\delta^{15}N_{organic}$ over this interval is difficult to interpret, but it is probably not tracking aquatic productivity, as the sedimentology, TOC, TN, and organic matter data indicate a productivity increase and $\delta^{15}N_{organic}$ would be expected to move towards higher values under these circumstances. The transition is probably driven by some change in the contribution of terrestrial organic matter in the dynamic post-glacial environment, but the specific change is unknown.

The onset of the Younger Dryas cold reversal is marked by the sediment transition observed in Unit III from ~12,500 – 11,500 cal yr BP. During this episode, conditions approximating those of Unit I returned, as low TOC, TN, and organic matter values are recorded, although rebound toward the top of the unit. Nitrogen isotopes also show a similar trend, suggesting that for this period changes may have been driven by decreases in productivity resulting in greater nitrogen availability and therefore increased fractionation (Fig.2.4). The lack of change in the TOC/TN ratio indicates that the relative contribution of terrestrial and aquatic matter probably remained constant. The lack of response by $\delta^{13}C$ may indicate that the vegetation change was still underway, although a component of the signal is likely the result of the productivity changes occurring in the lake. Interestingly, the geochemical data that record a Younger Dryas signal begin to respond around 12,700 cal yr BP, slightly before the lithological transition between Units II and III at 12,500 cal yr BP (Fig.2.4). This may indicate the more sensitive nature the geochemical proxies compared to the general sedimentology.

Following the Younger Dryas, a vegetation regime dominated by *Artemesia* (sagebrush), Gramineae (grass), and diploxylon pines (yellow pines) was established, implying a warmer climate than that experienced in Unit III, though not warmer than today (Mack et al., 1979). The high TOC, TN, and organic matter values reflect the establishment of a sustained and relatively stable vegetation regime, while the TOC/TN ratio suggests a generally increasing contribution of terrestrial organic matter to the lake water (Fig.2.4). This may have been the result of increasing catchment vegetation and topsoil accumulation, which would have in turn made a greater contribution to the organic matter budget from surface runoff in the catchment at the expense of mineral soil flux. The general decline seen in clastic sediment contribution is likely the result of this increase in soil and slope-stabilizing vegetation, which limited the amount of terrigenous mineral matter that could be delivered to the lake by surface runoff. The increase in carbonate content over this unit may also be attributed to this change, as more terrestrial organic matter and topsoil accumulation would have lead to increases in dissolved carbon dioxide in surface runoff and subsurface groundwater, which would in turn have resulted in increased carbonate dissolution in the catchment. Increased carbonate saturation of lake water inflow would then have led to increased carbonate precipitation in the lake due to differences in carbonate solubility between the inflow and the lake water. The general long-term increase in $\delta^{13}C_{organic}$ may be the result of increased productivity over this period, but the TOC/TN ratios do not suggest an increasing contribution of aquatic vegetation. Alternatively, the increase may be attributable to a greater contribution of $C_3$ plant material (~-27‰) compared to phytoplankton (~-30‰) (McKenzie, 1985). The $\delta^{15}N_{organic\ signal}$ is likely responding in a similar fashion. Visual correlation of $\delta^{13}C_{organic}$ and $\delta^{15}N_{organic}$ data is good for most of this unit, with the exception of the period between 9,500 cal yr BP and 8,000 cal yr BP (Fig.2.4). The reason for the lack of correlation is unclear but it could be the result of a decline in aquatic productivity, as the increase in TOC/TN ratio might be the result of a decreased contribution of aquatic material rather than an increasing contribution of that from the terrestrial environment.

The unique nature of the sedimentary sequence in Unit V alone is indicative of major change. The unlaminated sediments in this unit suggest frequent overturn of the water column, probably as a result of more effective wind mixing due to declining lake-level. Slightly after the onset of sediment Unit V, at ~7,585 cal yr BP (Hallett et al., 1997), the climactic eruption of Mount Mazama deposited a ~30 cm-thick tephra sequence in the lake sediment record. This event undoubtedly had a major influence on the landscape and lake system. Although the actual tephra sequence itself has been removed from the depth scale due to its instantaneous nature, LOI residue data and smear slide analyses show that tephra continued to be an important contributor to the sediment for a significant period as it was carried to the lake in the form of surface runoff from the catchment (Fig.2.3). Smear slides also reveal, however, a far greater abundance of diatom frustules in the period immediately following the deposition of the tephra. This apparent increase in aquatic productivity is probably the result of several factors, but the massive influx of silica from the tephra dissolution is likely to have been a contributor. Recent work in the Trans-Mexican Volcanic Belt have also identified similar diatom responses in lake sediment to tephra deposition, and attributed the change to massive silica loading as well (Telford et al., 2004). The increase in clastic material and diatom frustules in Castor Lake serves to dilute the signal seen in TOC, TN, and organic matter content (Figs.2.3&2.4). Despite this dilution, a relative high in each of these proxies at approximately 7,000 cal yr BP indicates a period of maximum lake productivity. This interpretation is also supported by the elevated $\delta^{13}C_{organic}$ values, as increased productivity and carbon limitation resulted in the decreased ability of photosynthetic organisms to fractionate carbon through preferential utilization of $^{12}C$ (Fig.2.4). The lack of significant $\delta^{15}N_{organic}$ response during this unit may be due to a variety of things, including the possibility that productivity periodically reached levels high enough to induce blooms of cyanobacteria capable of fixing atmospheric nitrogen (0‰), thus diluting the productivity signal (Gu et al., 1996). The decrease in TOC/TN values indicates a greater contribution of aquatic vegetation. This could be the result of increased productivity, or alternatively, decreased precipitation, which would in turn lead to decreased runoff and a subsequent decrease in the delivery of terrestrial organic material to the lake. Ultimately, productivity changes were probably driven by a warming and drying climate, which caused an increase in water temperatures, and a concentration of nutrients in the water as lake volume declined.

It is interesting to note that such profound sedimentological and geochemical changes as those seen in Unit V occur at nearly the same time as the deposition of the massive Mazama tephra sequence. Any reason for the correlation between these two events remains unclear at this time, but it is clear that the sedimentary changes did not occur in response to this event as these changes predate the tephra. It is unclear at this time whether the massive eruption served to exacerbate climate shifts that were already underway, or if shifts to warmer and drier conditions somehow influenced volcanic activity.

The onset of Unit VI marks the transition to the modern vegetation regime (Mack et al., 1979), and therefore facilitates more detailed interpretation of the geochemical data and extrapolation of modern conditions to the past. In the early part of Unit VI little change is apparent in TOC, TN, organic matter, $\delta^{13}C_{organic}$, or $\delta^{15}N_{organic}$, indicating relatively stable conditions following the rapid Unit V-VI transition (Figs.2.3&2.4). Ratios of TOC/TN increase slightly, possibly suggesting an increasing contribution of terrestrial organic matter. Mount Saint Helens erupted at approximately 3,790 cal yr BP and distributed the MSH Y tephra across much of the region surrounding Castor Lake (Mullineaux, 1986). Although this tephra was not present in a thick enough sequence to positively identify, the changes observed in the sediment record around this time seem to indicate at least some affect similar to those seen surrounding the Mazama tephra in Unit V. Total organic carbon, total nitrogen, organic matter, and carbonate content all decline, as LOI-residue increases (Figs.2.3&2.4), but in this case these changes might be interpreted as a dilution signal only. The associated increases in $\delta^{13}C_{organic}$ and $\delta^{15}N_{organic}$ seem to suggest otherwise, however, as they also indicate a slight increase in productivity and are not subject to the effects of dilution. Such a slight productivity increase may simply be a diatom productivity increase resulting from the large tephra-induced influx of silica to the lake. This hypothesis cannot be tested without quantitative measurements of biogenic silica, as qualitative analysis of smear slides will not resolve such minor changes. Interestingly, TOC/TN values begin to decline at ~4,200 cal yr BP, indicating a shift towards greater contribution of aquatic matter approximately 300 years before the eruption of Mount Saint Helens. Careful examination of the $\delta^{13}C_{organic}$ data reveals that the shift towards increasing values begins around this time as well, suggesting that productivity increases may have begun slightly before MSH Y. Full investigation of this transition requires more detailed sampling and analysis of this specific time period.

After ~3,500 cal yr BP, TOC, TN, TOC/TN, and organic matter indicate a return to the relatively stable conditions that prevailed prior to the MSH Y eruption (Figs.2.3&2.4). The gradual increase in $\delta^{13}C_{organic}$ and $\delta^{15}N_{organic}$ that begins here and continues to the top of the core at ~400 cal yr BP may indicate a gradual increase in productivity through time. However, it could also be a signal of small-scale changes in vegetation that were not substantial enough to be resolved by pollen records. The decreases in TOC, TN, TOC/TN, that occur from ~2,000 cal yr BP to the top of the core are also not easily interpreted (Fig.2.4). Stable isotope data indicate increasing productivity, and the TOC and TN data show the opposite signal. The discrepancy cannot be resolved with a dilution explanation, as all LOI data remain constant over this period (Fig.2.3). One possible, but unlikely explanation is that aquatic productivity decreased due to carbon limitations, which in turn lead to decreased fractionation by photosynthetic processes. However, carbon is almost never a limiting nutrient in aquatic systems. More probable is the possibility of minor vegetation changes that were not significant enough to appear in the pollen record, associated with climate changes that caused decreases in productivity.

## 2.6. Conclusion

The general sequence of environmental changes identified in this research correlate well with local pollen data from Mud Lake and Bonaparte meadows (Figs.2.1, 2.3&2.4) (Mack et al., 1979). Composite pollen records assembled from the greater Pacific Northwest also show the same large-scale trends as those outlined here (Whitlock, 1992), where following deglaciation, the Holocene is divided by a prolonged period of significantly warmer and drier conditions between approximately 8,000 and 6,000 cal yr BP. The strength with which the Castor Lake sediment record resolves the Younger Dryas cold reversal is another noteworthy discovery to come out of this research. Additional investigation of this period, with more radiocarbon dates, may be warranted in order to identify the exact timing of this event with as much precision as possible. Preliminary efforts outlined here indicate that the Younger Dryas began to affect local climate between 12,700 and 12,500 cal yr BP, and that conditions rebounded by approximately 11,500 cal yr BP.

The Castor Lake sediment record, like many other paleoenvironmental investigations in the Pacific Northwest, documents evidence for severe drought conditions in the middle Holocene (Bennett et al., 2001; Clague and Mathewes, 1989; Doerner and Carrara, 2001; Lowe et al., 1997; Whitlock, 1992). Although evidence for these conditions is strong, questions persist surrounding the influence of the Mazama tephra deposition on this portion of the sediment record. It is interesting to note the similar response in geochemical proxy data, though smaller in magnitude, to the less severe eruption of Mount Saint Helens at 3,790 cal yr BP. While such responses may be mere coincidence, the data are interesting. The fact that changes begin to occur before the tephra deposition in both cases would seem to indicate that climate changes preceded the eruptions in both cases. Tephra deposition may therefore have exacerbated changes that were already underway, or some other unknown forcing factor may possibly have been at work affecting both systems. This raises interesting questions requiring further research regarding the influence of tephra deposition on lake systems and sediment proxy data, as well as the influence of climate on volcanic processes.

# 3. LATE-QUATERNARY ENVIRONMENTAL HISTORY FROM STABLE ISOTOPES AND TRACE ELEMENT GEOCHEMISTRY AT CASTOR LAKE, NORTH-CENTRAL WASHINGTON STATE

Understanding moisture variability and other paleoenvironmental changes in Washington State is increasingly important given the current state of severe drought conditions in the western United States. A sediment core from Castor Lake in Washington State was used to investigate such events over the late Pleistocene and Holocene. The local topography and small size of Castor Lake create an environment where the lake responds to larger-scale regional change, and not localized effects that could mask the climate signal. This paleoenvironmental record thus provides a window into the relationship between ocean variability and terrestrial climate on millennial timescales. Loss on ignition (LOI), magnetic susceptibility, bulk density, x-ray diffraction (XRD), and scanning electron microscopy (SEM) were utilized to understand the character of the sediment and related paleoenvironmental conditions at the time of deposition. Trace element and stable isotope geochemistry of endogenic carbonates were also measured to document fluctuations in the hydrologic state of the lake. Mack et al. (1979) produced a local pollen record from Mud Lake and Bonaparte Meadows that is incorporated into interpretations of proxy data presented here. Chronological control is provided by eleven accelerator mass spectrometer (AMS) radiocarbon dates, and tephrochronology. The most prominent millennial-scale features identified through this research are a strong Younger Dryas signal occurring from approximately 12,500 to 11,500 cal yr BP, and a strong and prolonged period of conditions significantly drier than present between about 8,200 and 5,900 cal yr BP.

## 3.1. Introduction

Paleoenvironmental investigations in the Pacific Northwest are increasingly important given the rapid human population growth and the ever-increasing demand for dwindling water resources. Understanding the natural cycle of drought variability is crucial to current and future planning and legislation regarding the distribution of this limited resource. Increasing the range of long-term drought prediction through more thorough understanding of past variability will enable policy decisions to be made that rely on known or statistically probable water resource fluctuations rather than the rigid baseline averages that are used today.

The drought conditions of the past ~5 years in the western United States are among the worst in the past 80 years, and many major water reservoirs that service most of the largest metropolitan centers in the area are near catastrophic low levels (Piechota et al., 2004). Legislation governing the allocation of these resources was drafted in the middle of the 20$^{th}$ century, a period that appears to have been anomalously wet compared to the emerging paleoclimate record (Gedalof, 2002). The possibility that the current drought will continue for years into the future, or that the 'drought' based on historic standards really just marks a return to more average conditions of the past few thousand years, raises serious concern for the region. If either of these scenarios unfolds, policy makers will need every tool available to cope with the complex changes that will occur as human adaptation to a drier climate intersects with attempts to understand and accommodate anthropogenic increases in average global temperature.

The record of environmental change presented here from Castor Lake is a multi-proxy investigation aimed at understanding drought variability on millennial time-scales in order to attempt to address some of the issues described above. The analysis of physical sediment characteristics along with measurements of $\delta^{13}C$, $\delta^{18}O$, and trace element ratios from carbonate sediment makes possible the resolution of short-term climate changes that might normally be overlooked using other methods. Such multi-proxy investigation also improves the level of confidence with which conclusions from the data may be drawn. Although the current body of work on Castor Lake lacks the necessary sampling resolution to make interpretations about centennial and sub-centennial-scale changes, the success of this millennial scale investigation allows future studies to proceed with greater confidence.

In addition to the data presented here, a regional pollen record is used from Mud Lake approximately eight kilometers northwest of Castor Lake, and Bonaparte Meadows, approximately 46 km northeast of Mud Lake (Fig.3.1), to aid in the interpretation of paleoenvironmental conditions (Mack et al., 1979).

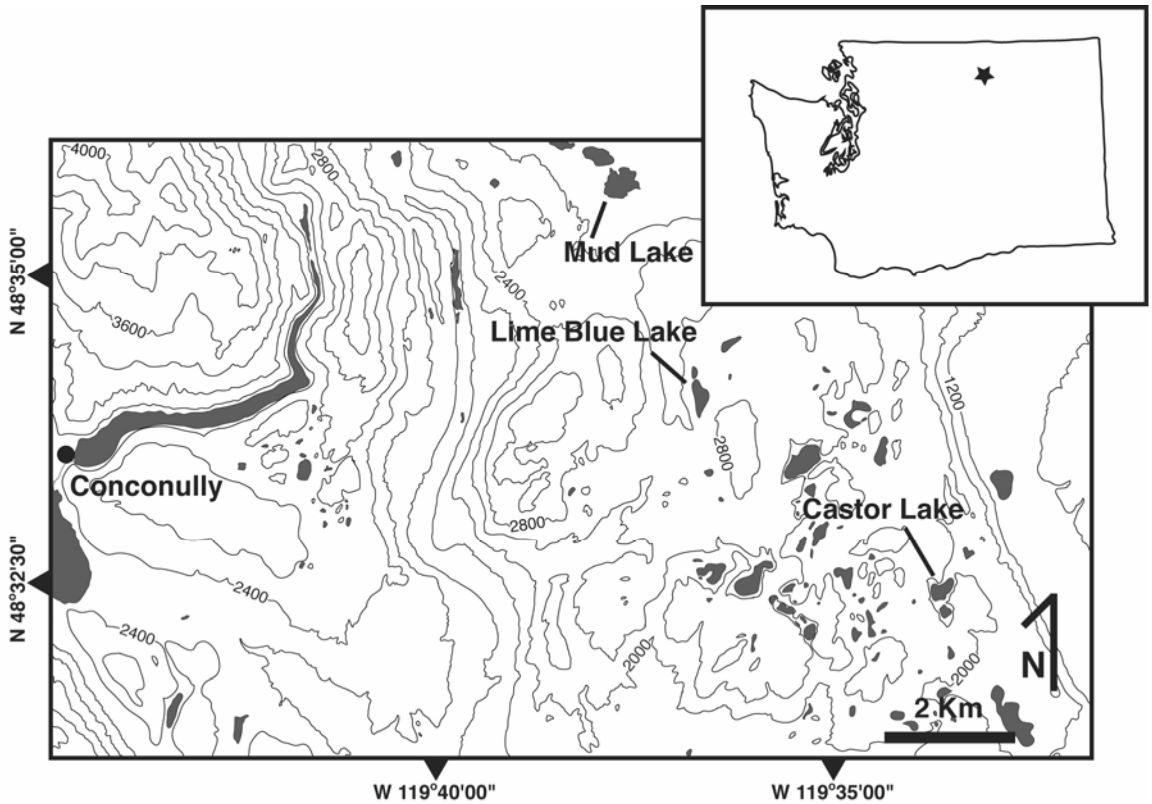


**Figure 3.1 Base map showing Castor Lake, Mud Lake, and Conconully, WA. Bonaparte Meadows is located approximately 46 km northeast of Mud Lake. Weather station data is from Conconully. Regional pollen data are from Mud Lake and Bonaparte Meadows (Mack et al., 1979). Contour interval = 400 feet.**

Based on palynological evidence, the sediment sequence from Mud Lake is divided into four zones that are mostly temporally correlative with the lithologic units described here in the Castor Lake sediment record. Minor age discrepancies between the two sites may be explained by limited age control in the Mud Lake study, given that the work was done before the advent of accelerator mass spectrometer (AMS) radiocarbon dating and therefore relied on bulk sediment radiocarbon dates.

Pollen Zone I is interpreted as colder and moister than today, and marks the initial introduction of vegetation into the area following ice retreat. Initial flora included haploxylon pine, *Artemisia* (sage brush), Cyperaceae (grass-like), Gramineae (grass), and *Shepherdia* *canadensis* (soapberry). Zone II climate was warmer than Zone I, though not as warm as today. The vegetation shift that occurs includes the invasion of a large componant of *Artemisia*, Gramineae, and some diploxylon pines that were probably confined to north facing slopes or foothills. Zone III climate is interpreted as warmer than present. The Mud Lake record also contains a ~1,000 year disconformity in the lower portions of the unit between ~7,000 and 8,000 cal yr BP. Pollen records show a return of *Artemisia* dominated vegetation and a low pine concentration. Zone IV pollen records are incomplete because sediments became too calcareous to use bulk sediment for radiocarbon dating. This un-dated portion of the record indicates a decrease in the importance of *Artemisia*, and its replacement by diploxylon pines and *Pseudotsuga menziesii* (Douglas fir) at the beginning of the zone as the modern vegetation established itself and the modern climate regime took hold.

## 3.2. Study Area

Castor Lake (48.54° N, 119.56° W) is located in Okanogan County in Washington State on a terrace margin of the Okanogan River. It is a kettle lake formed by the retreating Cordilleran Ice Sheet near the end of the Pleistocene (Fig.3.1). There is no active surface outflow and it is therefore effectively closed-basin. However, surface water level currently resides only a few meters below overflow level in the northeast portion of the lake, so it is possible that during wetter times the hydrology was open. The lake sits on a relative topographic high, making it unlikely that distal groundwater from deep aquifers make any significant contribution. Residence time was not calculated for Castor Lake, but estimates from lakes in similar environmental settings in central and northern Alberta range from 0.2 to 20 calendar years, depending on whether the hydrology is open, closed, or somewhere in between (Gibson et al., 2002). Given the nearly closed-basin hydrology of Castor Lake, residence time is probably closer to the upper limits of this range. Surface water pH was 8.5 in late July of 2003, and alkalinity measured 565 mg/L. Although the dissolved inorganic carbon (DIC) pool was not directly measured, it is likely that the majority of inorganic carbon is in the form of bicarbonate, given the high alkalinity and pH of the lake water. Lake surface elevation is about 591 m above sea level, maximum water depth is ~11.5 m, and lake surface area is ~0.07 $km^2$. The catchment is approximately 3.2 $km^2$, and is almost entirely undeveloped. Field-based bathymetric surveys reveal a single large, flat basin with gently sloping sides rising to the shores.

Based on sedimentological analyses and limited limnological investigations conducted in July of 2003 and February of 2004, Castor Lake appears to be a warm monomictic or meromictic water body. Winter temperature, conductivity, and pH profiles exhibit an unstratified water column indicating seasonal vertical mixing, but dissolved oxygen profiles show very low bottom-water concentrations suggesting permanent anoxia in the hypolimnion (Fig.3.2).

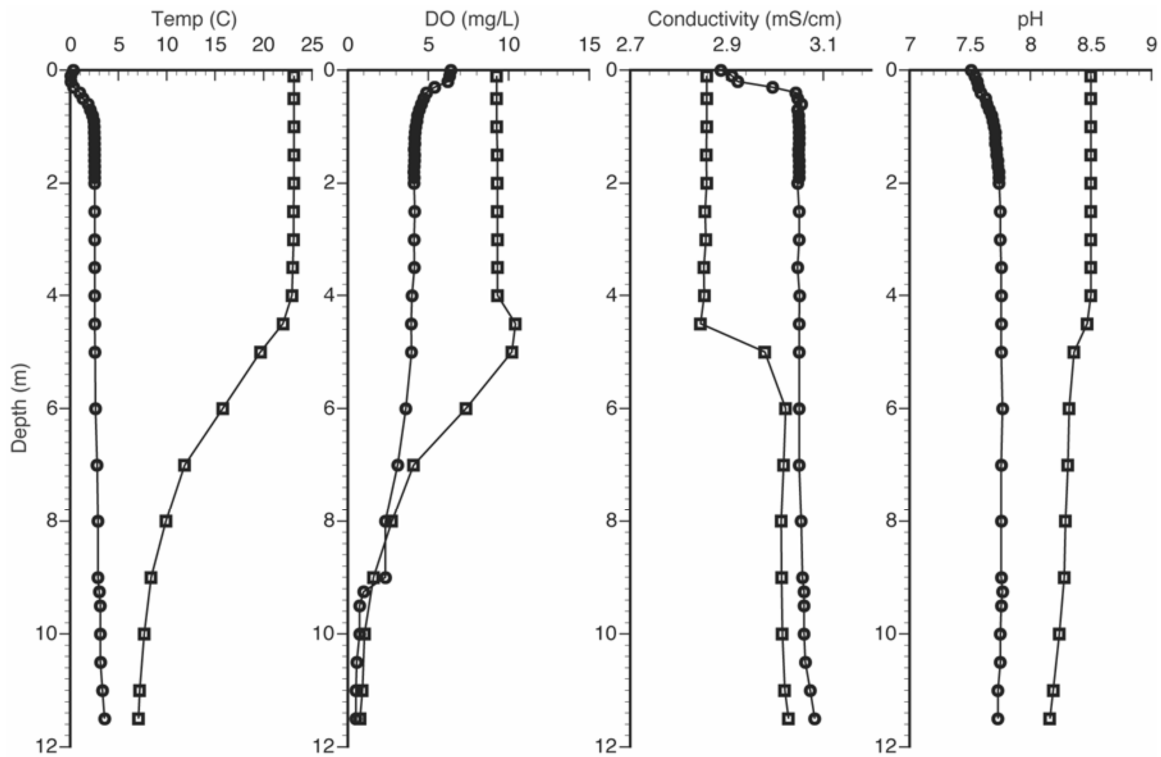


**Figure 3.2 Temperature, dissolved oxygen, conductivity, and pH data from Castor Lake water column in the primary coring location from summer 2003 (open squares) and winter 2004 (open circles).**

The cause of deepwater anoxia remains unclear, as only two profile measurements were made, but it may be a result of the topographic protection of the basin. The lake is surrounded by relatively steep, forested hill slopes, which might serve to limit the water surface wind speed, thus preventing complete seasonal overturn. Hypolimnetic anoxia is unlikely to be the result of lake-water eutrophy, as the lake is currently too alkaline to support fish populations and water column visibility extends up to several meters, indicating low to moderate productivity levels. Whatever the cause of the permanent anoxia, the effect has been to inhibit sediment bioturbation, and allow for the deposition of undisturbed, finely laminated sediments throughout the Holocene sedimentary sequence. These conditions of constant bottom water anoxia have an additional effect of severely inhibiting benthic ostracod growth.

The area surrounding Castor Lake was last glaciated during the Fraser advance in the late Pleistocene when the thickness of the Okanogan lobe of the Cordilleran ice sheet reached as much as 2000 m in this location (Waitt and Thorson, 1983). The distribution of tephra layers associated with the Glacier Peak ‘layer G’ eruption, ca. 13,160 cal yr BP (Foit et al., 1993), indicates that areas north of Chelan along the Columbia River were most likely totally ice free by approximately 13,000 cal yr BP (Waitt and Thorson, 1983). Areas to the north of this became free of ice after this date as ice retreated to progressively higher latitudes (Waitt and Thorson, 1983).

The climate of north-central Washington is dominated primarily by the Pacific westerlies (Bryson and Hare, 1974). These winds, strongest between 45° and 50°N, are controlled by the strength and position of the Aleutian low-pressure system, and the North Pacific high-pressure system. During winter months, the Aleutian low strengthens and shifts to more southern latitudes, delivering cool, moist air to the coast of Washington State. In summer, the Aleutian low weakens, moves northward, and is replaced by the North Pacific high. The presence of this pressure center during the summer months results in the delivery of more arid air masses to the state. Arctic air masses occasionally enter the region as well, but are generally replaced quickly by incoming Pacific westerlies (Bryson and Hare, 1974). Modern climate data, acquired from the National Climatic Data Center (NCDC), indicate that the closest weather station to Castor Lake is at Conconully, WA. Average annual adjusted precipitation values for the period from 1960 to 1990 were 277 mm/yr, average summer temperatures (Jun-Aug) were 18.0°C, and average winter temperatures (Dec-Feb) were ~3.6°C.

## 3.3. Methods

### 3.3.1. Sediment Recovery, Field Methods, and Sampling

In June 2003, a 4.5 m sediment core was collected from Castor Lake using a 5 cm diameter modified Livingstone-type piston core (Wright et al., 1984). Overlapping sections were taken to a depth of 3.78 m. Cores were transported to the University of Pittsburgh for analysis and stored at ~4°C in plastic wrap placed in polyvinyl chloride (PVC) tubes prior to sampling.

Cores were split, photographed, and described, and bulk density measurements were conducted at 2 cm intervals using a known volume of sediment and a drying oven to remove water. The same samples were subsequently used for loss on ignition (LOI) analysis at 500° and 1000°C in order to determine approximate weight percent of organic matter, and carbonate, respectively (Dean, 1974). Loss on ignition sample residue was comprised of a combination of terrigenous clastic sediment and biogenic silica. Smear slides were made from samples taken over the length of the sediment sequence.

### 3.3.2. Chronology

Sediment age-depth relations were derived from eleven accelerator mass spectrometry radiocarbon dates (Table3.1), and two tephra layers of known age.

**Table 3.1 Radiocarbon dates from Castor Lake.**

| Core | Drive Depth (cm) | $^{14}C$ age ($^{14}C$ yr B.P.) with error | Median calibrated age (cal yr B.P.) | 2-sigma calibrated age range (cal yr B.P.) | Material | Lab accession number |
|---|---|---|---|---|---|---|
| A-03 D-1 | 23 | 435 ± 40 | 492 | 328-540 | Grass | CAMS# 104906 |
| A-03 D-1 | 75 | 1530 ± 35 | 1416 | 1334-1518 | Charcoal | CAMS# 104907 |
| B-03 D-2 | 9 | 1890 ± 35 | 1833 | 1725-1919 | Pine Needle | CAMS# 104908 |
| B-03 D-2 | 75 | 3385 ± 35 | 3622 | 3479-3715 | Charcoal | CAMS# 104910 |
| B-03 D-3 | 8 | 4095 ± 45 | 4608 | 4442-4816 | Seed | UCI# 7527 |
| B-03 D-3 | 36 | 5160 ± 100 | 5911 | 5661-6173 | Charcoal | CAMS# 104909 |
| B-03 D-3 | 56 | 5815 ± 25 | 6628 | 6502-6721 | Seed | UCI# 7488 |
| B-03 D-4 | 52 | 6720 ± 80 | 7582 | 7432-7682 | Seed | CAMS# 104911 |
| B-03 D4 | 88 | 9425 ± 30 | 10648 | 10557-11035 | Seed | UCI# 7590 |
| B-03 D-5 | 16 | 10025 ± 35 | 11465 | 11259-11908 | Seed | UCI# 7491 |
| B-03 D-5 | 40 | 11020 ± 35 | 13022 | 12675-13169 | Seed | UCI# 7493 |

Radiocarbon ages were generated from charcoal or identifiable macrofossils, including seeds from the *cyperaceae* sedge family in many cases. Possible hard-water effects were avoided by ensuring that only identifiable remains from terrestrial plants were used for dating. Analyses were completed at the Center for Accelerator Mass Spectrometry (CAMS) at Lawrence Livermore National Laboratory, and the W.M. Keck Carbon Cycle Accelerator Mass Spectrometry lab at the University of California, Irvine (UCI). Samples that were sent to the UCI lab were pre-treated at the University of Pittsburgh following standard acid-base-acid procedure (Abbott and Stafford, 1996). All radiocarbon ages were calibrated using the CALIB online software program version 4.4.2 (Stuiver and Reimer, 1993; Stuiver et al., 1998). Subsequent discussions of proxy data will be made with regard to age, not depth.

Several tephra layers were present in the sediment sequence, although many were thin (<1 mm) and not readily identifiable with the unaided eye. Two tephras of significant thickness were sampled and sent to Washington State University for identification by electron microprobe. The first of these tephras was identified as the Mount Saint Helens (MSH) W tephra, which has been dated at 1480 AD (470 BP) by dendrochronology (Mullineaux, 1986). The second identified tephra unit is from the Mazama climactic eruption that formed Crater Lake in Oregon. The most recently published age determined by radiocarbon dating places this tephra deposition at 6,730 ± 40 $^{14}C$ yr BP (7,585 cal yr BP) (Hallett et al., 1997). Age determinations from annual layer counting in the GISP2 ice core place the age at 7,627 ± 150 yr BP (Zdanowicz et al., 1999). In either case, the ages are in close enough agreement that substituting one for the other in the development of an age-depth model for the Castor Lake record results in no significant change to the overall chronology. We have chosen to use the radiocarbon-determined age of 7,585 cal yr BP in this study.

The age-depth model developed for Castor Lake was constructed using linear interpolation between measured ages on an age-depth plot (Fig.3.3).

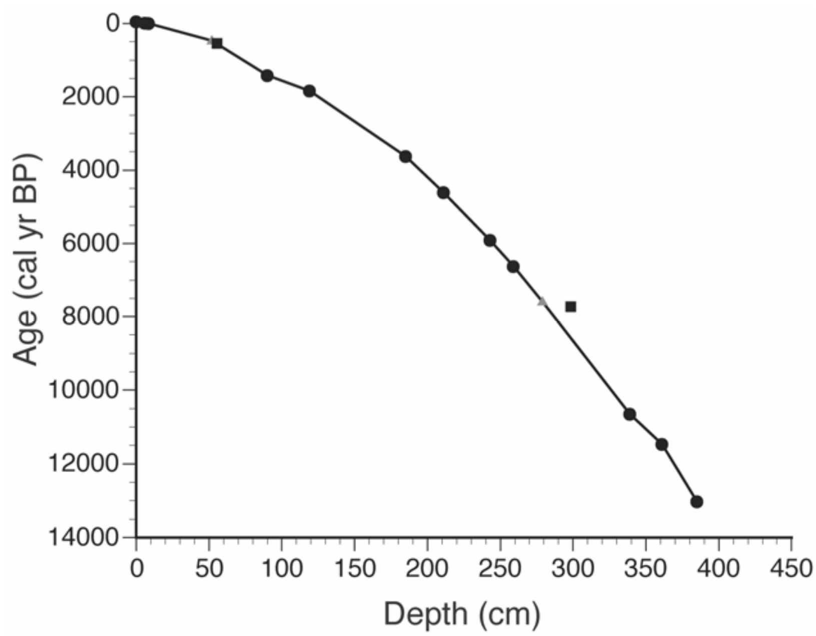


**Figure 3.3 Age vs. depth plot for Castor Lake radiocarbon and tephra dates. Radiocarbon ages used in age model shown as closed circles, radiocarbon ages shown as closed squares were not used in age model. Tephra ages shown as gray triangles.**

Tephra unit thicknesses were subtracted from the age-depth model due to their deposition as instantaneous events. Two radiocarbon dates were excluded from this model as well: 435 ± 40 $^{14}$C yr BP, and 6,720 ± 80 $^{14}$C yr BP (Table 3.1). The first of these dates were excluded due to the close proximity to the very well dated MSH W tephra. The radiocarbon date does not contradict the age model, given the range of error in the radiocarbon measurement, but accuracy is improved by using only the tephra age. The second excluded age lies approximately 20 cm below the Mazama tephra, but was reported to be slightly younger. Given the very well established age of the Mazama tephra, this age must have been contaminated with a small amount of modern $^{14}$C.

### 3.3.3. Carbonate Sample Preparation

Endogenic carbonate refers to those carbonate mineral grains that precipitated directly from the lake water in the pelagic region or epilimnion. Sediment samples used for x-ray diffraction (XRD), scanning electron microscopy (SEM), stable isotope, and trace element analyses were all treated initially to isolate this endogenic carbonate component of the sediment. These samples were taken from the core at the same 2 cm intervals that bulk density and LOI samples were collected from. Raw sediments were disaggregated with a ~7% $H_2O_2$ solution. This process also served to oxidize and remove some of the organic portion of the sediment. Samples were sieved at 63μm to remove biogenic carbonate shell material. The portion of sediment smaller than 63μm was recovered, bleached, and freeze-dried. Dried samples were then gently homogonized using an agate mortar and pestle.

### 3.3.4. XRD & SEM

X-ray diffraction (XRD) analyses were performed at the University of Pittsburgh on seventeen samples at random intervals throughout the core using a Phillips X-pert Powder Diffractometer over a 2θ range of 10° to 80°. In all cases, only a small amount of sample was used so the powder was spread evenly on an amorphous silicon wafer using ethyl alcohol and allowed to dry. Comparison of this method with the traditional back-fill sample preparation showed no difference in the resultant mineralogical identification. Treated samples were also analyzed in a scanning electron microscope (SEM) at the Matco Associates Incorporated office in Pittsburgh, PA.

### 3.3.5. Stable Isotopes

Treated carbonate sample aliquots were sent to the University of Florida, Gainesville for stable isotope measurements of $\delta^{13}C$ and $\delta^{18}O$. Analyses were performed using a Finnigan-MAT 252 mass spectrometer with an online automated carbonate preparation system (Kiel II). Results are expressed relative to a standard in typical per-mille notation:

$$\delta_x^E = (R_{sample} / R_{stnd} - 1) * 1000$$

Where $\delta_x^E$ is the heavy isotope of element E, and $R_{sample}$is the ratio of the heavy isotope to the light isotope of the sample, and $R_{stnd}$ is the ratio of the heavy isotope to the light isotope of the standard. Analytical precision of measurements was reported to be within 0.04‰ for $\delta^{13}C$ and 0.08‰ for $\delta^{18}O$.

### 3.3.6. Trace Elements

Additional carbonate sample aliquots were weighed dry, leached with ammonium acetate ($NH_4Ac$, pH = 8.11) and rinsed twice to remove any possible contaminant coatings or exchangeable materials on the carbonate grains. Leach residues were dried and weighed, leached twice with 8% acetic acid (HOAc), and rinsed twice. HOAc leachate and rinses were saved, and aliquots were analyzed for Ca, Mg, K, Na, Sr, Ba, Mn, Fe, and Zn by inductively coupled plasma – atomic emission spectrometry (ICP-AES). Trace element analyses were performed with quality assurance/quality control adherence to Environmental Protection Agency (EPA) protocol SW-846 (EPA, 1996).

## 3.4. Results

### 3.4.1. Lithology, Bulk Density & LOI

Six zones were identified based on the lithology of the Castor Lake sediment core (Fig.3.4).

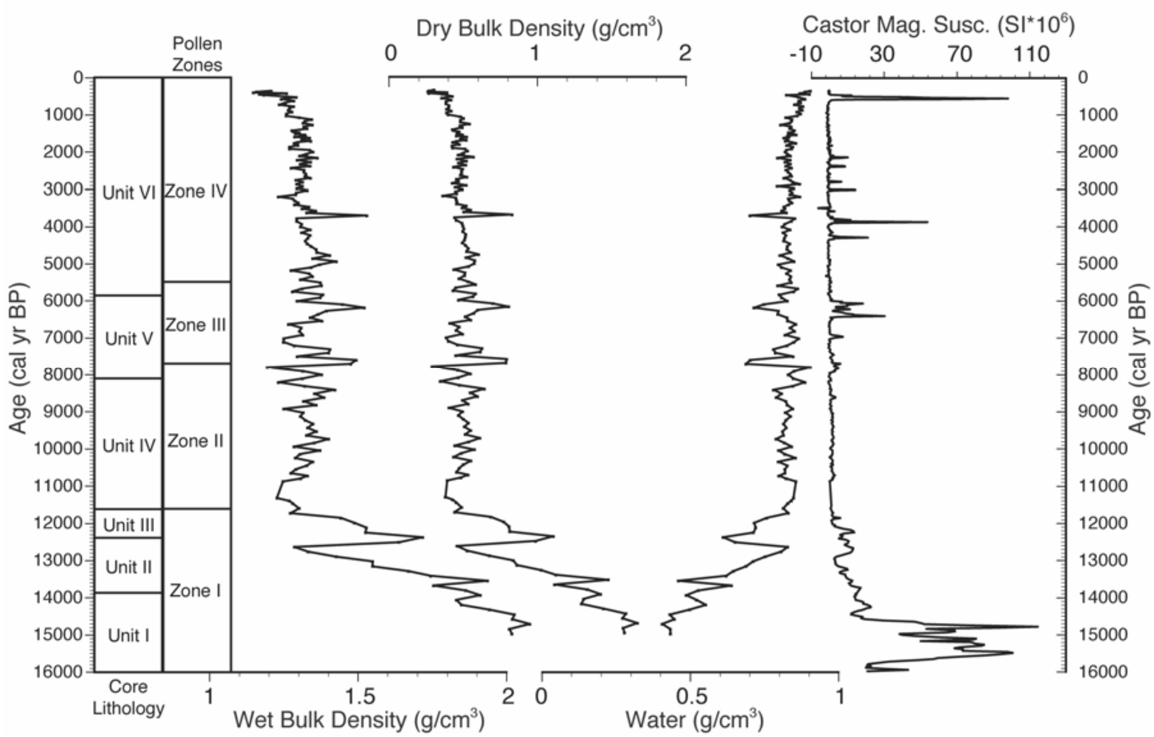


**Figure 3.4 Lithological, bulk density, and magnetic susceptibility data from Castor Lake. Pollen data are from Mud Lake and Bonaparte Meadows (Mack et al., 1979).**

Unit I (>~14,000 cal yr BP) is composed of massive, and laminated grey silt sequences. Bulk densities reach the highest values seen in the sediment core in this unit (dry bulk density >1.5 g/cm$^3$), and magnetic susceptibility is consistently high over this interval (Fig.3.4). Organic matter is almost entirely absent, and carbonate content is also very low, between 0 and 20% (Fig.3.5).

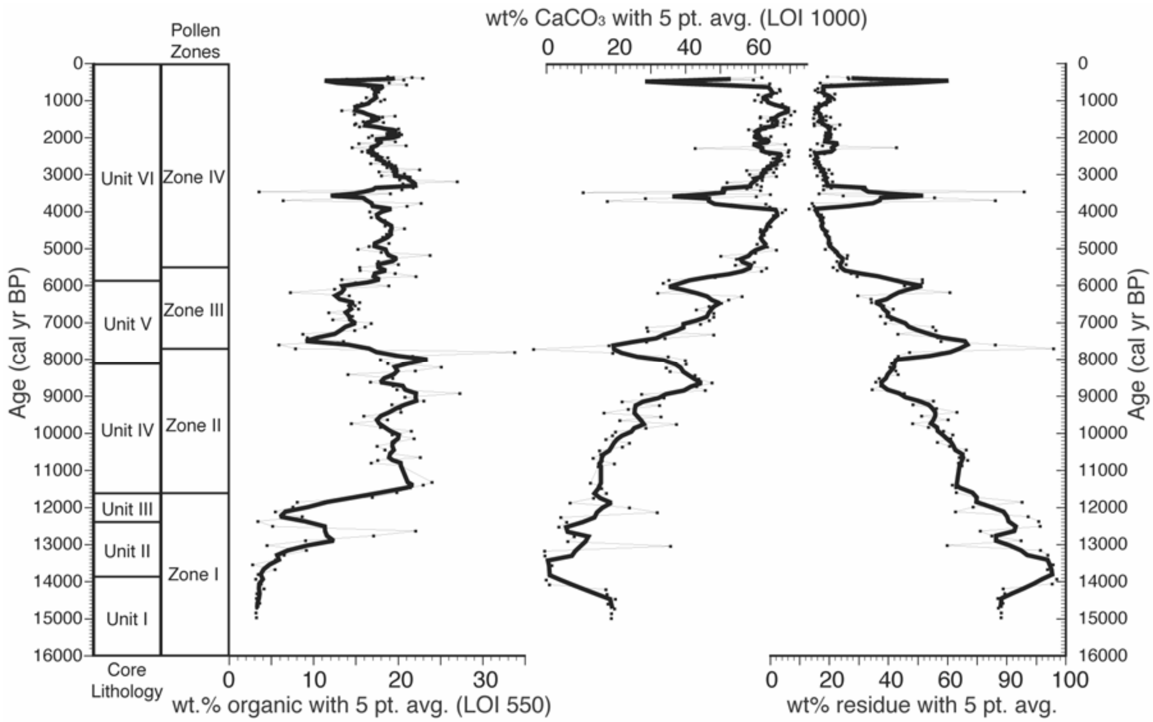


**Figure 3.5 Lithological, and loss on ignition (LOI) data from Castor Lake. LOI data expressed as a weight percent of total sediment mass. LOI 'residue' is composed of biogenic silica and clastic sediment. Thick line on LOI plots represents a 5-point running average of the data. Pollen data are from Mud Lake and Bonaparte Meadows (Mack et al., 1979).**

Qualitative smear slide analyses of several sample locations reveal an abundance of fine-grained angular quartz clasts. The concentration of non-quartz clasts is greatest near the bottom of Unit I.

Unit II (~14,000 – 12,500 cal yr BP) is characterized by sediment color shifts from grey to dark brown, and laminated structures are present. Three bands of coarse-grained material with high magnetic susceptibility most likely represent the Glacier Peak B, M, G tephra sequence, ca. 13,160 cal yr BP (Foit et al., 1993), although the material was not sent for positive identification. Dry bulk density decreases substantially in this unit from ~1.5 to 0.5 g/cm$^3$ (Fig.3.4), and organic matter and carbonate content both increase from ~3 to 20%, and ~3 to 10%, respectively (fig.3.5). Smear slides indicate abundant fine-grained angular quartz clasts similar to Unit I, but unlike Unit I, some organic matter is also present.

In Unit III (~12,500 – 11,500 cal yr BP), sediment properties become similar to those observed in Unit I, with laminated and massive inorganic grey silt. Bulk density increases again to levels approaching those observed in Unit I, and magnetic susceptibility also increases, but to a lesser degree (Fig.3.4). Organic matter decreases to almost zero, and carbonate content also shows a decline of a few percent (Fig.3.5). Smear slides from Unit III look much like Unit I slides, although the minor amount of non-quartz clasts seen in Unit I are mostly absent in Unit III.

Unit IV (~11,500 – 8,200 cal yr BP) consists of a sequence of finely laminated sediments that become lighter in color near the top of the unit. Bulk density and magnetic susceptibility reach values of approximately 0.5 g/cm$^3$ and 0 SI*10$^{-6}$, respectively, at the beginning of this unit (Fig.3.4). Little change is seen in either of these two proxies after this period throughout the rest of the sediment sequence, excluding minor short-term fluctuations. Organic matter content varies around its highest average sustained value in the record of approximately 20% before declining sharply at the transition to Unit V (Fig.3.5). Carbonate content increases steadily from about 20% at the base of the unit to about 40% at the top before experiencing a sharp decline near the transition to Unit V (Fig.3.5). Clastic grain abundance in this unit is greatest at the bottom, near 70%, and decreases to ~30% with decreasing age. Smear slide analysis indicates that an increasingly significant portion of the LOI residue is composed of diatom frustules towards the top of the unit.

Unit V (~8,200 – 5,900 cal yr BP) is the only portion of the Holocene sediment sequence that does not contain sub-millimeter-scale laminations. Sediments in this unit have an identifiable horizontal orientation, but discrete laminae are not present, and abundant rip up clasts are observed. The Mazama tephra occurs near the beginning of this unit. Bulk density and magnetic susceptibility continue to fluctuate around the baseline values reached in Unit IV (Fig.3.4). Organic matter mass fractions reach the lowest sustained values over the entire Holocene sequence of approximately 10-15%, and carbonate content initially declines, then increases to peak values of ~50% before declining again toward the top of the unit (Fig.3.5). Smear slides reveal the most abundant concentrations of diatom frustules in the record; particularly over the interval in which the LOI residue (clastic + biogenic silica) values show a strong increase (Fig.3.5).

Unit VI (~5,900 cal yr BP – present) is made up of finely laminated sediments up to the top of the sediment core, and there is no evidence for major disturbance during the period represented by this sediment package. Bulk density and magnetic susceptibility continue to fluctuate around the values obtained in Unit IV (Fig.3.4). Average organic matter content increases slightly to the 15-20% range, and the gradual increase in carbonate content that began in the early Holocene stabilizes around 60% by the beginning of the unit (Fig.3.5). Smear slides indicate that sediments are composed primarily of carbonaceous mud and diatom frustules, with a sparse clastic component.

### 3.4.2. XRD

X-ray diffraction (XRD) analysis of treated carbonate samples provides strong evidence that the only carbonate mineral phase present in significant amount in Castor Lake sediment is aragonite (Fig.3.6).

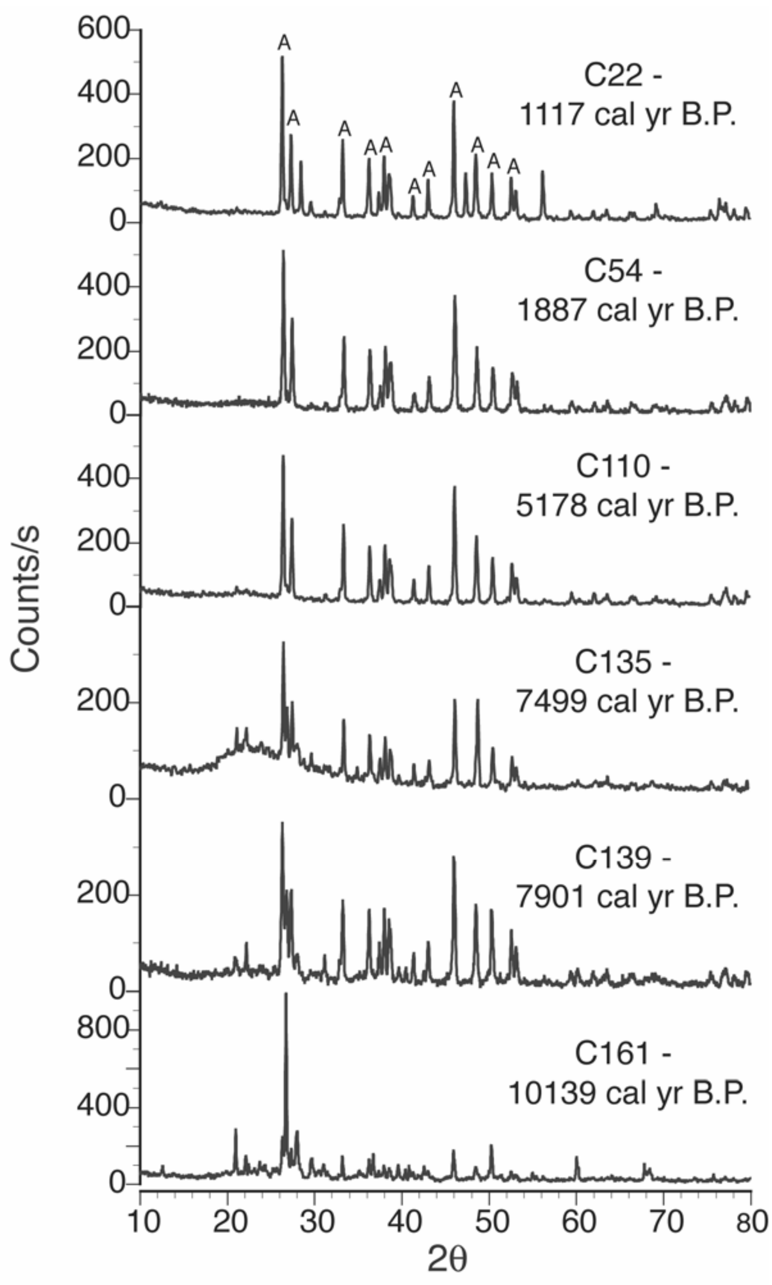


**Figure 3.6 X-ray diffraction (XRD) data from Castor Lake carbonate sediment. Expected location of aragonite peaks indicated by multiple letter 'A' markings on top plot.**

In most of the sediment sequence, there are no additional peaks present other than those attributable to aragonite. Near the base of the core, however, where terrigenous clastic sediment becomes a significant component, additional peaks begin to appear in the x-ray scans. In no cases, however, can these additional peaks be attributed to another carbonate mineral phase such as calcite (the probable carbonate phase from terrigenous sources), the effects of which might complicate trace element or stable isotope investigations. These additional peaks are instead attributed to the presence of quartz, albite, and other aluminosilicate minerals, a finding that is supported by smear slide analysis. An additional observation comes from scans made on samples from lithological Unit V (sample C135) (Fig.3.6), which contain a low, broad increase over the interval from approximately 10 to 20 $2\theta$ indicative of high concentrations amorphous opal, a characteristic feature of diatoms. This result is also supported by smear slide analysis.

### 3.4.3. SEM

Images collected at 10,000 times magnification using SEM show individual aragonite grains one to four microns in length (Fig.3.7).

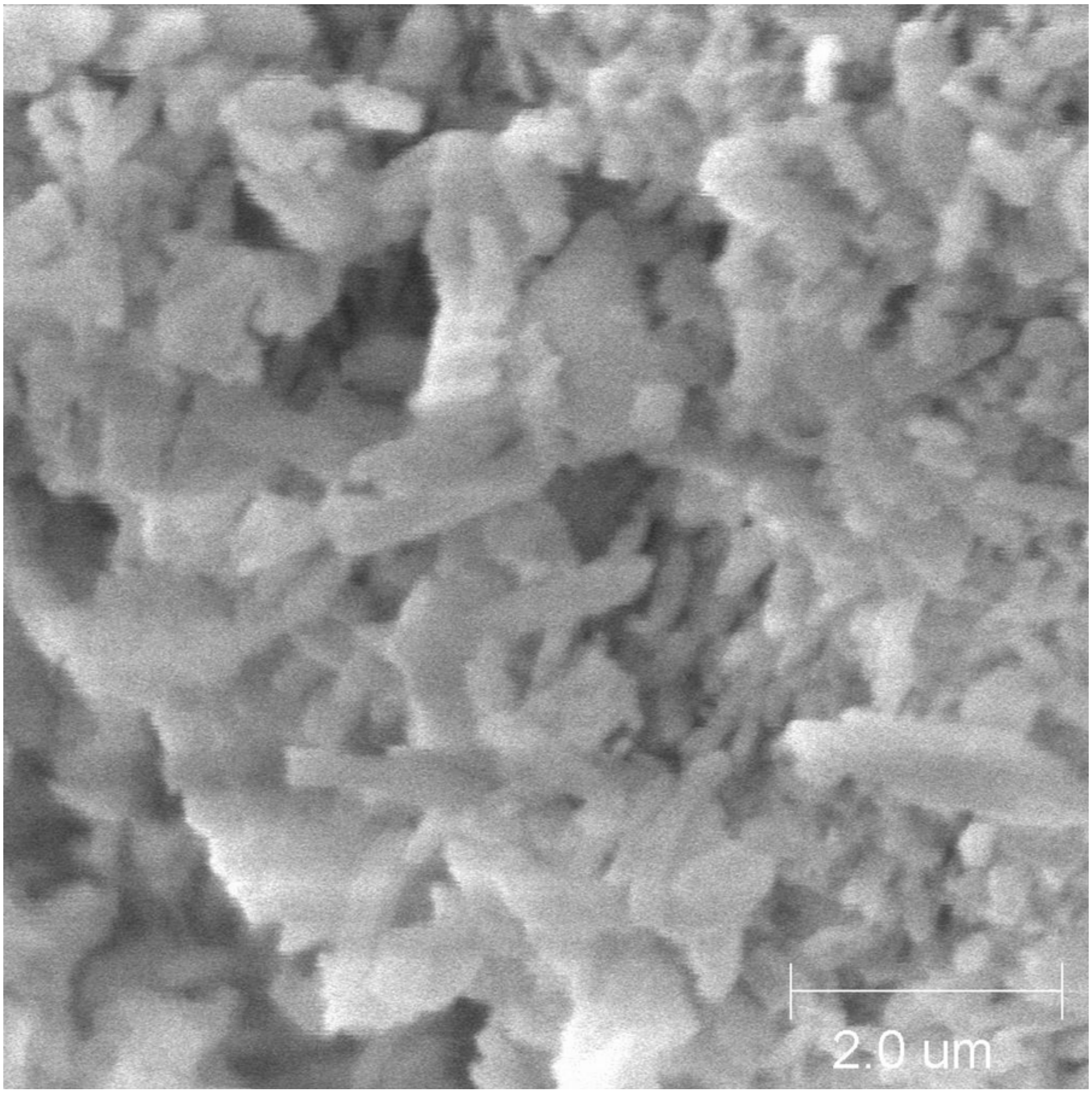


**Figure 3.7 Example scanning electron microscopy (SEM) image of Castor Lake treated carbonate sediment samples. Rice-shaped grains are indicative of endogenic aragonite. Lack of large rounded grains suggests that no terrigenous carbonate is present. Biogenic carbonate is also absent in all samples.**

The size and elongated shape of the observed crystals offers another line of support for the notion that the treated sediment samples are overwhelmingly composed of endogenic aragonite, and very little if any, terrigenous carbonate, biogenic carbonate, or other materials that might contaminate or confound any trace element or stable isotope analyses. Terrigenous carbonate, if it were present in the core, would be expected to have a more rounded shape than the aragonite grains, and show other signs of surface transport to the lake. Biogenic carbonate grain shapes vary based on the organism, but all are easily discernable from that of endogenic aragonite on the basis of shape and size.

#### 3.4.4. Stable Isotopes

Stable isotope $\delta^{18}O_{aragonite}$ and $\delta^{13}C_{aragonite}$ data measured over the entire sediment sequence from Castor Lake (late Pleistocene and Holocene) show a generally covariant relationship at millennial time-scales (Fig.3.8), indicative of long-term closed-basin hydrology (Li and Ku, 1997; Talbot, 1990).

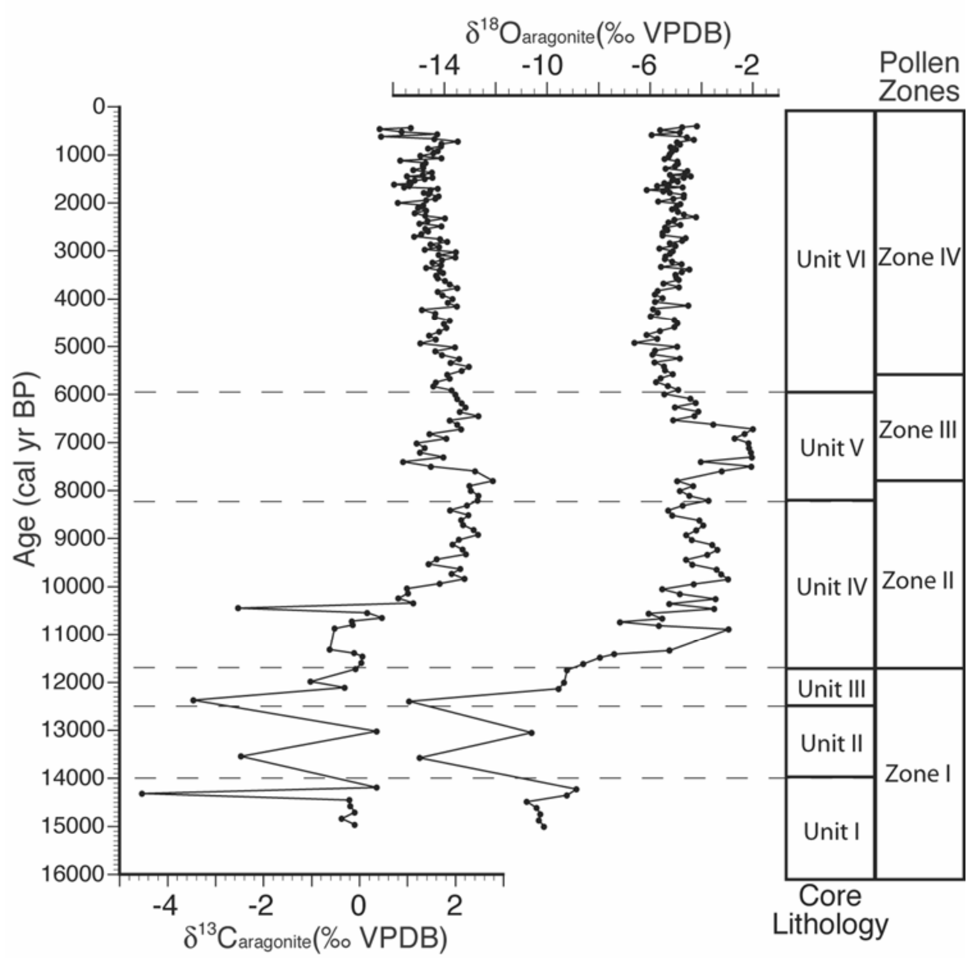


**Figure 3.8 Stable isotope data from Castor Lake carbonate sediment shown with core lithology and regional pollen data (Mack et al., 1979).**

Even though the lake is currently only a few meters below overflow, and would have had a surface outflow at certain periods in its history if conditions had become wetter, the isotope data do not support the conclusion that lake-level reached overflow height for any significant period in the Holocene. Isotope interpretation is based only on the Holocene sequence because of the limited late Pleistocene data and the large shift in values that occurs over the glacial to interglacial transition (Fig.3.8).

In the early Holocene at approximately 10,000 cal yr BP, $\delta^{13}C_{aragonite}$ increases abruptly and substantially from ~0‰ to ~2.5‰. Carbon isotope values show a slight but steady increase into the lower portions of Unit V, with little fluctuation around the average. At approximately 7,800 cal yr BP, $\delta^{13}C_{aragonite}$ declines abruptly by ~1.5‰, but rebounds by about 6,500 cal yr BP. After this change, and to the top of the sediment record, $\delta^{13}C_{aragonite}$ trends slightly towards more negative values, with averages decreasing about 1‰ over this time span. Variability is also greater during the late Holocene sequence represented by lithological Unit VI than during other periods of the record.

Although millennial-scale trends in $\delta^{18}O_{aragonite}$ correlate well with trends in $\delta^{13}C_{aragonite}$ for the majority of the record, this pattern reverses in Unit V, and the records are anticorrelated for this period (Fig.3.8). Significant discrepancies also appear when the records are examined at sub-millennial timescales. Oxygen and carbon isotopic compositions increase across the Pleistocene-Holocene transition. Variation in $\delta^{18}O_{aragonite}$ around the average is greatest in the early Holocene. At around 7,800 cal yr BP, $\delta^{18}O_{aragonite}$ values increase sharply by almost 3‰, but decrease again to around 6‰ at about 6,500 cal yr BP. There is a very slight increasing trend in $\delta^{18}O_{aragonite}$ in lithologic Unit VI of no more than 0.5‰, but most variation is small and occurs at centennial time-scales.

### 3.4.5. Trace Elements

Although a large number of cation concentrations were measured for aragonite samples from Castor Lake (Appendix B), only Ca, Mg, Sr, and Ba will be discussed here given their more important role in lacustrine carbonates (Haskell et al., 1996; Valero-Garcés et al., 1997). Trace element substitution rates for calcium in the carbonate crystal lattice vary by element, and are different between aragonite and calcite due to the different shape of the two minerals. Magnesium, for example, readily substitutes into the calcite lattice, but is much less likely to be accommodated into the aragonite lattice. Calcium, strontium, and barium were measured in

Castor Lake carbonate samples because these elements tend to be strongly partitioned into aragonite (Lippmann, 1973). Magnesium concentrations were included in the discussion because of the highly important role that this element plays in other carbonate mineral systems such as calcite and dolomite, and the important regulatory role that lake water Mg/Ca serve in determining carbonate mineralogy (Müller et al., 1972).

Due to the low sampling resolution of cation concentrations relative to stable isotope measurements, only millennial scale relationships between trace element data and isotope data may be explored at this time. Trace element data were converted to molar ratios in order to understand the relative changes in cation concentrations, which can be more meaningful than measures of absolute concentration (Fig.3.9).

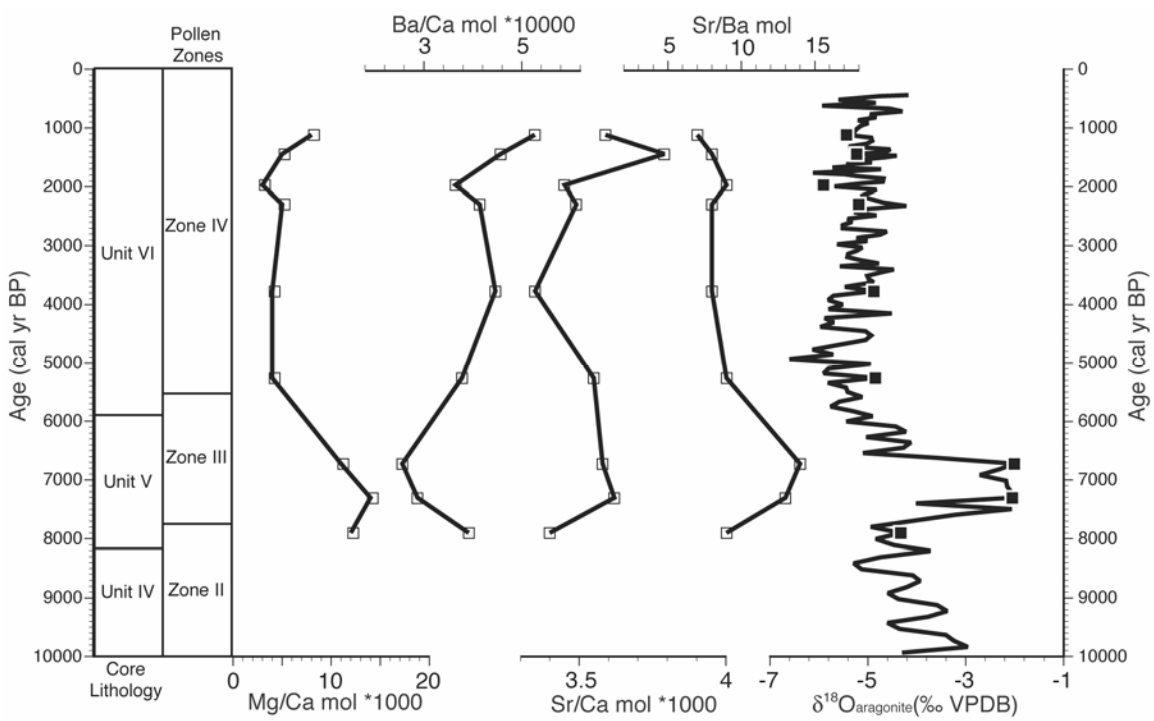


**Figure 3.9 Trace element ratio data from Castor Lake shown with core lithology, oxygen isotope data, and regional pollen record (Mack et al., 1979). Trace element ratios have been multiplied by an integer value in some cases in order to produce more convenient numbers, as absolute values are not important.**

Magnesium-calcium ratios show elevated values at the same time that $\delta^{18}O_{aragonite}$ increases between 8,000 and 7,000 cal yr BP. The Mg/Ca data are also observed to decrease slightly at 2,000 cal yr BP. Measurements of Ba/Ca indicate a decrease during the 8,000 to 7,000 cal yr BP interval, as well as a decrease at 2,000 cal yr BP. Strontium-calcium values are slightly elevated during the interval from 8,000 to 7,000 cal yr BP, and a similar response is also seen at 1,500 cal yr BP. Data from Sr/Ba measurements show great similarity to the general trends of the $\delta^{18}O_{aragonite}$ data. There is a strong response to the 8,000 to 7,000 cal yr BP period, and also at 2,000 cal yr BP, but it is not as pronounced.

## 3.5. Discussion

### 3.5.1. Model for Interpretation

Results from SEM, XRD, and smear slide analyses all suggest that aragonite is the only carbonate mineral phase present in the sediment record in any appreciable quantity. This indicates that mineralogical changes are not the cause of large-scale shifts in stable isotopes and trace elements such as those that occur between 8,000 and 7,000 cal yr BP. Due to the large magnitude and duration, geochemical and sedimentary events observed in lithologic Unit V are the main features that may be explained using the combination of sedimentary, isotopic, and trace metal proxies outlined above given the low sampling resolution of trace element analyses.

Interpretations of stable isotope records from lake sediments are often complicated, as there are many possibly causes of variability. The oxygen isotopic composition of a standing body of water is controlled by the initial isotopic composition and volume of water flowing into the lake, the lake volume, the isotopic composition and volume of water flowing out of the lake, and the evaporation flux or vapor exchange from the surface water (Gat, 1995). Precipitation of endogenic carbonate from lake water introduces an additional temperature-dependant oxygen isotopic fractionation. A water temperature increase of 1°C reduces the $\delta^{18}O$ of sedimentary calcite by ~0.24‰, and vice versa (Kelts and Talbot, 1990). This is a $\delta^{18}O$ shift that will occur in addition to whatever changes the lake water is experiencing from other environmental factors such as changes in the ratio of precipitation to evaporation (P/E) balance.

Existing paleotemperature records and glacial studies from the proximal Cascade Range (Benson et al., 2002; Clague and Mathewes, 1989; Rosenberg et al., 2004; Thomas et al., 2000) can adequately rule out the dramatic Holocene temperature shifts that would be required to produce the observed millennial-scale changes in the Castor Lake $\delta^{18}O_{aragonite}$ record. If source water changes were responsible for the large shifts in the stable isotope record, trace element data, particularly Sr/Ba ratios, would not be expected to respond in tandem, as the rates of dissolution of these cations in the catchment would not change under such circumstances. Trace element data thus provide additional lines of evidence to support the assumption that neither changes in temperature, nor source water, are significant factors in the stable isotope signal from Castor Lake. Lake volume changes and changes in evaporative flux are the remaining factors that may play important roles in the Castor Lake $\delta^{18}O_{aragonite}$ record, but the controls on lake volume are likely to be primarily controlled by changes in aridity, which would also affect evaporation rates. The concentration of $^{18}O$ in waters increases by the process of evaporation (Craig, 1961), and the relative isotopic impact of evaporation on a body of water increases with decreasing volume due to changes in the surface area/volume ratio. The $\delta^{18}O$ value of the lake water would therefore increase with increasing aridity, whether due to increased evaporative flux or decreased lake volume. These two factors therefore need not be separated unless efforts to quantify changes in aridity are undertaken.

Endogenic carbonate trace element data can be linked to changes in sediment mineralogy and/or solute chemistry (Haskell et al., 1996). Because Castor Lake carbonates have been demonstrated to be dominantly aragonite (no changes in sediment mineralogy), data from this system is most likely indicative of changes in solute chemistry. Trace element concentration is greater in water with more total dissolved solids (TDS), so carbonates precipitated in waters with high TDS will be more likely to have cation substitution in place of calcium (Chivas et al., 1985). Studies of trace element chemistry in lake sediment carbonate have more commonly relied on the use of Mg/Ca and Sr/Ca ratios of ostracod shell carbonate to understand environmental change because the mineralogy is known to always be low Mg-calcite (Chivas et al., 1993; Chivas et al., 1985; Curtis and Hodell, 1993; Rosenmeier et al., 2002). In these applications, increases in Mg/Ca are shown to be salinity and temperature dependant, while Sr/Ca is only salinity dependant. Trace element data are perhaps most useful when coupled with stable isotope data because they can be used to rule out influences on the isotope record such as changes in precipitation source, and can differentiate between changes in temperature and changes in salinity (Curtis and Hodell, 1993; Rosenmeier et al., 2002).

The model for interpretation of Mg/Ca and Sr/Ca ratios in ostracod shells cannot be translated to endogenic aragonite due to differences in the rates in which calcite and aragonite incorporate magnesium, strontium and calcium into their mineral lattice. Unlike ostracod calcite, aragonite actually favors the uptake of strontium and barium over calcium, and discriminates against magnesium. In fact, during periods of heavy carbonate precipitation, and presumably high TDS, Ba/Ca and Sr/Ca ratios may actually *decrease* as the respective reservoirs are consumed (Haskell et al., 1996). These facts have limited the number of trace element studies using endogenic carbonate as a measure of solute chemistry due to the additional complications involved, although the techniques have been more commonly applied as an indicator of changes in mineralogy (Valero-Garcés et al., 1997). Castor Lake does not contain ostracods in the sediment record due to the hypolimnetic anoxia, but trace element studies of systems of similar size and water chemistry that do contain ostracods have shown that Sr/Ba ratios in endogenic aragonite replicate the ostracod Mg/Ca signal quite faithfully (Haskell et al., 1996). Although barium geochemistry in natural waters is poorly understood, the previous success of this application, along with the apparent success in Castor Lake warrants the cautious use of these data.

Lake water $\delta^{13}C$ values are primarily influenced by vapor exchange, inflow, exchange with sediment pore water, photosynthesis, and respiration (McKenzie, 1985). Vapor exchange becomes increasingly important as water residence time increases (Lamb et al., 2002), so it is not a major factor in a site with short residence time like Castor Lake. Lake water inflow $\delta^{13}C$ values can be influenced by changes in the source of the water, and through interaction with local bedrock, soil, and catchment vegetation prior to entering the lake. Although large-scale changes in groundwater source account for changes in $\delta^{13}C$ of input waters in some settings, it is unlikely that this occurred in Castor Lake as the vast majority of water is thought to come from surface and sub-surface flow within the catchment. This implies that the ultimate water source is direct, and stored local precipitation, which would have entered the catchment at equilibrium with the relatively constant $\delta^{13}C$ values of atmospheric carbon dioxide throughout the Holocene. Although significant changes in $\delta^{13}C$ of atmospheric $CO_2$ occurred during the Pleistocene-Holocene transition, the lack of sufficient quantities of carbonate sediment over this interval do not allow for meaningful isotopic analysis. While bedrock properties probably remained relatively constant over the time period represented in the Castor carbonate record, vegetation changes, particularly between $C_3$ and $C_4$ plants, could have strongly influenced the $\delta^{13}C_{aragonite}$ signal. By incorporating palynological data from Mud Lake and Bonaparte Meadows (Mack et al., 1979) into the interpretation of the Castor Lake carbon isotope data, periods of major vegetation change can be identified in order to separate isotopic shifts caused by such changes from isotope shifts resulting from other factors.

Photosynthesis and respiration are likely the dominant controls on Castor Lake $\delta^{13}C_{aragonite}$ values apart from periods of major changes in catchment vegetation. Photosynthetic uptake of dissolved inorganic carbon (DIC) will act to preferentially remove $^{12}C$ and convert it to particulate organic carbon (POC), which eventually becomes incorporated into the lake sediment (McKenzie, 1985). Increased photosynthetic productivity may lead to increased $\delta^{13}C$ values in the lake water DIC, and decreased $\delta^{13}C$ values in the POC of the sediment. This is particularly true under conditions of hypolimnetic anoxia because aerobic respiration, which can convert the POC and sediment pore water carbon back into DIC with low $\delta^{13}C$ values, cannot be carried out in the sediment by benthic organisms (McKenzie, 1985).

Endogenic aragonite ultimately precipitates from the DIC reservoir in lakes, but either $HCO^-_3$ or $CaCO_3$ may be the dominant phase depending on a variety of controlling factors, especially pH. At 25°C the carbon isotopic fractionation between dissolved $HCO^-_3$ and gaseous $CO_2$ is approximately 8‰, and between dissolved $CaCO_3$ and gaseous $CO_2$ it is 10‰ (Emrich et al., 1970), but for $CaCO_3$ precipitated from the DIC pool, there is no apparent fractionation that occurs (McKenzie, 1985). Because Castor Lake is thought to have always been predominantly a $HCO^-_3$ system due to the high alkalinity, the offset in $\delta^{13}C$ between lake water DIC and atmospheric $CO_2$ has probably remained constant throughout the Holocene. The $\delta^{13}C$ value of carbonate sediment may therefore be regarded as an accurate recorder of the lake water DIC pool from which it precipitated.

It should also be noted that because the carbonate source for isotope and trace element analyses is endogenic aragonite, which is primarily formed in the summer months, the $\delta^{13}C_{aaragonite}$, $\delta^{18}O_{aragonite}$, and trace element signals are probably a record of summer lake water conditions. The summer P/E balance is directly influenced by the amount of winter precipitation that is received, however, as the majority of all precipitation in the area falls during the winter and spring. In addition, because the residence time of the lake is on the order of 10-20 years, there is a lagged response to environmental change in the lake water that averages out seasonal variation.

### 3.5.2. Paleoenvironmental Interpretation

Prior to 10,000 cal yr BP and the beginning of the Holocene, stable isotope and trace element data may not be confidently interpreted due to the extremely low levels of carbonate concentration in the sediment. Lithologic information from Unit I (>~14,000 cal yr BP), including bulk density, magnetic susceptibility (Fig.3.4), LOI (Fig.3.5), sedimentology, and the regional pollen stratigraphy from this period (Mack et al., 1979) all support the interpretation that at this time the area surrounding Castor Lake was a periglacial environment freshly devoid of ice cover. Very little vegetation would have existed and almost no organic soil would have been present in the catchment. Smear slides from Castor Lake support this interpretation, as the sediments are composed almost entirely of clastic material. Climate conditions were most likely cooler and more wet than today, as the retreating ice sheet to the north still maintained a significant control on regional climate, and elevated groundwater saturation from meltwater may have made some contribution to the lake.

By the beginning of lithologic Unit II (~14,000 – 12,500 cal yr BP), which corresponds roughly to the Bolling/Allerod warming period observed in records from the north Atlantic, some vegetation had likely moved into the area as evidenced by the increase in organic matter in the sediment observed in LOI data (Fig.3.5) and seen in smear slides. The decline in magnetic susceptibility is also a result of the introduction of terrestrial vegetation into the region, which limited terrigenous clastic runoff. Conditions were probably still cooler and wetter than present, although perhaps less so than in Unit I.

Unit III (~12,500 – 11,500 cal yr BP) indicates a return to periglacial-like conditions, as magnetic susceptibility, bulk density, and organic matter all return towards levels observed in Unit I. This unit corresponds well with accepted ages for the Younger Dryas cold reversal. The regional pollen data do not record this event (Mack et al., 1979), but this is probably an effect of the low temporal resolution inherent in pollen studies, as well as the overall scarcity of pollen grains at this time.

Unit IV (~11,500 – 8,200 cal yr BP) represents the beginning of the Holocene and the first period for which carbonate sediment is present in significant enough quantity to justify the use of stable isotope and trace element data in the climatic interpretation. The lake is established as a carbonate system at this time, although there was still a significant contribution to the sediment from terrigenous clastic material. The steady decline in the mass fraction of clastic sediment over this unit was likely the result of the gradual accumulation of catchment topsoil and vegetation through time, which covered the exposed mineral soil deposits and decreased the likelihood of their erosion by surface runoff. Pollen data suggest that the period was still wetter than today, although drier than the previous periods (Mack et al., 1979). The laminated nature of the sediments, higher organic matter content, and relatively high $\delta^{13}C_{aragonite}$ values suggest that aquatic productivity was higher than it had previously ever been. The fine sediment laminations also indicate that permanent anoxia existed in the hypolimnion. This is indicative of permanent water column stratification, as seasonal overturn would have caused sediment mixing and the introduction of increased levels of dissolved oxygen, which would have in turn allowed for the presence of benthic organisms capable of sediment bioturbation. Oxygen isotope data seem to suggest slightly more arid and variable conditions than in the late Holocene (Fig.3.8), although the higher $\delta^{18}O_{aragonite}$ values may also be a result of the slightly different vegetation regimes and the resultant effects on catchment hydrology (Rosenmeier et al., 2002). However, solar insolation reached maximum Holocene values between 10,000 and 9,000 cal yr BP, so the possibility exists that this period was more comparable to modern conditions than the pollen record would seem to indicate. Trace element data do not indicate substantial differences from modern conditions.

Unit V (~8,200 – 5,900 cal yr BP) contains by far the most pronounced changes in the Holocene record. The abrupt decrease in organic matter and carbonate content (Fig.3.5) may be due to a dilution effect from the massive increase in diatom frustules, which usually signifies an increase in aquatic productivity, and minor increase in clastic sediment observed in smear slides. The sharp and sustained increase in the oxygen isotopes would seem to indicate the rapid onset of a sustained arid period, but the $\delta^{13}C_{aragonite}$ might normally be expected to increase in tandem given the likelihood that increased aridity would concentrate nutrients and lead to an increase in productivity (Fig.3.8) (McKenzie, 1985). The opposite response from the $\delta^{13}C_{aragonite}$ is probably the result of the breakdown of permanent water column stratification, the possibility of which is supported by the lack of laminated sediment. This breakdown probably resulted from decreased lake level and the subsequent release of low-$\delta^{13}C$ carbon from organic sediment as benthic organisms, which would have then been able to thrive due to the presence of oxygen in the hypolimnion, utilized this carbon source and recycled the material back into the water column DIC reservoir. This interpretation is supported by Sr/Ba data, which increased in response to increasing salinity, and the Ba/Ca data, which decreased as rapid aragonite precipitation depleted the limited barium reservoir from the lake water (Fig.3.9). Magnesium-calcium ratios also increased as the lake water became more concentrated in dissolved solids and aragonite precipitation was less able to discriminate against the incorporation of magnesium into the mineral lattice. Although changes in the rate of delivery of dissolved cations like Ba, Sr, and Mg to the lake could also have produced a similar response in the trace element signal it is unlikely that this occurred, as it would have required large-scale changes in the geomorphology of the catchment, an event for which no evidence exists. Even if changes in catchment geomorphology were responsible for changes in the delivery rates of these cations to the lake and thus, the trace element signal, the oxygen isotopes would not be expected to respond in similar fashion, as they are observed to do in the Castor Lake record. The increased influx of clastic sediment was also the probable result of a more arid period where ground-stabilizing terrestrial vegetation became sparser, thus increasing delivery to the basin by surface runoff. The deposition of the Mazama tephra sequence also played a role in the increased clastic sediment influx, as it probably blanketed the landscape and continued to be washed into the lake for centuries after the initial deposition in the catchment. Mud Lake pollen data indicates a more arid environment, and the presence of a disconformity in that record during this time also supports the idea of lower lake-levels (Mack et al., 1979).

It is unclear whether the events of Unit V, apart from the increased clastic sediment influx, were totally climate driven or if they were partially the result of the deposition of the Mazama tephra sequence. The increase in diatom frustules may have been a result of more silica availability in the water (Telford et al., 2004), as the apex of the increase occurred after the deposition of the tephra. However, the changes that mark this unit clearly begin below the tephra layer, indicating that these events were already beginning as the tephra was deposited. The timing of the onset of this unit is coincident with the so-called “8.2ka event” seen in the GISP2 cores and elsewhere, and marked by a cooling episode in the north Atlantic (Alley et al., 1997). It is unclear at this time if the 8.2 ka event is related to the onset of this warm, dry period in Washington. The cooling event in the north Atlantic may have led to a reorganization of circulation patterns that caused the warming and drying that is thought to have occurred in Castor Lake.

Unit VI (~5,900 cal yr BP – ~400 cal yr BP) marks the onset of modern conditions from a lithological and palynological standpoint. Given the lack of large millennial-scale changes, and the high temporal resolution of the sediment sequence over this period, it would be possible to extend an interpretation of sediment variability based on instrumental calibration from the past 100 years throughout the entirety of this unit. At this time, little can be said about this period given the lack of surface sediment recovery for this study, the relatively poor temporal resolution of the current data set, and the lack of millennial-scale changes. Although the trace element data appear to show some response to an event around 2,000 to 1,500 cal yr BP, the lack of a large $\delta^{18}O_{aragonite}$ response at the same interval makes the cause of such a change difficult to interpret. The one inference that may be drawn is that there have been no major changes or systematic reorganizations to the region over the last 6,000 years compared to what took place in the early and middle Holocene.

### 3.5.3. Comparison with Other Paleoenvironmental Records

Regional climate records for the early Holocene in the Pacific Northwest are difficult to synthesize, as many glacial studies from the Cascade Range, Coast Range, and Rocky Mountains show evidence for glacial advances (Beget, 1981; Heine, 1998a; Heine, 1998b; Luckman and Osborn, 1979; Thomas et al., 2000; Waitt et al., 1982; Waitt and Thorson, 1983), while several pollen records, lake studies, and some glacial studies show evidence for drier conditions (Bennett et al., 2001; Clague and Mathewes, 1989; Doerner and Carrara, 2001; Lowe et al., 1997; Whitlock, 1992; Whitlock and Bartlein, 1993). It is unlikely that these seemingly contradictory findings come from misinterpreted observations, given the number of studies involved. It is more probable that the complex topography and reorganization of the regional circulation system led to non-uniform spatial response.

Most records from the middle Holocene in the Pacific Northwest suggest the existence of drought conditions, although the exact timing of these events do not always agree completely (Bennett et al., 2001; Clague and Mathewes, 1989; Doerner and Carrara, 2001; Lowe et al., 1997; Whitlock, 1992). The paucity of evidence for glacial advances in the region during the middle Holocene lends support to the notion of low effective moisture during this interval due to the close relationship demonstrated between glacial advance and moisture availability (Luckman and Osborn, 1979; Ryder and Thomson, 1986; Waitt et al., 1982). The timing of this lack of glacial activity correlates with the well-documented xerothermic interval of the early middle Holocene (Lowe et al., 1997; Ryder and Thomson, 1986; Whitlock, 1992). In spite of the general lack of evidence for major middle Holocene glaciation, however, a few isolated episodes have been recognized during this interval (Ryder and Thomson, 1986). The timing of return to cooler and moister conditions after the period of drought also varies depending on location throughout the Pacific Northwest, but is generally inferred to have occurred between 6,000 and 5,000 cal yr BP.

Little significant change is reported from paleoecological studies in the Pacific Northwest after the end of the phase of middle Holocene drought conditions, although some evidence suggests a slight shift towards more arid conditions near 4,000 or 3,000 cal yr BP (Bennett et al., 2001; Clague and Mathewes, 1989; Doerner and Carrara, 2001; Lowe et al., 1997; Whitlock, 1992). Most glacial studies report that the largest advances since the early Holocene and late Pleistocene are late neo-glacial in age (~450 yr old) (Luckman and Osborn, 1979; Ryder and Thomson, 1986; Waitt et al., 1982). The lack of resolution of these climatic events by other paleoecological proxies may illustrate the insensitivity of the proxy/sensitivity of glacial response, uncertainties in dating more recent events, or effects of regional topography.

### 3.6. Conclusion

The Castor Lake sediment record supports and refines the complex preexisting regional environmental history in the Pacific Northwest. The successful application of trace element geochemistry of endogenic carbonates also provides additional foundation for the cautious application of this technique to future studies, given careful preliminary evaluation and accompanying proxy records. Before the application of barium trace element studies can become more widespread, significant work is needed to gain a more thorough understanding of the behavior of this element in modern lake systems.

The most promising result to come from this investigation is the potential for more detailed centennial to sub-centennial-scale results from rapidly responding proxies like stable isotopes to investigate more short-term climate fluctuations over the last ~6,000 years. Future work may also include the collection of transect cores to gain a better understanding of lake volume changes, and the deployment of sediment traps and lake level monitors to gain a more thorough understanding of the modern system.

The lack of significant anthropogenic impact on the catchment facilitates the use of the instrumental climate record of the past ~100 years as a tool for calibrating and interpreting sedimentary evidence for environmental changes before this period. The added confidence that this will bring to interpretations of the proxy records will greatly improve our knowledge of climate and drought cycles in the increasingly drought-stricken Pacific Northwest. In any event, it is clear from this work that at least one very long-term drought, which was much more severe than anything humans have experienced in recorded history, persisted for nearly 1,000 years in the middle Holocene.

# 4. A DROUGHT RECORD OF THE PAST 6,000-YEARS FROM OXYGEN ISOTOPES IN ENDOGENIC ARAGONITE AT CASTOR LAKE, NORTH-CENTRAL WASHINGTON STATE

Rapid population growth in the Pacific Northwest places increased demand on water resources making the region increasingly susceptible to drought. Current understanding of natural climate variability is limited by the short duration of the instrumental record. Here we present a drought reconstruction for the last ~6,000 years based on oxygen isotope measurements of endogenic aragonite from sediment cores collected from Castor Lake in north-central Washington State. Chronological control is based on tephrochronology, radiocarbon dates from terrestrial material, and a cesium activity profile. There is a strong correlation between the Castor Lake isotope record and the 1,500-year reconstruction of the Palmer Drought Severity Index (PDSI) from central Washington State. This provides an extensive calibration period on which to base the interpretation spanning the period from ~6,000 to 1,500 cal yr BP. Several drought episodes are revealed, some with much greater duration than any experienced during the historic record or identified in proxy reconstructions of the past ~500 years. This contrasts with the lack of any major drought events in the past half-century, which is a concern given that this period has been used to develop average precipitation baselines on which much of the water resource allocation in the Pacific Northwest is based.

## 4.1. Introduction

The growing population of the Pacific Northwest has placed increased reliance on limited water resources from spring snowmelt in and around the Cascade Range (Gedalof, 2002). Several studies have suggested that the last half-century, which is the period when most legislation that governs water resource allocation was written, may have been anomalously wet and devoid of multi-year drought events (Cook et al., 2004; Gedalof, 2002; McKee et al., 2000; Woodhouse et al., 2002). The combination of these two factors outlines the importance of working towards a better understanding of the natural cycle of drought in the region. The Pacific Northwest has been identified as a so-called “core region” for drought (Knapp et al., 2004). Such regions have been described elsewhere in the West and are thought to mark locations where droughts first take hold, expand from, and persist in even as the arid events conclude in other localities (McKee et al., 2000; Woodhouse et al., 2002). Information regarding drought history in the Pacific Northwest may therefore lead to a better understanding of regional drought frequency and duration, such as the mega-drought that affected much of the American West during the Dust Bowl of the 1930’s.

In order to investigate drought history on multi-decadal to centennial time scales using lake sediments, certain issues must be acknowledged regarding chronological control, as changes in sedimentation rate and the errors inherent in radiocarbon dating introduce a degree of uncertainty. However, as long as these issues are taken into account it is possible to generate highly relevant and useful data. Each lake system must also be approached from a unique perspective because lakes exist in a variety of forms and environments. Despite these complications, lakes offer an advantage because they archive longer records than other proxy sources, such as tree-rings, can provide. Furthermore, the development of an increasingly extensive network of tree-ring based drought reconstructions in North America (Cook et al., 2004; Cook et al., 1999) extends the currently available calibration period that may be used for understanding how lake sediment proxy records record drought events back as far as 2,000 years in some locations.

## 4.2. Study Area

Castor Lake (48.54° N, 119.56° W) is located in Okanogan County in Washington State on a terrace margin of the Okanogan River. It is a kettle lake formed by the retreating Cordilleran Ice Sheet near the end of the Pleistocene (Fig.4.1).

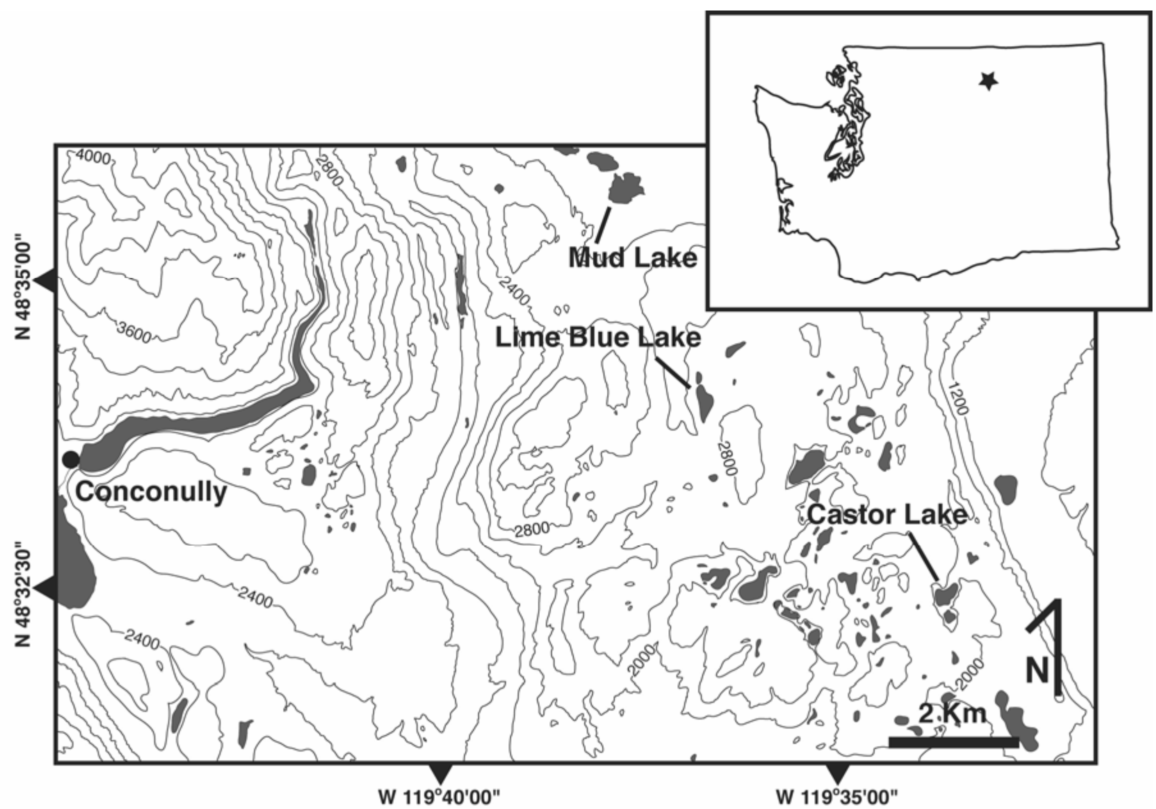


**Figure 4.1 Base map showing Castor Lake, Mud Lake, and Conconully, WA. Bonaparte Meadows is located approximately 46 km northeast of Mud Lake. Weather station data is from Conconully. Regional pollen data are from Mud Lake and Bonaparte Meadows (Mack et al., 1979). Contour interval = 400 feet.**

There is no active surface outflow and it is therefore effectively closed-basin. The lake sits on a relative topographic high, making it unlikely that distal groundwater from deep aquifers contribute significantly to the lake. Residence time was not calculated for Castor Lake, but estimates from lakes in similar environmental settings in central and northern Alberta range from 0.2 to 20 calendar years, depending on whether the hydrology is open, closed, or somewhere in between (Gibson et al., 2002). Given the apparent closed-basin hydrology of Castor Lake, residence time is probably closer to the upper limits of this range. Surface water pH was 8.5 in late July of 2003, and alkalinity measured 565 mg/L. Although the dissolved inorganic carbon (DIC) pool was not directly measured, it is likely that the majority of inorganic carbon is in the form of bicarbonate, given the high alkalinity and pH of the lake water. Lake surface elevation is about 591 m above sea level, maximum water depth is ~11.5 m, and lake surface area is ~0.07 $km^2$. The catchment is approximately 3.2 $km^2$, and is almost entirely undeveloped. Field-based bathymetric surveys reveal a single large, flat basin with gently sloping sides rising to the shores. Modern water $\delta^{18}O$ values from Castor Lake are 10-15‰ higher than local precipitation, suggesting a strong influence by evaporation on the system (Fig.4.2)

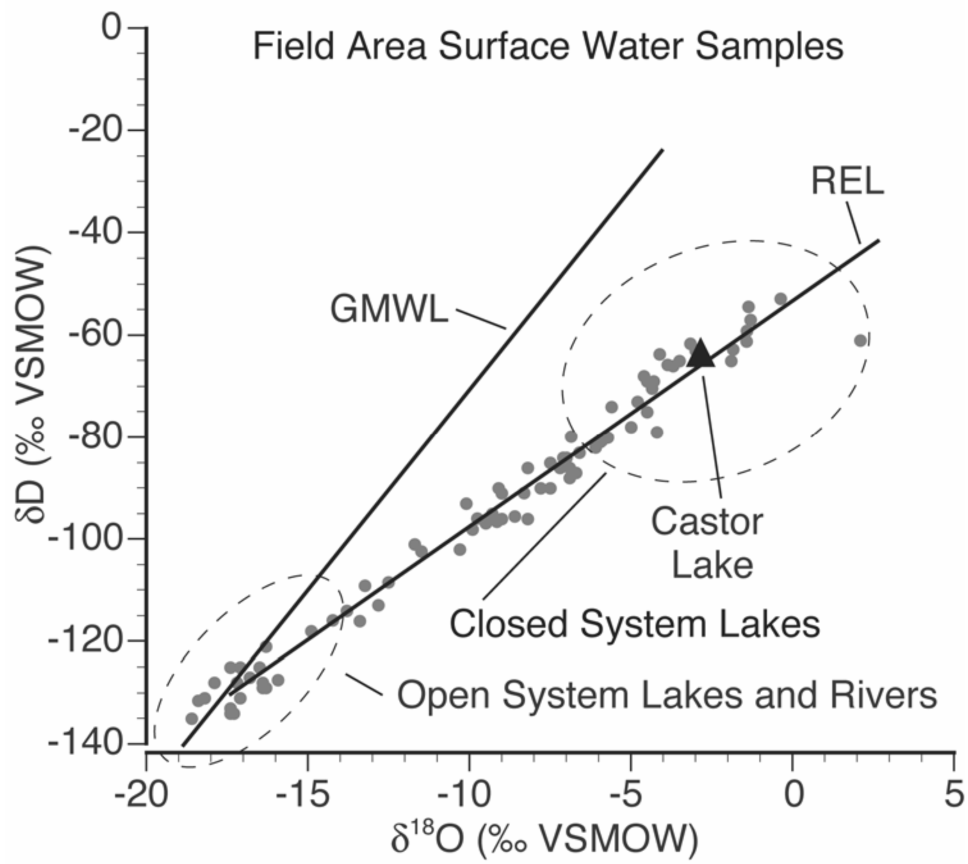


**Figure 4.2 Modern surface water isotope data from vicinity of Castor Lake. Samples collected between 2000 and 2004, over an area from 48° N to 49° N latitude, and 119° W to 121° W longitude. Open system lakes and rivers plot near the Global Meteoric Water Line (GMWL) due to limited atmospheric interaction. Closed system lakes plot far from the GMWL along the Relative Evaporation Line (REL) due to increased influence by evaporation.**

Based on sedimentological analyses, and limited limnological investigations conducted in July of 2003 and February of 2004, Castor Lake appears to be a warm monomictic or meromictic water body. Winter temperature, conductivity, and pH profiles exhibit an unstratified water column indicating seasonal vertical mixing, but dissolved oxygen profiles show very low bottom-water concentrations suggesting permanent anoxia in the hypolimnion. The cause of deepwater anoxia remains unclear, as only two profile measurements were made, but it may be a result of the topographic protection of the basin. The lake is surrounded by relatively steep, forested hill slopes, which might serve to limit the water surface wind speed, thus preventing complete seasonal overturn. Hypolimnetic anoxia is unlikely to be the result of lake-water eutrophy, as the lake is currently too alkaline to support fish populations, and water column visibility extends up to several meters, indicating low to moderate productivity levels. Whatever the cause of the permanent anoxia, the effect has been to inhibit sediment bioturbation, and thereby allow for the deposition of undisturbed, finely laminated sediments throughout the Holocene sedimentary sequence. These conditions of constant bottom water anoxia have an additional effect of severely inhibiting benthic ostracod growth.

The climate of north-central Washington is dominated primarily by the Pacific westerlies (Bryson and Hare, 1974). These winds, strongest between 45° and 50°N, are controlled by the strength and position of the Aleutian low-pressure system, and the North Pacific high-pressure system. During winter months, the Aleutian low strengthens and shifts to more southern latitudes, delivering cool, moist air to the coast of Washington State. In summer, the Aleutian low weakens, moves northward, and is replaced by the North Pacific high. The presence of this pressure center during the summer months results in the delivery of more arid air masses to the state. Arctic air masses occasionally enter the region as well, but are typically are replaced quickly by incoming Pacific westerlies (Bryson and Hare, 1974). Modern climate data, acquired from the National Climatic Data Center (NCDC), indicate that the closest weather station to Castor Lake is at Conconully, WA. Average annual adjusted precipitation values for the period from 1960 to 1990 were 277 mm/yr, average summer temperatures (Jun-Aug) were 18.0°C, and average winter temperatures (Dec-Feb) were ~3.6°C.

## 4.3. Methods

### 4.3.1. Coring and Field Measurements

Three sediment cores were recovered from Castor Lake between 2003 and 2004. During summer 2003, one 4.5 m modified Livingstone piston core was collected from a water depth of 11.5 m, with overlapping sections down to approximately 3.78 m (Wright et al., 1984). An additional 1.25 m percussion core was collected in the summer of 2003 in an effort to increase the amount of usable sediment in the upper sequence. A 52 cm freeze core was collected in the winter of 2004 to preserve an undisturbed sequence of the uppermost sediments that were lost in the cores collected the previous summer.

Cores were transported to the University of Pittsburgh for analysis. The freeze core was stored in dry ice during shipping and kept frozen in the lab prior to sampling. The Livingstone and percussion cores were wrapped in plastic wrap, placed in polyvinyl chloride (PVC) tube, and stored at ~4°C until they were sampled.

### 4.3.2. Chronology

Chronological control is provided by eleven accelerator mass spectrometry (AMS) radiocarbon dates (Table 4.1), two tephra layers of known age, and measurements of $^{137}Cs$ activity near the top of the core.

**Table 4.1 Radiocarbon dates from Castor Lake.**

| Core | Drive Depth (cm) | $^{14}C$ age ($^{14}C$ yr B.P.) with error | Median calibrated age (cal yr B.P.) | 2-sigma calibrated age range (cal yr B.P.) | Material | Lab accession number |
|---|---|---|---|---|---|---|
| A-03 D-1 | 23 | 435 ± 40 | 492 | 328-540 | Grass | CAMS# 104906 |
| A-03 D-1 | 75 | 1530 ± 35 | 1416 | 1334-1518 | Charcoal | CAMS# 104907 |
| B-03 D-2 | 9 | 1890 ± 35 | 1833 | 1725-1919 | Pine Needle | CAMS# 104908 |
| B-03 D-2 | 75 | 3385 ± 35 | 3622 | 3479-3715 | Charcoal | CAMS# 104910 |
| B-03 D-3 | 8 | 4095 ± 45 | 4608 | 4442-4816 | Seed | UCI# 7527 |
| B-03 D-3 | 36 | 5160 ± 100 | 5911 | 5661-6173 | Charcoal | CAMS# 104909 |
| B-03 D-3 | 56 | 5815 ± 25 | 6628 | 6502-6721 | Seed | UCI# 7488 |
| B-03 D-4 | 52 | 6720 ± 80 | 7582 | 7432-7682 | Seed | CAMS# 104911 |
| B-03 D4 | 88 | 9425 ± 30 | 10648 | 10557-11035 | Seed | UCI# 7590 |
| B-03 D-5 | 16 | 10025 ± 35 | 11465 | 11259-11908 | Seed | UCI# 7491 |
| B-03 D-5 | 40 | 11020 ± 35 | 13022 | 12675-13169 | Seed | UCI# 7493 |

Lead-210 activity was measured, but the results were ambiguous and will be discussed later. Radiocarbon measurements were made on charcoal or identifiable terrestrial macrofossils, including seeds from the *cyperaceae* sedge family in many cases. Possible hard-water effects were avoided by ensuring that only identifiable remains from terrestrial plants were used for dating. Measurements were made at the Center for Accelerator Mass Spectrometry (CAMS) at Lawrence Livermore National Laboratory, and at the W.M. Keck Carbon Cycle Accelerator Mass Spectrometry lab at the University of California, Irvine (UCI). Samples analyzed at the UCI lab were pre-treated at the University of Pittsburgh following standard acid-base-acid procedure (Abbott and Stafford, 1996). All radiocarbon ages were calibrated using the CALIB online software program version 4.4.2 (Stuiver and Reimer, 1993; Stuiver et al., 1998).

Several tephra layers were present in the sediment sequence, although many were very thin and not readily identifiable with the unaided eye. Two tephras of significant thickness were analyzed by electron microprobe at Washington State University. The first of these tephras was identified as the Mount Saint Helens (MSH) W tephra which has been dated at 1480 AD (470 BP) by dendrochronology (Mullineaux, 1986). The second identified tephra unit is from the Mazama climactic eruption that formed Crater Lake in Oregon ca. 6,730 ± 40 $^{14}C$ yr BP (7,585 cal yr BP) (Hallett et al., 1997).

Lead-210 and Cesium-137 activity measurements were made at the Freshwater Institute at the University of Manitoba in Winnipeg, Canada. The $^{210}Pb$ profile showed several activity reversals, and the age model generated through the application of the constant rate of supply (CRS) model to the measured $^{210}Pb$ activities did not include the $^{137}Cs$ peak at 1964 AD, even within a 2-sigma error range. Although $^{137}Cs$ can sometimes be mobile in the sediment column, it is unlikely that this occurred in Castor Lake. The presence of laminated sediments indicates that very little sediment mixing occurs in this system, which would aid in cesium migration. Also, cesium migration tends to be more common in lakes where organic matter content in the sediment is high. The relatively low organic matter content (10-20%) in the upper sequence of the Castor Lake sediments therefore further suggests that cesium migration is not an issue in this system.

A more likely explanation for the discrepancy between the $^{137}Cs$ and the $^{210}Pb$ dates is that variation in supported $^{210}Pb$ has introduced inaccuracies to the CRS age model. Because supported $^{210}Pb$ was not measured on a level-by-level basis, the average asymptotic value of

$^{210}Pb$ activity at depth was used as an estimate for supported $^{210}Pb$ throughout the entire sequence. While this commonly applied approach is often successful, it may account for the age discrepancies in this case. When additional age models are generated where supported $^{210}Pb$ values are assigned at random within the range of asymptotic values observed in the Castor Lake profile (1.64-2.16 dpm), significantly different chronologies are produced. Although none of these attempted age model iterations accurately intersected with the $^{137}Cs$ peak at 1964 AD, this result was achieved by increasing the range of possible values of supported $^{210}Pb$ to include values closer to 1 dpm. Given the uncertainties regarding the supported $^{210}Pb$ activity values used in applying the CRS age model, and the significant changes and reversals in total $^{210}Pb$ activity that occur with depth, more confidence may be placed in ages based on the $^{137}Cs$ profile. Cesium-137 activity measurements are therefore used as the basis for the final age model in the upper section of the Castor Lake sediment record.

The $^{137}Cs$ profile matched the typical pattern of increase through the 1950's to 1964 AD when atmospheric nuclear testing was banned and $^{137}Cs$ levels began to decline. In order to increase the number of age control points in light of the ambiguous $^{210}Pb$ profile, a date of 1959 AD was assigned to the beginning of $^{137}Cs$ increase based on the shape of published atmospheric activity curves in addition to assigning a date of 1964 AD to the $^{137}Cs$ activity peak. A straight line was then drawn on an age vs. depth plot from the top of the sediment at zero age, through the two cesium inferred dates, down to the point corresponding to 1954 AD. At this depth the linear relationship between bulk density and depth changes, indicating a probable end to the linear relationship that exists between sediment age and depth in the upper ~50 years of the sequence. From this depth, identified as 1954 AD, through the remainder of the sediment core, sediment ages were calculated by regression analysis using linear interpolation between dated samples. All subsequent discussions of proxy data will be made with regard to age, not depth.

### 4.3.3. Stable Isotopes

Inorganic carbonate sediment sub-samples were collected continuously from the upper 2,000-year sequence of the Castor Lake sediment record at an average sampling interval of 3.7 mm per sample. One-centimeter-thick sub-samples were collected every other centimeter for the portion of the record older than 2,000 years. All samples were disaggregated in 7% $H_2O_2$ and sieved at 63μm to remove any possible biogenic carbonate contamination. X-ray Diffraction (XRD) and Scanning Electron Microscopy (SEM) analyses were performed at the University of Pittsburgh to determine mineral phase and origin of fine-grain sediment.

Prepared carbonate samples were sent to the University of Florida, Gainesville for stable isotope measurements of $\delta^{13}C$ and $\delta^{18}O$. Analyses were performed using a Finnigan-MAT 252 mass spectrometer with an online automated carbonate preparation system (Kiel). Results are expressed relative to a standard in typical per-mille notation:

$$\delta_x^E = (R_{sample} / R_{stnd} - 1) * 1000$$

Where $\delta_x^E$ is the heavy isotope of element E, and $R_{sample}$is the ratio of the heavy isotope to the light isotope of the sample, and $R_{stnd}$ is the ratio of the heavy isotope to the light isotope of the standard. Analytical precision of measurements was reported to be within 0.04‰ for $\delta^{13}C$ and 0.08‰ for $\delta^{18}O$.

### 4.3.4. Palmer Drought Severity Index Correlation

Sediment records are often confounded by chronologies that contain considerable error as a result of variation in sedimentation rates, stretching and compression of the sediment sequence upon recovery, and the errors inherent in radiocarbon dating. While it is impossible to escape such errors entirely, steps can be taken to minimize their effects. Increasing the number of radiocarbon measurements on each core, and removing instantaneous tephra events from the depth scale can improve the quality of the chronology, but uncertainties will still persist. Chronological tuning of one record to another on the basis of common changes in proxy data is one of the most effective and easily applied methods to improve age models beyond the limits of radiocarbon.

In order to investigate the high-resolution variability observed in the Castor Lake stable isotope record, data from the past 6,000 years were normalized to a unit variance and the linear trend was removed by simple interpolation using a linear function in the AnalySeries® software program. The segment of this record representing the past 1,500 years was then tuned to a 1,500-year reconstruction of the Palmer Drought Severity Index (PDSI) obtained from the World Data Center for Paleoclimatology website (http://www.ncdc.noaa.gov/paleo/) (Cook et al., 2004). The basis for the correlation between the Castor Lake isotope record and the PDSI will be discussed later. Tuning was also carried out using the AnalySeries® software program, and care was taken to ensure that changes to the sediment chronology did not violate the ages determined by radiocarbon measurements.

## 4.4. Results

XRD and SEM analyses reveal that the fine-grain sediment from Castor Lake is overwhelmingly composed of endogenic aragonite. Alumino-silicate minerals occur in sediments of late Pleistocene and early Holocene age, but not after (tephra deposits excluded). No evidence for the presence of calcite or other carbonate mineral phases can be found anywhere in the sediment sequence. This fact both eliminates the need to account for changes in isotopic fractionation caused by changes in carbonate mineralogy, and provides compelling evidence that the carbonate sediment is entirely endogenic, because carbonate with a terrigenous source is generally calcite due to the fact that aragonite is instable at surface conditions.

Isotopic and sedimentological results show broad, large-scale changes occurring across the Pleistocene/Holocene transition, and several lithological changes prior to ~6,000 cal yr BP (Fig.4.3).

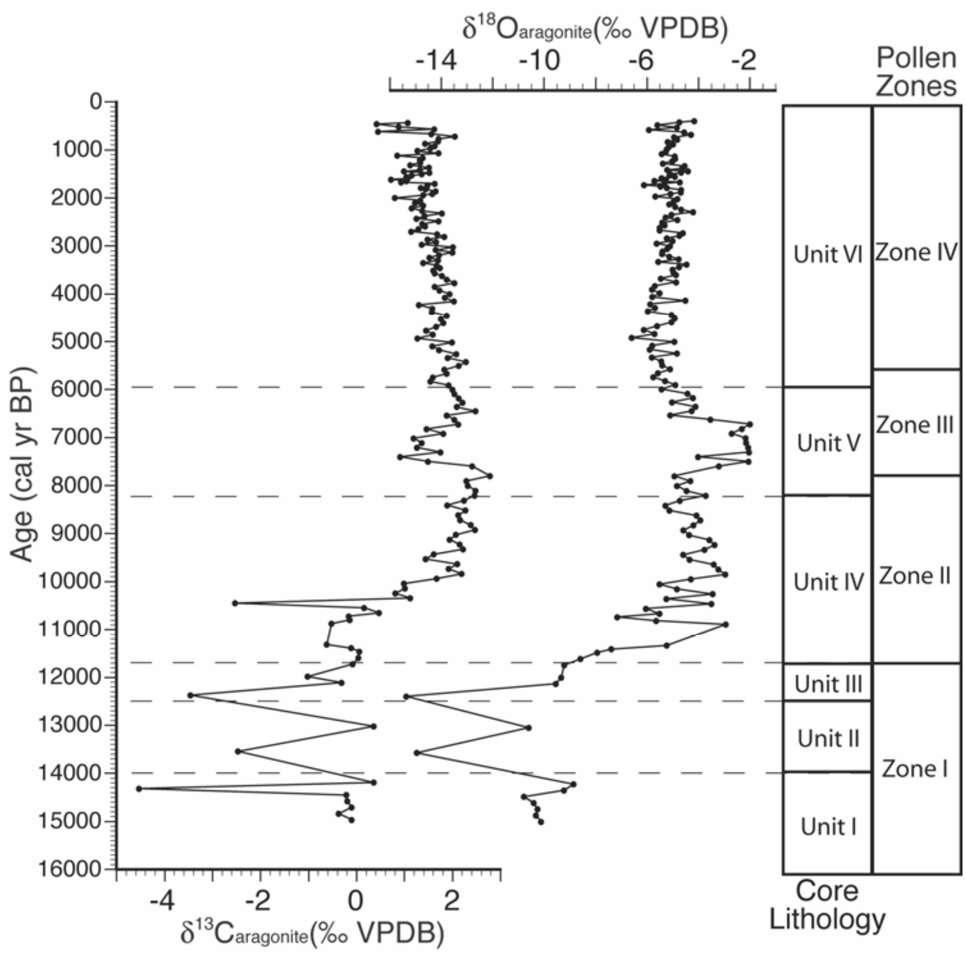


**Figure 4.3 Stable isotope data from carbonate sediment in the entire Castor Lake sediment core. Core lithological units shown at right next to regional pollen record (Mack et al., 1979). Dashed lines indicate lithological unit boundaries.**

This paper is focused on the high-resolution variability during the past 6,000 years. However, compared to the earlier portions of the Holocene sediment record, it is apparent the most recent ~6,000 year period was characterized by more stable conditions, with no major changes in regional vegetation or hydrology.

The sediment sequence from the past ~2,000 years is sampled at higher temporal resolution than the rest of the sediment sequence, and shows strong covariance ($R^2$=0.60) between carbon and oxygen isotope measurements made on endogenic aragonite (Fig.4.4).

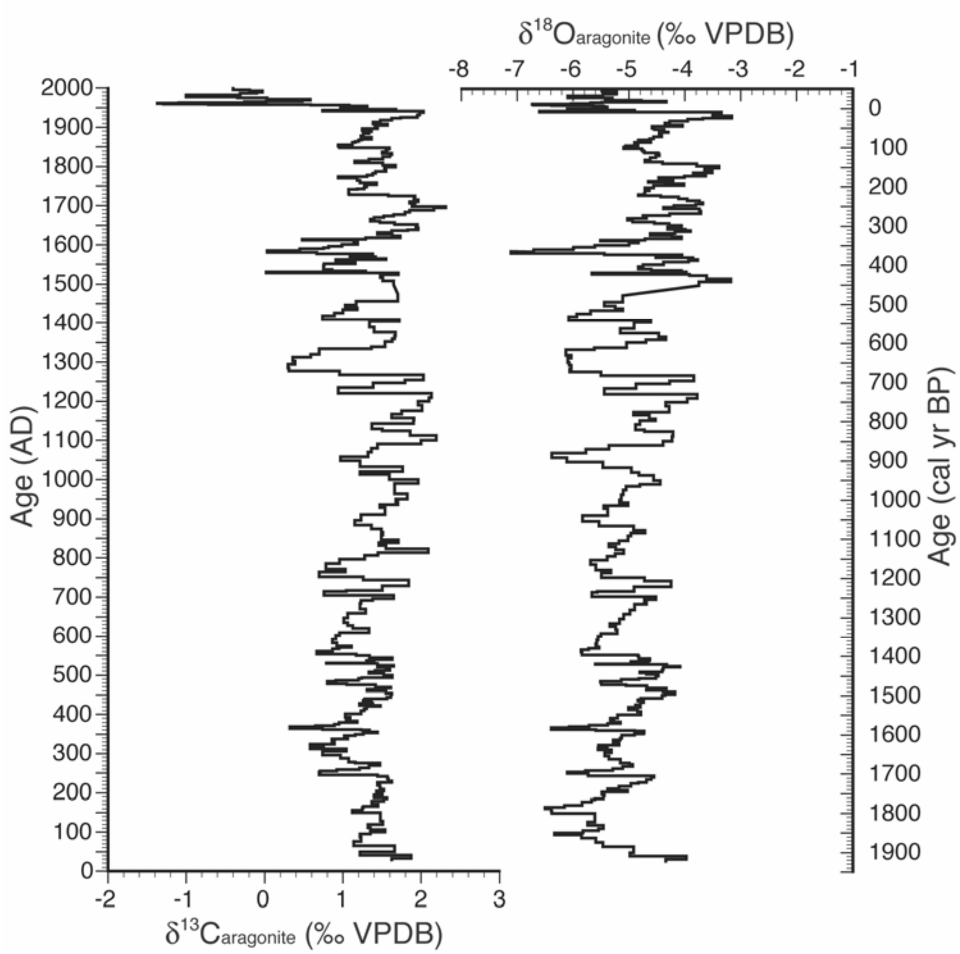


**Figure 4.4 High resolution stable isotope data from the past ~2,000 years at Castor Lake. Data are plotted to show sample thickness, as the core was sampled continuously every 3.7 mm (~7 years) on average. Note high degree of covariance between records on decadal time scales ($r^2$=0.60).**

During the 20th century the oxygen isotope data from Castor Lake has a relatively strong correlation with the Palmer Drought Severity Index (PDSI) calculated from instrumental data (Fig.4.5).

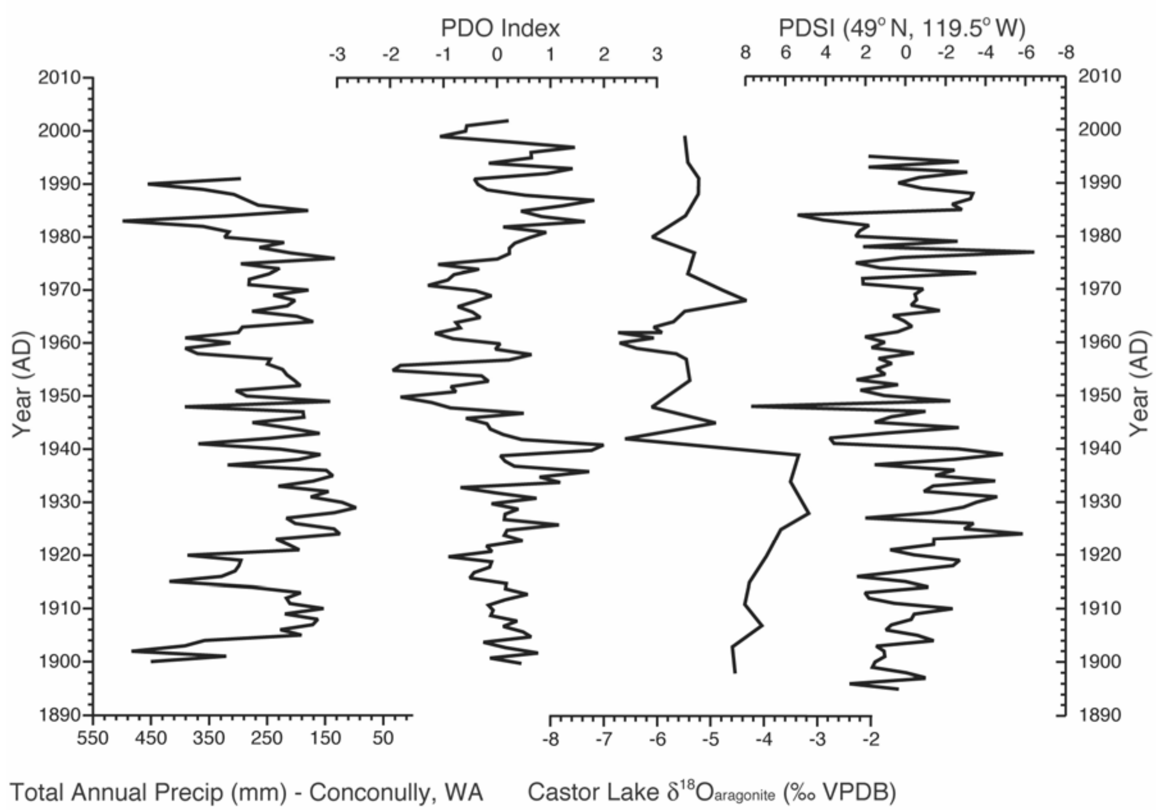


**Figure 4.5 Castor Lake oxygen isotope data compared to 20th-century records of precipitation at Conconully, WA, the Pacific Decadal Oscillation (PDO) index, and 20-year low-pass filter of Palmer Drought Severity Index (PDSI) data. Precipitation and PDSI axes are reversed to show drier conditions increasing to the right, PDO axis is not reversed, but also shows increasing aridity to the right. Note correlation between Castor Lake isotope and PDSI data ($r^2$=0.43) despite difference in sampling resolution. Conconully precipitation data are incomplete after the 1980's. Precipitation data were obtained from the National Climatic Data Center (NCDC). PDO data were obtained from the Joint Institute for the Study of the Ocean and Atmosphere (JISAO) via the World Wide Web (http://tao.washington.edu/main.html). PDSI data were obtained at the NOAA World Data Center for Paleoclimatology website (http://www.ncdc.noaa.gov/paleo/).**

The correlation is particularly good ($R^2$=0.43) in light of the fact that no adjustments were made to the isotope chronology, and the sampling resolution between the two records is different. It is also interesting to note that the oxygen isotope data appear to respond to changes in local precipitation (measured at Conconully, WA) during periods where the data do not appear to correlate well with the PDSI, for example, during the 1950's (Fig.4.5). This may reflect the fact that Castor Lake and the center of the PDSI grid point used for correlation are actually several kilometers apart, and therefore should not be expected to correlate perfectly.

As discussed previously, in order to examine centennial and multi-decadal-scale changes seen in the oxygen isotope record, the data from the past 6,000 years were normalized to a unit variance and the linear trend was removed before tuning the past 1,500 years to the PDSI reconstruction (Fig.4.6).

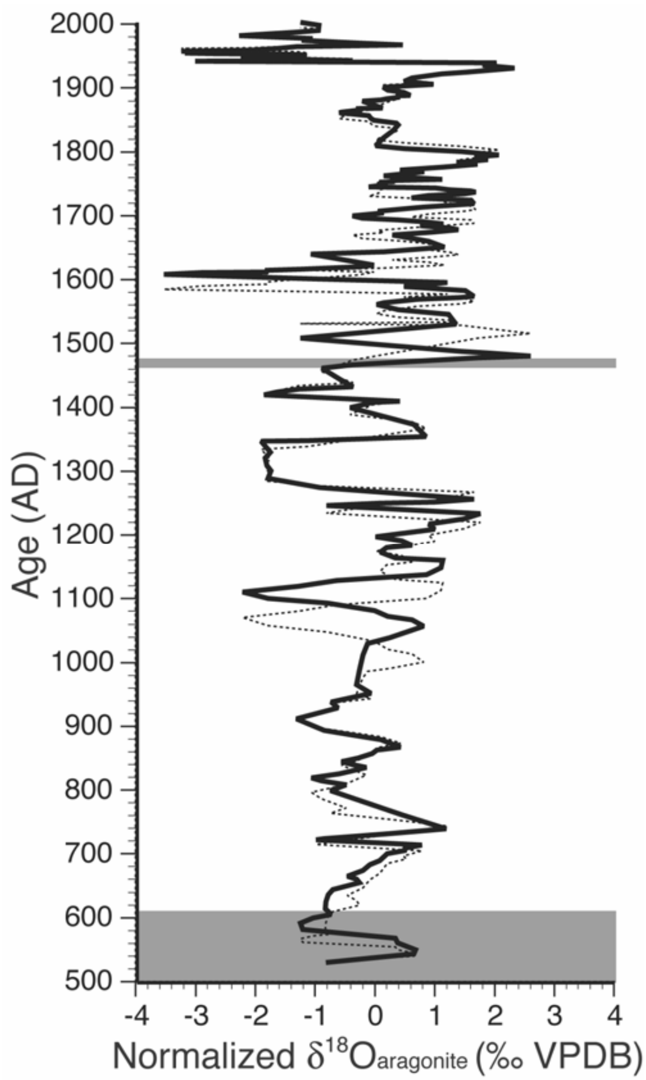


**Figure 4.6 Chronology changes from adjusting the 1,500-year oxygen isotope record from Castor Lake to the Palmer Drought Severity Index (PDSI) reconstruction from 47.5° N, 120° W. Data normalized to unit variance. Thin line represents isotope record plotted using the original chronology based on radiocarbon dates. Thick line represents adjusted chronology. Gray zones indicate radiocarbon dates, with thickness representative of error range.**

Tuning resulted in a remarkably high correlation ($R^2$=0.45) between the normalized oxygen isotope record from Castor Lake and the 1,500-year reconstruction of the PDSI (Fig.4.7).

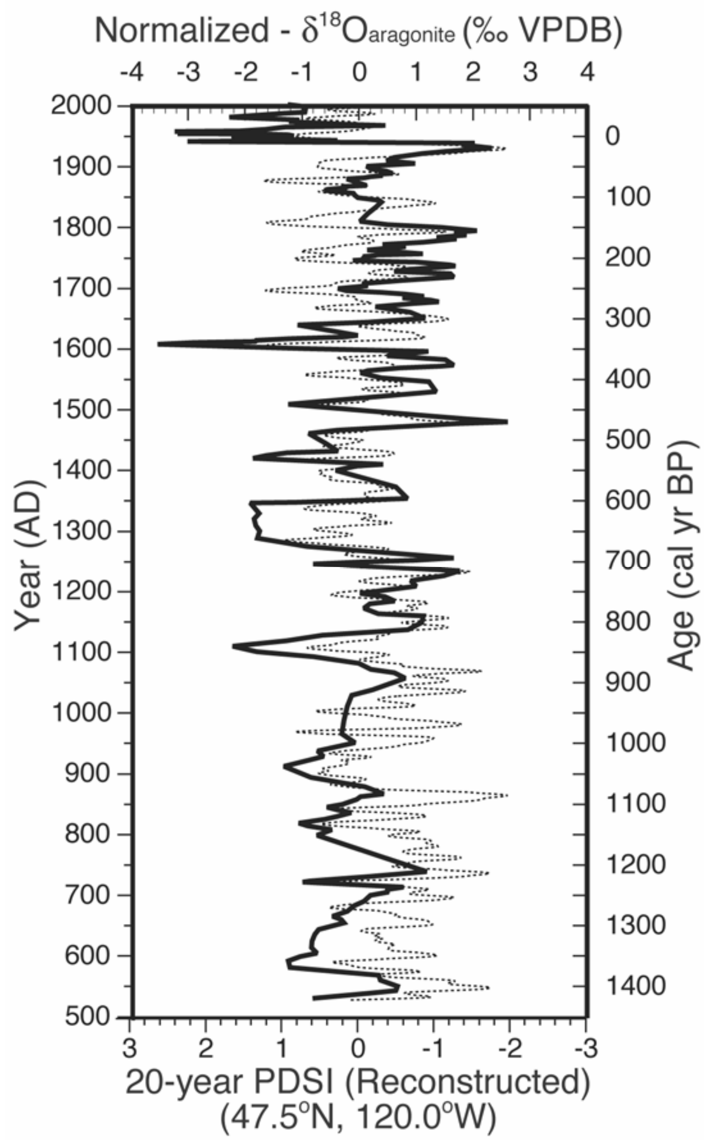


**Figure 4.7 Adjusted Castor Lake oxygen isotope record shown with Palmer Drought Severity Index (PDSI) reconstruction from 47.5° N, 120° W ($r^2$=0.45). Castor Lake data have been normalized to unit variance. PDSI data have been smoothed with a 20-year low-pass filter. PDSI data were obtained from the NOAA World Data Center for Paleoclimatology website (http://www.ncdc.noaa.gov/paleo/).**

The final result includes the tuned 1,500-year portion of the isotope record spliced with the un-tuned period spanning the period from 6,000 to 1,500 cal yr BP (Fig.4.8).

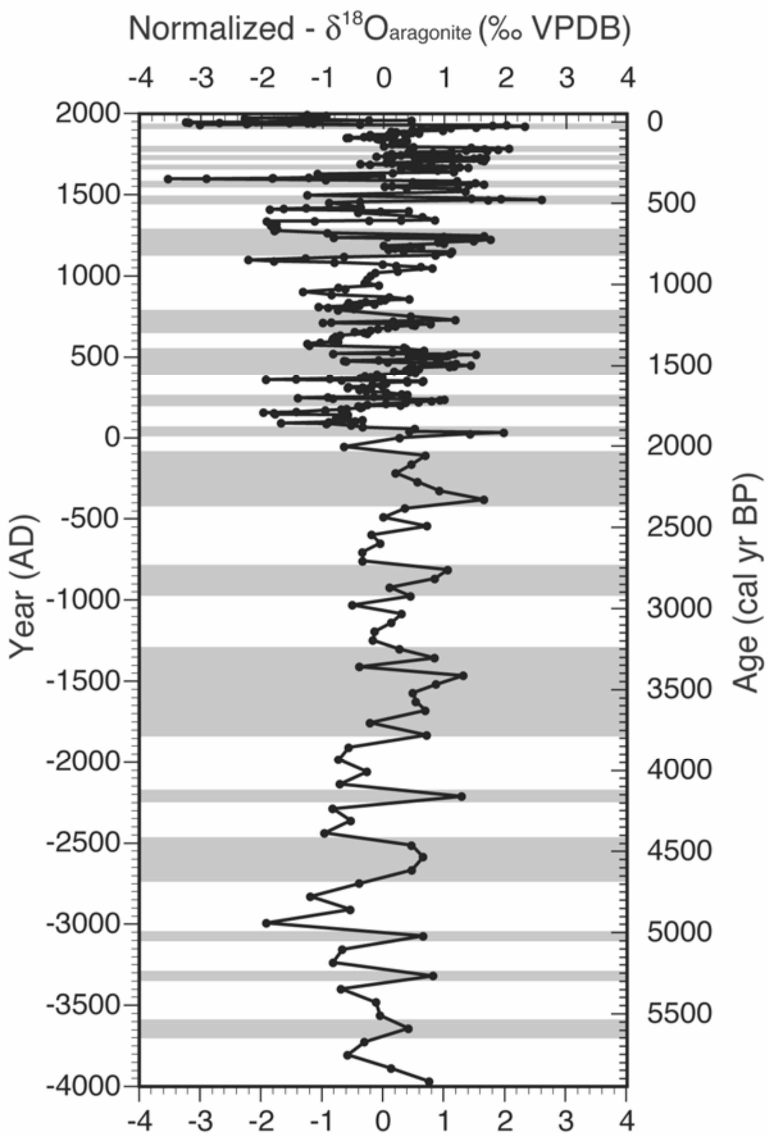


**Figure 4.8 Composite oxygen isotope record from Castor Lake. Data show 1,500-year tuned sequence with 6,000 cal yr BP to 1,500 cal yr BP sequence plotted using radiocarbon chronology. Data normalized to unit variance. Dry periods designated by gray bars.**

The complete 6,000-year oxygen and carbon isotope records from Castor Lake record several periods of elevated values. Due to the chronological errors inherent in lake sediment records, the precise beginning and end of each period may not be known, but approximations accurate to within 50 or 100 years may be given. These periods include ~5,650 to 5,550 cal yr BP, ~5,300 to 5,250 cal yr BP, ~5,050 to 5,000 cal yr BP, ~4,700 to 4,400 cal yr BP, ~4,200 to 4,100 cal yr BP, ~3,800 to 3,250 cal yr BP, ~2,950 to 2,700 cal yr BP, and ~2,350 to 2,250 cal yr BP for the period prior to ~2,000 cal yr BP. Events of the past ~2,000 years are observed from ~0 to 50 AD, ~200 to 300 AD, ~400 to 550 AD, ~650 to 800 AD, ~1150 to 1300 AD, and more recent events are observed occurring around 1500 AD, the late 1500's the late 1600's the 1740's around 1800 AD, and in the 1930's (Fig.4.8).

## 4.5. Discussion

### 4.5.1. Drought in the Pacific Northwest

An adequate definition of drought is central to any discussion regarding changes in aridity, although creating one that is universally applicable is problematic. The lack of satisfactory terminology is partially due to the fact that no one set of rules outline all types of precipitation deficits, as severe single-year events may not appear significant when focusing on multi-year arid spells. For example, some attempts to identify drought may look only at precipitation totals from the preceding and subsequent years surrounding that in question as a comparison to identify single-year events (Knapp et al., 2002). Others may compare precipitation totals from each year against the annual average from the length of the entire climate record (McCabe et al., 2004). The effects of drought are often cumulative over many years, however, so neither definition is adequate for exploring sustained events. At present, the Palmer Drought Severity Index (PDSI) is one of the most comprehensive methods to quantify drought, as it takes into account several factors other than precipitation including temperature, evapotranspiration, and soil moisture (Palmer, 1965). Although the PDSI does well measuring the intensity of long-term droughtinducing circulation patterns, it has certain limitations. These include inherent difficulties in calculating potential evapotranspiration, an overall lack of allowance for the effect of snowmelt or frozen ground, and the use of arbitrary methods for determining drought intensity as well as starting and end times (Alley, 1984). Despite these shortcomings continued application of this index is warranted given its widespread use in both instrumental and proxy data. PDSI reconstructions from tree-ring data are possible and available on a gridded-network (2° latitude x 3° longitude) over much of North America extending back to 2,000 years (Cook et al., 2004; Cook et al., 1999).

The factors leading to drought in the Pacific Northwest vary based on severity, duration, and regional extent. The development of high-pressure systems over Vancouver Island results in a blocking effect on the cyclonic airflow from the Pacific. This is often invoked as a main causal mechanism for large-scale regional drought (Knapp et al., 2004; Namais, 1983; Woodhouse et al., 2002). Localized droughts occur for a wider variety of reasons, but in general, sustained drought events are most likely to result from changes in ocean dynamics because only the oceans have the thermal inertia necessary to sustain changes in temperature and precipitation for a number of years (Namais, 1983). Other mechanisms for the causes of long-term drought have been explored, most notably changes in solar irradiance (Cook et al., 1997), and the influence of feedback dynamics, but currently the role of the oceans remains the most probable (McCabe et al., 2004).

The recent identification of several bimodal oscillations in ocean dynamics that occur over a range of timescales has improved understanding of the role of the oceans in sustained drought events. Such oscillations include the Pacific Decadal Oscillation (PDO)(Mantua et al., 1997), the El Niño/Southern Oscillation (ENSO), and the Atlantic Multidecadal Oscillation (AMO)

(Kerr, 2000). Because these modes of variability operate over a variety of time-scales their effects vary over time as they affect one another through constructive and deconstructive phase relations (Knapp et al., 2004; McCabe et al., 2004). For example, the Pacific Northwest is more likely to experience drought events when the PDO and AMO are both positive (McCabe et al., 2004). Conversely, substantial drought events have been shown to have occurred during both El Niño and La Niña events, suggesting that the influence of this phenomena is not as important in regard to long-term arid periods (Knapp et al., 2004). ENSO variability does have a significant impact on annual precipitation in the western US, however, but the strength of this teleconnection ultimately varies with the phase of the PDO (McCabe and Dettinger, 1999).

The influence of the oceans on climate variability in the Pacific Northwest is demonstrated at Castor Lake by the strong correlation between the stable isotope record and the PDSI and PDO records from instrumental data (Fig.4.5). The relationship between the Pacific Decadal Oscillation (PDO) and drought explored by previous authors (Gedalof, 2002; Gedalof and Smith, 2001; Knapp et al., 2004; McCabe et al., 2004), is confirmed by these broad correlations. Despite the fact that the correlations between the Castor oxygen isotope record, the PDSI, and the PDO are not as strong on annual to sub-decadal time-scales, the general trends of the 20$^{th}$ century are the same. This implies that moisture availability in north-central Washington responds to the same forcing factors as the north Pacific, or that one system is driving the other. Given the large size and thermal inertia of the north Pacific, it is far more likely that ocean dynamics are responsible for influencing conditions in the terrestrial system rather than the reverse scenario.

### 4.5.2. Proxy record of Drought in the Pacific Northwest

Several studies have explored the occurrence of drought in the Pacific Northwest, but tree-ring records provide the vast majority of proxy data (Gedalof, 2002; Graumlich, 1987; Knapp et al., 2002; Knapp et al., 2004; Mitchell, 1976). Tree-ring width measurements provide some of the best sources of data for examining drought variability due to the fact that they record climate information on a definite annual basis, but the relatively short temporal duration of most tree-ring records limits the ability to examine longer periods. Alternatively, reconstructions of drought based on lake sediments typically provide data much further into the past. However, it must be acknowledged that sediment records are often confounded by imperfect chronologies as a result of variation in sedimentation rates, and the errors inherent in radiocarbon dating. Additional complexity arises from the fact that lakes exist in a wider variety of forms and settings than trees, and variability in proxy data can therefore occur for a wider variety of reasons. It is therefore even more important for lake records than for tree-ring records that data be interpreted from a unique perspective developed on a site-by-site basis. Despite these minor difficulties, lakes can generate highly useful records of environmental change, particularly when the data are interpreted within the context of other regional records.

Comparisons of proxy records across the Pacific Northwest are complicated because the meteorological parameters used to describe climate, such as mean temperature and precipitation, are modified by substantial orographic effects (Mitchell, 1976). Regional records derived from tree-ring investigations that attempt to account for such effects have resulted in the identification of periods of widespread drought, most notably the late 1600’s to early 1700’s, 1740’s to 1760’s, the late 1700’s to early 1800’s, the 1840’s, the early 1900’s, and the 1930’s (Gedalof, 2002; Graumlich, 1987; Knapp et al., 2004). However, few of these records extend past the 1600’s because most are procured by tree-ring research. There is also considerable variation among records with respect to duration and intensity of any one event within these generalized periods.

Few continuous drought records exist from lake sediments in the Pacific Northwest. Lake sediment proxy records from southern British Columbia and Alberta, Canada show episodes of drought during the Medieval Warm Period (MWP) (900-1200AD), in the early 1600's, and around 1800 AD (Campbell, 1998; Hallett et al., 2003). These periods are consistent with tree-ring studies from the Pacific Northwest during the time interval over which the records overlap.

Although substantially further away geographically than the records discussed thus far, a large body of work using lake sediments as a proxy for drought has been completed in the vicinity of Pyramid and Mono lakes on the California-Nevada boarder between 38° N and 40° N latitude (Benson et al., 2002; Li and Ku, 1997; Mensing et al., 2004; Stine, 1990). These efforts have produced a general outline of drought vs. wet conditions. This work has shown that after ~6,000 cal yr BP, dry phases are occurred at Pyramid Lake from ~5,200 to 5,000 cal yr BP, ~4700 to 4,300 cal yr BP, ~3,900 to 3,800 cal yr BP, ~2,500 to 2,000 cal yr BP, ~1,500 to 1,250 cal yr BP, ~800 to 725 cal yr BP, and ~600 to 450 cal yr BP. Wet phases occurred from ~5,000 to 4,700 cal yr BP, ~4,300 to 3,900 cal yr BP, and ~3,800 to 3,400 cal yr BP (Benson et al., 2002; Mensing et al., 2004). The wet interval in Pyramid Lake around 3,500 cal yr BP is seen around much of the Great Basin, along with an apparent shift in general climate to coder and wetter conditions around 3,100 cal yr BP (Benson et al., 2002). Work at Mono Lake based on lake-level reconstructions correlates well with the wet and dry events observed in the Pyramid Lake record, with the highest Holocene lake-level reached at approximately 3,770 cal yr BP (Stine, 1990).

### 4.5.3. Lake Sediment Stable Isotopes as a Proxy for Drought

The oxygen isotopic composition of lake water is controlled by the volume and initial isotopic composition of inflowing water, the total lake volume, the isotopic composition and volume of outflowing water, and the evaporation flux or vapor exchange from the lake surface-water (Gat, 1995). Depending on the system, any one of these factors can provide a controlling influence on the lake-water $\delta^{18}O$ value. In some rare cases it may be possible to quantify these factors through the use of a combination of proxy data. More often it is only possible to quantify some of these variables and assumptions must be made regarding those that cannot be directly measured. Similarly, a variety of factors also control lake water $\delta^{13}C$ values. The greatest influence is exerted by the dissolved inorganic carbon (DIC) pool in lake water because it is the primary carbon source used by photosynthesis and the reservoir from which $CaCO_3$ precipitates (McKenzie, 1985). Lake water $\delta^{13}C$ values are primarily influenced by vapor exchange, inflow, photosynthesis and respiration within the lake, and lake water exchange with sediment pore water (McKenzie, 1985). As with oxygen isotopes, the relative importance of each of these factors varies on a lake-by-lake basis.

### 4.5.4. Oxygen Isotopes

Castor Lake, in many ways, represents a nearly ideal site for examining changes in aridity through the application of oxygen isotope measurements of inorganic carbonate. Because of its small size, residence time is limited and probably does not exceed 20 years in spite of its closed-basin hydrology. Modern lake water clearly responds to drought, as evidenced from its highly enriched $\delta D/\delta^{18}O$ value relative to local meteoric waters and hydrologically open lake systems (Fig.4.2) (Craig, 1961). The large, 10-15‰, differences between the $\delta^{18}O$ values of lake water and average local precipitation are substantially greater than that which could be accounted for under any realistic Holocene temperature change scenario. Assuming the estimated isotope-precipitation temperature relationship value for temperate latitude sites of 0.59‰/1°C (Rozanski et al., 1992), and the minimum enrichment of Castor Lake water from precipitation of 10‰, a temperature change of 16.9°C would be required to produce the observed values. This has certainly not occurred over the last 20 years (maximum estimated lake-water residence time), and further illustrates the sensitivity of this system to changes in aridity. Water residence time in Castor Lake is long enough to allow measurable evaporative enrichment of $^{18}O$, but short enough that the temporal resolution of the climate signal preserved in the sediment remains relatively high. The anoxic nature of the hypolimnion in Castor Lake also allows the sedimentary record to be preserved in discrete lamina, without significant mixing or bioturbation.

The oxygen isotope composition of Castor Lake aragonite is predominantly influenced by changes in evaporative enrichment. Although lake-water temperature has a quantifiable influence on the oxygen isotopic composition of aragonite precipitated from the epilimnion of -0.24‰/1°C (Kelts and Talbot, 1990), the estimated range of regional temperatures over the last ~6,000 years is only ~1-2°C (Kienast and McKay, 2001; Rosenberg et al., 2004; Wiles et al., 1996). Such minor changes in temperature would produce changes in the oxygen isotope record of only 0.5‰. Changes in the source of precipitation are also unlikely to account for the variability observed in the Castor Lake $\delta^{18}O_{aragonite}$ record, as such events would have probably caused more substantial changes in vegetation than those that are observed in regional pollen records (Mack et al., 1979). Changes in evaporative enrichment thus remain the only possible factor that can adequately explain the ~4‰ range displayed by the Castor Lake oxygen isotope record. Although temperature changes do not completely obscure the aridity-driven component, they do introduce a level of noise to the data so that the measured values of $\delta^{18}O_{aragonite}$ cannot be interpreted in a strictly quantifiable sense as a measure of aridity. However, future efforts to reconstruct temperature changes at this site may allow for the removal of this component of the $\delta^{18}O_{aragonite}$ signal. Additional uncertainties are raised by the effect of basin infill through time as sediment accumulates, effectively reducing total lake volume for non-climatic reasons, although such an effect is generally regarded as negligible in all but extreme circumstances.

The temporal resolution of the semi-quantitative drought record of paleo-aridity from Castor Lake $\delta^{18}O_{aragonite}$ is limited as a result of lake water response time to environmental change, limitations imposed by the sedimentation rate, and limitations in the ability to sub-sample the core for analytical purposes. According to age-depth models, the sedimentation rate for the last ~6,000 years is approximately 0.41mm/yr. Samples dating between ~0 AD and the present average 3.7mm in thickness and represent approximately 7 years each. Samples dating between ~6,000 cal yr BP and ~2,000 cal yr BP were all 10mm thick, and therefore each represent about 25 years of sedimentation. The isotope record from the upper 2,000-year sequence, thus represents a ~7-year running average of lake water conditions, while the values from ~6,000 cal yr BP to ~2,000 cal yr BP are discrete averages of lake water conditions spanning approximately 25 years each. Because lake-water residence time is probably ~10 to 20 years, the temporal resolution of the aridity signal represented by the $\delta^{18}O_{aragonite}$ data is about 20 to 30 years for the upper 2,000 year portion of the sequence. Since the remaining portion of the record was not sampled continuously, the resolution of the period from ~6,000 cal yr BP to ~2,000 cal yr BP is about 35 to 45 years for each measurement, with gaps of equal duration between each sample for this portion of the record. These estimates take into account the lag-time of the lake water response to changes in aridity, and the time averaging induced by sub-sampling.

### 4.5.5. Carbon Isotopes

The covariant nature of the $\delta^{13}C_{aragonite}$ and the $\delta^{18}O_{aragonite}$ records from Castor Lake indicate that closed-basin hydrology was persistent for at least the last 2,000 years (Fig.4.4), and probably persisted for the last 6,000 years (Fig.4.3). Regional vegetation reached modern conditions by approximately 6,000 years ago (Mack et al., 1979), ruling out the possibility that changes in vegetation between $C_3$ and $C_4$ plants had a major affect on the Castor Lake $\delta^{13}C_{aragonite}$ record over this interval. Given the lake's small catchment size and relative topographic isolation, it is also unlikely that major changes occurred in the amount or type of bedrock interaction that groundwater receives. Although no measurements of modern $\delta^{13}C_{aragonite}$ values from Castor Lake DIC are available, when these factors are taken into account, it is reasonable to interpret the $\delta^{13}C$ record from this system in the context of a photosynthetic productivity driven model (McKenzie, 1985).

Under such a scenario, originally proposed by McKenzie (1985), kinetic fractionation during uptake causes particulate organic carbon (POC) produced by photosynthesis to be low in $^{13}C$ relative to the DIC pool from which carbon dioxide is drawn. This leads to an increase in $\delta^{13}C$ in the DIC reservoir of the epilimnion. As dead organic matter sinks to the lake bottom, its POC may be utilized by organisms through respiration, or undergo decay before it reaches the sediment, in which case the low $\delta^{13}C$ carbon is re-released into the lake water. In settings where bottom water conditions are anoxic, such as those present in Castor Lake, the portion of POC that reaches the sediment is effectively removed from the lake-water carbon cycle, as benthic organisms are primarily aerobic. This causes the remaining carbon pool, especially the DIC pool in the epilimnion, to increase significantly with respect to $\delta^{13}C$ during periods of high productivity as a result of the removal of $^{12}C$. These changes are then preserved by the precipitation of carbonate from the DIC reservoir in the epilimnion. The net result of this process is a $\delta^{13}C$ record preserved in the endogenic carbonate where increases in productivity levels are recorded as increases in $\delta^{13}C$.

### 4.5.6. Castor Lake Record

The high degree of correlation between the Castor Lake isotope record and the 1,500-year reconstruction of the PDSI ($R^2$=0.45) supports the assertion that the oxygen isotope signal can be interpreted as a proxy for drought conditions (Fig.4.5). Although the degree of variability in the isotope record does not match that seen in the PDSI reconstruction, it is clear that the isotope record is responding to changes in aridity on multi-decadal time-scales. The lack of short-term variability in the Castor sequence is probably a result of the sampling resolution and the lagged response time to environmental change imposed by lake water residence time. As discussed previously, the Castor Lake record may be regarded as only semi-quantitative in that the temporal occurrence and duration of droughts may be identified within the range of chronological error, but the magnitude of individual events cannot be known.

Changes in the carbon isotope record from Castor Lake generally track changes in the oxygen isotope record for the past ~2,000 years (Fig.4.4). Such tight correlation between carbon and oxygen isotopes from carbonates has been identified as an indicator of closed-basin hydrology (Talbot, 1990). The interpretation of the carbon isotope record as a proxy for aquatic productivity implies that productivity increases with increasing aridity. Alternatively, the carbon isotope record may be recording changes in lake-level coincident with changes in aridity resulting from changes is total lake volume and nutrient concentration (Benson et al., 1996; McKenzie, 1985). In either case, the evidence for closed-basin hydrology that comes from the carbon isotope record supports the interpretation of the oxygen isotope record as proxy for drought.

The period of overlap between the Castor Lake oxygen isotope record and the PDSI reconstruction document several episodes of drought seen elsewhere in the Pacific Northwest through other proxy reconstructions. The Dust Bowl event of the 1930's stands out as the most recent large-scale event in the record, with additional drought events occurring around 1800 AD, the 1740's, the late 1600's, the late 1500's and around 1500 AD (Fig.4.8). Events are also observed from approximately ~0-50 AD, ~200-300 AD, ~400-550 AD, ~650-800 AD, ~1150-1300 AD (Fig.4.8). A minor indication of a drought event in the 1840's can be seen, though it does not appear to have affected the region surrounding Castor Lake as significantly as it did in other regions of the Pacific Northwest as described by Gedalof (2002). Despite this discrepancy the generally strong agreement between the Castor Lake oxygen isotope record and other proxy reconstructions of drought from the Pacific Northwest, particularly the 1,500-year long PDSI reconstruction, enables the model for interpretation to be extended back to approximately 6,000 cal yr BP (4000 BC). This cutoff point was chosen because the period prior to this shows evidence for extremely arid conditions in the Castor Lake record (Fig.4.3). These changes more than likely resulted in a fundamental restructuring of the lake system dynamics, which was accompanied by a major change in regional vegetation (Mack et al., 1979). Such widespread changes probably introduced additional complications that limit the continued use of the interpretive model developed based on 20$^{th}$ century data.

The 6,000-year record of drought from Castor Lake shows evidence for several oscillating wet-dry episodes (Fig.4.8). Due to the long 1,500-year calibration period available for this record, and the high precision and reproducibility of isotope measurements made on the larger samples between 6,000 and 2,000 cal yr BP, more confident interpretations of single isotope measurements may be made for than would otherwise be possible. The apparent increase in frequency and decrease in duration of drought events in the most recent 2,000 years is almost certainly a result of the change in sampling interval and subsequent averaging of more time per sample after ~2,000 cal yr BP rather than a climate signal. Particularly noticeable drought events occur from approximately ~5,650 to 5,550 cal yr BP, ~5,300 to 5,250 cal yr BP, ~5,050 to 5,000 cal yr BP, ~4,700 to 4,400 cal yr BP, ~4,200 to 4,100 cal yr BP, ~3,800 to 3,250 cal yr BP, ~2,950 to 2,700 cal yr BP, and ~2,350 to 2,250 cal yr BP (Fig.4.8).

Few records exist in the Pacific Northwest of comparable temporal duration and detail for correlation. Some records do identify individual droughts or dry periods, such as the Medieval Warm Period (ca. 900-1200 AD) or the events of the early 1600's AD (Campbell, 1998; Hallett et al., 2003), but none provide a continuous record like that presented from Castor. Although not really located in the Pacific Northwest, the continuous drought record from Pyramid Lake (Mensing et al., 2004) agrees remarkably well with the record from Castor Lake, recording similar drought events and wet phases at all but one interval. Interestingly, it is during the largest and most extreme wet phase seen in this, and other Great Basin records around 3,500 cal yr BP (Benson et al., 2002), that the Castor Lake drought record shows evidence for some of the longest drought conditions of the past 6,000 years (Fig.4.8). A full explanation for why these records fail to correlate only at this time interval is unavailable at the present, although changes in atmospheric circulation, Pacific Ocean dynamics, and the associated bimodal precipitation regime in the western US may offer a possible explanation.

The presence of a north-south precipitation seesaw across the western USA has been identified from instrumental climate data (Dettinger et al., 1998), and has been postulated to have existed in the past (Graham, 2004). Presently, the transition between northwestern and southwestern precipitation regimes occurs between 38° N and 40° N latitude (Dettinger et al., 1998). If the circulation changes required to produce the large changes seen in the Pyramid-Mono Lake region at ~3,500 cal yr BP were of the appropriate scale to shift the boundary between precipitation zones north slightly it might explain why these systems would experience wetter conditions while Castor Lake experienced conditions that were more arid. This interpretation agrees with the current understanding of the dipole mechanism, where warmer than average tropical Pacific SSTs causes the eastern lobe of the Northeast Pacific high to weaken and the westerlies to expand southward, causing an increase in precipitation in the southern region of the dipole and a decrease in the north (Graham, 2004). In any event, further investigation is required to identify the causes and nature of large-scale climate changes that may have affected the western US around 3,500 cal yr BP.

## 4.6. Conclusion

The oxygen isotope record from Castor Lake reveals several multi-decadal droughts over the past ~6,000 years. Between ~6,000 cal yr BP and ~2,000 cal yr BP, droughts are observed from ~5,650 to 5,550 cal yr BP, ~5,300 to 5,250 cal yr BP, ~5,050 to 5,000 cal yr BP, ~4,700 to 4,400 cal yr BP, ~4,200 to 4,100 cal yr BP, ~3,800 to 3,250 cal yr BP, ~2,950 to 2,700 cal yr BP, and ~2,350 to 2,250 cal yr BP (Fig.4.8). Droughts of the past ~2,000 years are observed from ~0-50 AD, ~200-300 AD, ~400-550 AD, ~650-800 AD, ~1150-1300 AD, and recent droughts are observed occurring around 1500 AD, the late 1500's the late 1600's the 1740's around 1800 AD, and in the 1930's (Fig.4.8). Although the causal mechanisms behind these droughts are unclear, the long temporal duration of some events and the high degree of correlation between modern drought conditions and changes in oceanic variability such as those described by the PDO suggest that changes in Pacific Ocean dynamics are a dominant influence. Also noteworthy, is the apparent lack of drought events longer than a few decades during the past 500 years as compared to the rest of the record of the last 2,000 years, which was sampled at the same resolution.

The implications of this, and other records of drought for the Pacific Northwest and the western US in general, are that no drought events have occurred in the historic record that are of comparable duration to the maximum duration events seen in the proxy record from the past 6,000 years. The occurrence of such “mega-droughts” in the future may face municipalities with circumstances for which they are unprepared. This is particularly true in light of the fact that no major drought events, even those that would be considered minor in the context of the proxy record, have occurred in the last half-century.

# 5. CONCLUSION

The data presented in this thesis represents a detailed investigation of one selected lake sediment record from north-central Washington State. The combination of analyses including stable isotope geochemistry of bulk organic sediment and inorganic aragonite precipitates, trace element geochemistry of inorganic aragonite precipitates, various measures of sediment composition, and identification of general sedimentary changes, identify a series of environmental changes on time scales ranging from millennia to decades. These data provide one of the most detailed and long-term records of continental environmental change available to date in the Pacific Northwest. Ample opportunity for continued research into the nuances and regional relationships of paleoenvironmental change exists in this area, both from the Castor Lake sediment record, and from additional sites in the region.

## 5.1. Future Work at Castor Lake

Initial efforts to expand on the findings presented in this study should focus on the remaining work on the Castor Lake sediment record. The obvious first step in this process is to extend the ultra-high resolution sampling of bulk sediment for stable isotope measurements of aragonite from its current limit at ~2,000 cal yr BP, to the last major vegetation and lithological transition, approximately 6,000 cal yr BP. Such a task could reveal new information regarding drought cyclicity, and improve the confidence in interpretations made regarding this interval from the currently available lower-resolution data. Additional efforts could focus on measuring the grayscale variation in sediment color in the hopes of correlating color changes with geochemical proxies, such as the $\delta^{18}O_{aragonite}$ data. Any effort towards more precise knowledge of the oxygen isotope composition of the carbonate sediment will only serve to increase the resolution of a record of drought that is ultimately only semi-quantitative. In order for the full potential of the Castor Lake drought record to be realized, a second oxygen isotope record must be developed from a proximal site that is not influenced by evaporative enrichment, therefore recording only changes in the oxygen isotopic composition of source precipitation. Such a site may or may not exist, and the data need not come from a lake sediment record, but if this goal is attainable it should be vigorously pursued. The acquisition of a record of this nature, which would ideally come from an open-basin carbonate lake with very short residence time, would facilitate the removal of the temperature and source-water component from the Castor Lake isotope record. With such influences removed, the Castor Lake oxygen isotope record would provide an unencumbered and quantitative record of changes in precipitation-evaporation (P/E) balance.

Additional avenues for improving the quantitative nature of the Castor Lake $\delta^{18}O_{aragonite}$ record include independent methodologies for estimating temperature using species assemblage analyses of aquatic microfossils like diatoms and chironomids. Such species-level identification of diatom and chironomid taxa and the application of the appropriate transfer functions for temperature will require collaboration with a specialist trained in these areas. Provided this goal can be achieved, the associated temperature data may be incorporated in efforts to model the environmental changes required to produce the changes observed in the oxygen isotope and temperature data. Even without microfossil-based temperature reconstructions, the benefits of applying an isotope mass-balance model to the Castor Lake isotope record are many. Software programs like Stella® offer powerful and readily available tools to assist in creating quantitative estimates of the environmental changes required to produce the variability observed in the proxy record, and should therefore be utilized where the data are of a sufficient quality to do so.

Isotopic investigation of the modern ecology of Castor Lake may also aid in the interpretation of millennial and centennial scale changes, particularly with respect to the carbon isotopic composition of sediment organic matter. The TOC/TN data from Castor clearly show that the sediment organic matter is a mix of terrestrial and aquatic material. A study of the stable isotope compositions of modern contributors to sediment organic matter may reveal likely sources of organic matter in the sediment, and therefore facilitate more detailed interpretations of the nature of the changes observed in the isotopic record. Compound specific analyses of sediment organic matter present another alternative for resolving changes of this nature, as such analyses allow for the extraction of both a terrestrial and aquatic isotope signal from the organic fraction of the sediment. Compound-specific techniques also offer a potential pathway for resolving the issue surrounding the isotopic composition of source water with respect to the $\delta^{18}O_{aragonite}$ record discussed previously. Because terrestrial vegetation utilizes water that is at isotopic equilibrium with precipitation, the $\delta D$ value of terrestrial organic matter preserved in the lake sediment may serve as a tool for estimating the $\delta^{18}O$ value of precipitation through time, thus facilitating the quantitative reconstruction of P/E balance from the carbonate isotope record discussed previously.

Beyond the application of new geochemical and microfossil analyses, one additional area where future efforts should be focused in Castor Lake is on the development of a lake-level reconstruction based on a transect of sediment cores from shallow to deep water. Such data would significantly improve the robustness of the interpretations based on other proxy data. Transect data are unlikely to reveal changes on anything shorter than millennial time scales, but the data that result from such investigations are very sound. The current lack of significant littoral vegetation in Castor Lake, and the geochemical data that support the idea that littoral vegetation has always been minimal, increases the likelihood that radiocarbon dates on unconformities in the shallow-water sediment cores would be reliable, and not be confounded by penetrating root structures from aquatic macrophytes, as can often be the case.

## 5.2. Future Work in the Greater Region

Apart from the Castor Lake site, potential exists for the extraction of several additional records of comparable nature from other lake basins in north-central Washington State. While initial efforts should be focused on the completion of the work at Castor, future goals should include the identification and analysis of a lake site that may hold a record of the isotopic composition of source precipitation over the Holocene. As mentioned previously, such a site may be in the form of an open-basin carbonate lake. Alternatively, similar information could be extracted from the compound-specific analysis of $\delta D$ from a component of aquatic organic matter in an open-basin non-carbonate lake that records changes in lake water $\delta D$, which are related to changes in lake water $\delta^{18}O$. Compound specific analyses of $\delta D$ from organic matter in lake sediment are still rather difficult from an analytical standpoint; however, future advances in technology will undoubtedly overcome these impedances.

Another area where additional efforts may be applied is in completing analyses similar to those performed at Castor Lake on other closed-basin carbonate lakes in an attempt to replicate the changes seen in the Castor record in an entirely separate, yet similar watershed. Although such an exercise may not produce much new information, it would serve to substantiate the conclusions drawn from the Castor data, and may reveal additional information about spatial relationships and how localized processes affect the basins and their sediment records. Several sediment records of this nature have already been collected and analyses are at various stages of completion. These include cores from Lime Blue Lake, Little Twin Lake, Big Twin Lake, Round Lake, and others. The ultimate goal for researching paleoenvironmental change in the region from lake sediments should be to replicate the Castor Lake record from at least one other site, and to compliment these data with a record of the isotopic composition of precipitation such as that described above. The creation of a composite data set such as that described here will facilitate quantitative reconstructions of temperature, relative humidity, and precipitation at sub-centennial time scales.

Additional efforts may also be focused on tangential questions raised by this research. Perhaps the most notable of these is the investigation of the impact of the deposition of tephra layers of various sizes on the paleoenvironmental signal preserved in the sediment record.

# APPENDIX A

## Modern Surface Water Isotope Data

| Sample Location | Classification | $\delta^{18}O$ | $\delta D$ |
|---|---|---|---|
| Aeneas Lake | Lake | -11.5 | -102.4 |
| Alta Lake | Lake | -4.3 | -69.0 |
| Alta Lake | Lake | -3.7 | -66.0 |
| Beaver Pond | Lake | -16.3 | -129.0 |
| Big Twin | Lake | -9.0 | -96.0 |
| Big Twin | Lake | -7.0 | -84.0 |
| Big Twin | Lake | -7.5 | -85.0 |
| Big Twin Lake | Lake | -9.3 | -95.0 |
| Big Twin Lake | Lake | -6.6 | -83.0 |
| Big Twin Lake | Lake | -6.9 | -86.0 |
| Big Twin Lake | Lake | -6.0 | -80.9 |
| Big Twin Lake | Lake | -5.7 | -80.0 |
| Big Twin Lake | Lake | -6.1 | -82.0 |
| Big Twin Lake | Lake | -5.9 | -80.7 |
| Black Pine Lake | Lake | -9.9 | -98.1 |
| Bonaparte Lake | Lake | -9.8 | -95.9 |
| Brown Lake | Lake | -1.4 | -54.4 |
| Cambell Lake | Lake | -6.7 | -87.0 |
| Cambell Lake | Lake | -6.9 | -88.0 |
| Castor Lake | Lake | -2.9 | -63.1 |
| Cook Lake | Lake | -3.5 | -65.0 |
| Couger Lake | Lake | -12.8 | -112.9 |
| Davis Lake | Lake | -7.0 | -85.7 |
| Davis Lake | Lake | -7.2 | -86.0 |
| Davis Lake (Ferry County) | Lake | -9.0 | -91.0 |
| Duck Lake - NOCA | Lake | -13.8 | -114.0 |
| Ell Lake | Lake | -9.5 | -96.9 |
| Ferry Lake | Lake | -7.1 | -84.0 |
| Fish Lake | Lake | -11.7 | -101.0 |
| Green Lake | Lake | -6.9 | -79.8 |
| Ground water at Big Twin | Lake | -17.1 | -131.0 |
| Inflow Duck Lake | Lake | -14.9 | -118.0 |

| | | | |
|---|---|---|---|
| Lake | Lake | -4.6 | -68.0 |
| Leader Lake | Lake | -13.2 | -109.1 |
| Lime Blue Lake | Lake | -3.9 | -65.8 |
| Little Davis Lake | Lake | -10.3 | -102.0 |
| Little Goose Lake | Lake | -5.6 | -74.0 |
| Little Soap | Lake | -4.8 | -73.0 |
| Little Twin | Lake | -5.0 | -78.0 |
| Little Twin | Lake | -4.5 | -75.0 |
| Little Twin Lake | Lake | -8.6 | -95.5 |
| Little Twin Lake | Lake | -7.8 | -90.0 |
| Little Twin Lake | Lake | -1.8 | -62.8 |
| Little Twin Lake | Lake | -1.4 | -61.2 |
| Little Twin Lake | Lake | -1.9 | -65.0 |
| Long Lake | Lake | -9.2 | -96.5 |
| Long Lake | Lake | -10.1 | -93.0 |
| Lost Lake | Lake | -12.5 | -108.4 |
| Methew River at Twisp | River | -18.6 | -135.0 |
| Methow River at Twisp | River | -17.4 | -133.0 |
| No Name Lake | Lake | -1.3 | -57.0 |
| Patterson | Lake | -16.4 | -128.0 |
| Patterson Lake | Lake | -16.8 | -127.0 |
| Patterson Lake | Lake | -15.9 | -127.5 |
| Patterson Lake Outflow | Lake | -17.2 | -128.0 |
| Poison Lake | Lake | -0.4 | -52.8 |
| pond | Lake | 2.1 | -61.0 |
| Small Lake adj. to Little and Big Twin | Lake | -4.2 | -79.0 |
| Small Lake adjacent to Big Twin | Lake | -8.2 | -96.0 |
| Rainbow Lake | Lake | -17.1 | -125.0 |
| Rainy Lake | Lake | -18.4 | -131.5 |
| Rainy Pass Snow | Snow | -16.3 | -121.0 |
| Rainy Pass Stream | Stream | -17.4 | -125.0 |
| Round Lake | Lake | -8.3 | -90.9 |
| Sidley Lake | Lake | -4.3 | -70.4 |
| Sinlahekin Blue Lake | Lake | -14.2 | -115.8 |
| Soap Lake | Lake | -9.1 | -90.0 |
| Soap Lake | Lake | -4.5 | -69.0 |
| Spring | Lake | -17.4 | -134.0 |
| spring | Lake | -13.4 | -116.0 |
| spring | Lake | -16.5 | -125.0 |
| Swan Lake | Lake | -8.2 | -86.0 |
| Synder Lake | Lake | -3.0 | -63.0 |
| Teal Lake | Lake | -1.4 | -59.1 |

| | | | |
|---|---|---|---|
| Twin Lake | Lake | -7.5 | -90.0 |
| Twin Lake's Well | Lake | -16.4 | -129.0 |
| Waddell Lake | Lake | -17.9 | -128.0 |
| Waddell Lake inflow | Inflow | -18.2 | -131.0 |
| Wannacut Blue Lake | Lake | -3.2 | -61.6 |
| Wannacut Lake | Lake | -4.1 | -63.7 |
| Well | Lake | -17.3 | -134.0 |

# APPENDIX B

## Trace Element Data

| Depth (cm) | Age (cal yr BP) | Mg (ppm) | K (ppm) | Mn (ppm) | Al (ppm) | P (ppm) | Na (ppm) |
|---|---|---|---|---|---|---|---|
| 78 | 1117 | 1414 | 85 | 40 | 221 | 202 | 912 |
| 92 | 1445 | 975 | 79 | 30 | 200 | 198 | 846 |
| 124 | 1969 | 696 | 79 | 22 | 151 | 176 | 701 |
| 136 | 2294 | 1158 | 117 | 34 | 297 | 199 | 752 |
| 189 | 3774 | 718 | 72 | 2 | 170 | 199 | 837 |
| 227 | 5260 | 775 | 89 | 25 | 212 | 157 | 749 |
| 261 | 6725 | 2916 | 155 | 144 | 1010 | 225 | 1216 |
| 273 | 7306 | 2970 | 212 | 257 | 1299 | 197 | 1229 |
| 285 | 7901 | 2981 | 148 | 93 | 518 | 172 | 844 |

| Depth (cm) | Age (cal yr BP) | Fe (ppm) | Sr (ppm) | Ba (ppm) | Ca (ppm) | Zn (ppm) | Wt.% Leach Residue |
|---|---|---|---|---|---|---|---|
| 78 | 1117 | 345 | 2297 | 308 | 293013 | 12 | 21 |
| 92 | 1445 | 300 | 2731 | 301 | 330028 | 11 | 23 |
| 124 | 1969 | 271 | 3084 | 297 | 408956 | 7 | 24 |
| 136 | 2294 | 375 | 2817 | 305 | 369334 | 10 | 36 |
| 189 | 3774 | 250 | 2393 | 290 | 326377 | 14 | 25 |
| 227 | 5260 | 353 | 2584 | 251 | 333005 | 22 | 29 |
| 261 | 6725 | 1387 | 3276 | 214 | 419156 | 13 | 48 |
| 273 | 7306 | 1708 | 2698 | 195 | 341170 | 17 | 48 |
| 285 | 7901 | 1179 | 2954 | 311 | 397516 | 44 | 53 |

| Depth (cm) | Age (cal yr BP) | Mg (moles) | Sr (moles) | Ca (moles) | Ba (moles) |
|---|---|---|---|---|---|
| 78 | 1117 | 7.90E-06 | 3.56E-06 | 9.93E-04 | 5.24E-07 |
| 92 | 1445 | 4.94E-06 | 3.83E-06 | 1.01E-03 | 4.63E-07 |
| 124 | 1969 | 5.01E-06 | 6.16E-06 | 1.79E-03 | 6.52E-07 |
| 136 | 2294 | 5.11E-06 | 3.45E-06 | 9.88E-04 | 4.09E-07 |
| 189 | 3774 | 4.54E-06 | 4.20E-06 | 1.25E-03 | 5.58E-07 |
| 227 | 5260 | 5.18E-06 | 4.79E-06 | 1.35E-03 | 5.10E-07 |
| 261 | 6725 | 5.06E-06 | 1.58E-06 | 4.41E-04 | 1.13E-07 |
| 273 | 7306 | 6.91E-06 | 1.74E-06 | 4.82E-04 | 1.38E-07 |
| 285 | 7901 | 8.89E-06 | 2.44E-06 | 7.19E-04 | 2.82E-07 |

| Depth (cm) | Age (cal yr BP) | Mg/Ca* 1000 | Sr/Ca * 1000 | Sr/Ba | Ba/Ca* 10000 |
|---|---|---|---|---|---|
| 78 | 1117 | 7.95 | 3.59 | 6.80 | 5.27 |
| 92 | 1445 | 4.87 | 3.79 | 8.28 | 4.57 |
| 124 | 1969 | 2.81 | 3.45 | 9.46 | 3.65 |
| 136 | 2294 | 5.17 | 3.49 | 8.42 | 4.14 |
| 189 | 3774 | 3.63 | 3.35 | 7.52 | 4.46 |
| 227 | 5260 | 3.84 | 3.55 | 9.40 | 3.78 |
| 261 | 6725 | 11.47 | 3.58 | 13.97 | 2.56 |
| 273 | 7306 | 14.35 | 3.62 | 12.61 | 2.87 |
| 285 | 7901 | 12.37 | 3.40 | 8.67 | 3.92 |

# APPENDIX C

## Lead-210 and Cesium-137 Data

| Median Depth (cm) | $^{210}$Pb Activity (dpm / g) | + / - | Error | | $^{137}$Cs Activity (dpm / g) | + / - | Error |
|---|---|---|---|---|---|---|---|
| 0.5 | 31.70 | | 1.50 | | 3.91 | | 1.26 |
| 1.3 | 29.35 | | 0.96 | | 2.70 | | 0.90 |
| 1.95 | 24.46 | | 0.84 | | 4.13 | | 1.18 |
| 2.55 | 24.73 | | 0.85 | | 5.33 | | 1.17 |
| 3 | 36.78 | | 1.28 | | 0.00 | | 0.00 |
| 3.4 | 41.25 | | 1.21 | | 3.63 | | 1.05 |
| 3.85 | 17.24 | | 0.49 | | 3.81 | | 0.57 |
| 4.3 | 17.99 | | 0.51 | | 3.99 | | 0.72 |
| 4.75 | 8.22 | | 0.34 | | 3.58 | | 0.69 |
| 5.15 | 6.35 | | 0.33 | | 4.39 | | 1.20 |
| 5.5 | 7.66 | | 0.36 | | 7.88 | | 1.21 |
| 5.95 | 7.86 | | 0.32 | | 10.70 | | 0.90 |
| 6.4 | 10.03 | | 0.43 | | 6.41 | | 0.81 |
| 6.8 | 4.80 | | 0.29 | | 4.75 | | 0.82 |
| 7.15 | 4.32 | | 0.23 | | 1.64 | | 0.37 |
| 7.55 | 3.96 | | 0.27 | | 0.00 | | 0.00 |
| 7.95 | 3.92 | | 0.23 | | 1.35 | | 0.37 |
| 8.2 | 4.42 | | 0.20 | | 0.00 | | 0.00 |
| 8.5 | 3.60 | | 0.23 | | | | |
| 8.9 | 3.76 | | 0.18 | | | | |
| 9.35 | 3.26 | | 0.17 | | | | |
| 9.8 | 2.62 | | 0.15 | | | | |

| | | |
|---|---|---|
| 10.15 | 1.91 | 0.15 |
| 10.4 | 1.96 | 0.14 |
| 10.7 | 1.91 | 0.15 |
| 11.05 | 1.64 | 0.12 |
| 11.4 | 1.87 | 0.17 |
| 11.7 | 2.14 | 0.17 |
| 12 | 2.16 | 0.17 |
| 12.5 | 1.97 | 0.17 |
| 13 | 2.01 | 0.18 |
| 13.4 | 2.02 | 0.15 |
| 13.8 | 1.92 | 0.17 |
| 14.15 | 2.16 | 0.17 |

## BIBLIOGRAPHY


Abbott, M. B., and Stafford, T. W., Jr. (1996). Radiocarbon Geochemistry of Modern and Ancient Artic Lake Systems, Baffin Island, Canada. *Quaternary Research* **45,** 300-311.

Alley, R. B., Mayewski, P. A., Sowers, T., Stuiver, M., Taylor, K. C., and Clark, P. U. (1997). Holocene climatic instability: a prominent, widespread event 8200yr ago. *Geology* **25,** 483-486.

Alley, W. M. (1984). The Palmer Drought Severity Index: Limitations and Assumptions. *Journal of Climate and Applied Meteorology* **23,** 1100-1109.

Beget, J. E. (1981). Early Holocene Glacier Advance in the North Cascade Range. *Geology* **9,** 409-413.

Bennett, J. R., Cumming, B. F., Leavitt, P. R., Chiu, M., Smol, J. P., and Szeicz, J. (2001). Diatom, Pollen, and Chemical Evidence of Postglacial Climatic Change at Big Lake, South-Central British Columbia, Canada. *Quaternary Research* **55,** 332-343.

Benson, L., Kashgarian, M., Rye, R., Lund, S., Paillet, F., Smoot, J., Kester, C., Mensing, S., Meko, D., and Lindström, S. (2002). Holocene multidecadal and multicentennial droughts affecting Northern California and Nevada. *Quaternary Science Reviews* **21,** 659-682.

Benson, L., White, L. D., and Rye, R. (1996). Carbonate deposition, Pyramid Lake Subbasin, Nevada: 4. Comparison of the stable isotope values of carbonate deposits (tufas) and the Lahontan lake-level record. *Palaeogeography, Palaeoclimatology, Palaeoecology* **122,** 45-76.

Bird, M. I., Summons, R. E., Gagan, M. K., Roksandic, Z., Dowling, L., Head, J., Fifield, L. K., Cresswell, R. G., and Johnson, D. P. (1995). Terrestrial vegetation change inferred from *n*-alkane $\delta^{13}C$ analysis in the marine environment. *Geochim. Cosmochim. Acta* **59,** 2853-2857.

Brenner, M., Whitmore, T. J., Curtis, J. H., Hodell, D. A., and Schelske, C. L. (1999). Stable isotope (d13C and d15N) signatures of sedimented organic matter as indicators of historic lake trophic state. *Journal of Paleolimnology* **22,** 205-221.

Bryson, R. A., and Hare, K. F. (1974). Climates of North America. *In* "World Survey of Climatology." (H. E. Landsberg, Ed.), pp. 420. Elsevier Scientific Publishing Company, New York.

Campbell, C. (1998). Late Holocene Lake Sedimentology and Climate Change in Southern Alberta, Canada. *Quaternary Research* **49,** 96-101.

Chivas, A. R., De Deckker, P., Cali, J. A., Chapman, A., Kiss, E., and Shelly, J. M. G. (1993). Coupled Stable-Isotope and Trace-Element Measurements of Lacustrine Carbonates as Paleoclimatic Indicators. *In* "Climate Change in Continental Isotopic Records." (P. K. Swart, K. C. Lohmann, J. A. McKenzie, and S. Savin, Eds.), pp. 113-121. Geophysical Monograph Series. American Geophysical Union, Washington D.C.

Chivas, A. R., De Deckker, P., and Shelly, J. M. G. (1985). Strontium content of ostracods indicates lacustrine paleosalinity. *Nature* **316,** 251-253.

Clague, J. J., and Mathewes, R. W. (1989). Early Holocene thermal maximum in western North America: New evidence from Castle Peak, British Columbia. *Geology* **17,** 277-280.
Clark, D. H., and Gillespie, A. R. (1997). Timing and Significance of Late-Glacial and Holocene Cirque Glaciation in the Sierra Nevada, California. *Quaternary International* **38/39,** 21-38.
COHMAP. (1988). Climatic Changes of the Last 18,000 Years: Observations and Model Simulations. *Science* **241,** 1043-1052.
Cook, E. R., Meko, D., Stahle, D. W., and Cleaveland, M. K. (2004). North American Summer PDSI Reconstructions. *In* "Data Contribution Series # 2004-045." (W. D. C. f. Paleoclimatology, Ed.). NOAA/NGDC Paleoclimatology Program, Boulder, CO.
Cook, E. R., Meko, D. M., Stahle, D. W., and Cleaveland, M. K. (1999). Drought Reconstructions for the Continental United States. *Journal of Climate* **12,** 1145-1162.
Cook, E. R., Meko, D. M., and Stockton, C. W. (1997). A New Assessment of Possible Solar and Lunar Forcing of the Bidecadal Drought Rhythm in the Western United States. *Journal of Climate* **10,** 1343-1356.
Craig, H. (1961). Isotopic Variations in Meteoric Waters. *Science* **133,** 1702-1703.
Curtis, J. H., and Hodell, D. A. (1993). An Isotopic and Trace Element Study of Ostracods from Lake Miragoane, Haiti: A 10,500 year Record of Paleosalinity and Paleotemperature Changes in the Caribbean. *In* "Climate Change in Continental Isotopic Records." (P. K. Swart, K. C. Lohmann, J. A. McKenzie, and S. Savin, Eds.), pp. 135-152. Geophysical Monograph Series. American Geophysical Union, Washington D.C.
Davis, P. T., and Osborn, G. D. (1987). Age of Pre-Neoglacial cirque moraines in the central North American Cordillera. *Geographie physique et Quaternaire* **41,** 365-375.
Dean, W. E. J. (1974). Determination of carbonate and organic matter in calcareous sediments and sedimentary rocks by loss on ignition: comparison with other methods. *Journal of Sedimentary Petrology* **44,** 242-248.
Dettinger, M. D., Cayan, D. R., Diaz, H. F., and Meko, D. M. (1998). North-South Precipitation Patterns in Western North America on Interannual-to-Decadal Timescales. *Journal of Climate* **11,** 3095-3111.
Doerner, J. P., and Carrara, P. E. (2001). Late Quaternary Vegetation and Climatic History of the Long Valley Area, West-Central Idaho, U.S.A. *Quaternary Research* **56,** 103-111.
Emrich, K., Ehhalt, D. H., and Vogel, J. C. (1970). Carbon Isotope Fractionation During the Precipitation of Calcium Carbonate. *Earth and Planetary Science Letters* **8,** 363-371.
EPA. (1996). Test Methods for Evaluating Solid Waste - Physical and Chemical Methods (SW-846). Edition 3, Revision 2. United States Environmental Protection Agency, Washington, D.C.
Foit, F. F. J., Mehringer, P. J. J., and Sheppard, J. C. (1993). Age, distribution, and stratigraphy of Glacier Peak tephra in eastern Washington and western Montana, United States. *Canadian Journal of Earth Sciences* **30,** 535-552.
Gat, J. R. (1995). Stable Isotopes of Fresh and Saline Lakes. *In* "Physics and Chemistry of Lakes." (A. Lerman, D. M. Imboden, and J. R. Gat, Eds.), pp. 334. Springer-Verlag New York, Inc., New York.
Gedalof, Z. e. (2002). "Links Between Pacific Basin Climatic Variability and Natural Systems of the Pacific Northwest." Unpublished pHD thesis, University of Washington.
Gedalof, Z. e., and Smith, D. J. (2001). Interdecadal climate variability and regime-scale shifts in Pacific North America. *Geophysical Research Letters* **28,** 1515-1518.

Gibson, J. J., Prepas, E. E., and McEachern, P. (2002). Quantitative comparison of lake throughflow, residency, and catchment runoff using stable isotopes: modeling and results from a regional survey of Boreal lakes. *Journal of Hydrology* **262,** 128-144.

Graham, N. E. (2004). Late-Holocene teleconnections between tropical Pacific climatic variability and precipitation in the western USA: evidence from proxy records. *The Holocene* **14,** 436-447.

Graumlich, L. J. (1987). Precipitation Variation in the Pacific Northwest (1675-1975) as Reconstructed from Tree Rings. *Annals of the Association of American Geographers* **77,** 19-29.

Gu, B., Schelske, C. L., and Brenner, M. (1996). Relationship between sediment and plankton isotope ratios (d13C and d15N) and primary productivity in Florida lakes. *Canadian Journal of Fish and Aquatic Sciences* **53,** 875-883.

Hallett, D. J., Hills, L. V., and Clague, J. J. (1997). New accelerator mass spectrometry radiocarbon ages for the Mazama tephra layer from Kootenay National Park, British Columbia, Canada. *Canadian Journal of Earth Sciences* **34,** 1202-1209.

Hallett, D. J., Mathewes, R. W., and Walker, R. C. (2003). A 1000-year record of forest fire, drought and lake-level change in southeastern British Columbia, Canada. *The Holocene* **13,** 751-761.

Haskell, B. J., Engstrom, D. R., and Fritz, S. C. (1996). Late Quaternary paleohydrology in the North American Great Plains inferred from the geochemistry of endogenic carbonate and fossil ostracodes from Devils Lake, North Dakota, USA. *Palaeogeography, Palaeoclimatology, Palaeoecology* **124,** 179-193.

Hassan, K. M., Swinehart, J. B., and Spalding, R. F. (1997). Evidence for Holocene environmental change from C/N ratios, and d13C and d15N values in Swan Lake sediments, western Sand Hills, Nebraska. *Journal of Paleolimnology* **18,** 121-130.

Heine, J. T. (1998a). A minimal lag time and continuous sedimentation in alpine lakes near Mount Rainier, Cascade Range, Washington, USA. *Journal of Paleolimnology* **19,** 465-472.

Heine, J. T. (1998b). Extent, Timing, and Climatic Implications of Glacier Advances Mount Rainier, Washington, U.S.A., At the Pleistocene/Holocene Transition. *Quaternary Science Reviews* **17,** 1139-1148.

Hodell, D. A., and Schelske, C. L. (1998). Production, sedimentation, and isotopic composition of organic matter in Lake Ontario. *Limnology and Oceanography* **43,** 200-214.

Kelts, K., and Talbot, M. R. (1990). Lacustrine Carbonates as Geochemical Archives of Environmental Change and Biotic/Abiotic Interactions. *In* "Large Lakes: Ecological Structure and Function." (M. M. Tilzer, and C. Serruya, Eds.), pp. 288-315. Springer-Verlag Berlin Heidelberg, New York.

Kerr, R. A. (2000). A North Atlantic Climate Pacemaker for the Centuries. *Science* **288,** 1984-1985.

Kienast, S. S., and McKay, J. L. (2001). Sea Surface Temperatures in the subarctic Northeast Pacific reflect the millennial-scale Climate Oscillations during the last 16 kyrs. *Geophysical Research Letters* **28,** 1563-1566.

Knapp, P. A., Grissino-Mayer, H. D., and Soulé, P. T. (2002). Climatic Regionalization and the Spatio-Temporal Occurance of Extreme Single-Year Drought Events (1500-1998) in the Interior Pacific Northwest, USA. *Quaternary Research* **58,** 226-233.

Knapp, P. A., Soulé, P. T., and Grissino-Mayer, H. D. (2004). Occurrence of Sustained Droughts in the Interior Pacific Northwest (A.D. 1733-1980) Inferred from Tree-Ring Data. *Journal of Climate* **17,** 140-150.

Lamb, A. L., Leng, M. J., Lamb, H. F., Telford, R. J., and Mohammed, M. U. (2002). Climatic and non-climatic effects on the $\delta^{18}$O and $\delta^{13}$C compositions of Lake Awassa, Ethiopia, during the last 6.5ka. *Quaternary Science Reviews* **21,** 2199-2211.

Lamb, A. L., Leng, M. J., Mohammed, M. U., and Lamb, H. F. (2004). Holocene climate and vegetation change in the Main Ethiopian Rift Valley, inferred from the composition (C/N and d13C) of lacustrine organic matter. *Quaternary Science Reviews* **23,** 881-891.

Li, H.-C., and Ku, T.-L. (1997). $\delta^{13}$C-$\delta^{18}$O covariance as a paleohydrological indicator for closed-basin lakes. *Palaeogeography, Palaeoclimatology, Palaeoecology* **133,** 69-80.

Lippmann, F. (1973). "Sedimentary Carbonate Minerals." Springer-Verlag Berlin, Heidelberg.

Lowe, D. J., Green, J. D., Northcote, T. G., and Hall, K. J. (1997). Holocene Fluctuations of a Meromictic Lake in Southern British Columbia. *Quaternary Research* **48,** 100-113.

Luckman, B. H., and Osborn, G. D. (1979). Holocene Glacier Fluctuations in the Middle Canadian Rocky Mountains. *Quaternary Research* **11,** 52-77.

Mack, R. N., Rutter, N. W., and Valastro, S. (1979). Holocene Vegetation History of the Okanogan Valley, Washington. *Quaternary Research* **12,** 212-225.

Mantua, N. J., Hare, S. R., Zhang, Y., Wallace, J. M., and Francis, R. C. (1997). A Pacific Interdecadal Climate Oscillation with Impacts on Salmon Production. *Bulletin of the American Meteorological Society* **78,** 1069-1079.

McCabe, G. J., and Dettinger, M. D. (1999). Decadal Variations in the Strength of ENSO Teleconnections with Precipitation in the Western United States. *International Journal of Climatology* **19,** 1399-1410.

McCabe, G. J., Palecki, M. A., and Betancourt, J. L. (2004). Pacific and Atlantic Ocean influences on multidecadal drought frequency in the United States. *Proceedings of the National Academy of Sciences of the United States of America* **101,** 4136-4141.

McKee, T. B., Doesken, N. J., Kleist, J., Shrier, C. J., and Stanton, W. P. (2000). A History of Drought in Colorado: Lessons Learned and What Lies Ahead. *Water in the Balance* **9,** 1-20.

McKenzie, J. A. (1985). Carbon Isotopes and Productivity in the Lacustrine and Marine Environment. *In* "Chemical Processes in Lakes." (W. Stumm, Ed.). John Wiley & Sons, Zurich.

Mensing, S. A., Benson, L. V., Kashgarian, M., and Lund, S. (2004). A Holocene pollen record of persistent droughts from Pyramid Lake, Nevada, USA. *Quaternary Research* **62**.

Meyers, P. A., and Ishiwatari, R. (1995). Organic Matter Accumulation records in Lake Sediments. *In* "Physics and Chemistry of Lakes." (A. Lerman, D. M. Imboden, and J. R. Gat, Eds.), pp. 334. Springer-Verlag New York, Inc., New York.

Meyers, P. A., and Teranes, J. L. (2001). Sediment Organic Matter. *In* "Tracking Environmental Change Using Lake Sediments." (W. M. Last, and J. P. Smol, Eds.), pp. 239-269. Developments in Paleoenvironmental Research. Kluwer Academic Publishers, Dordrecht, The Netherlands.

Mitchell, V. L. (1976). The Regionalization of Climate in the Western United States. *Journal of Applied Meteorology* **15,** 920-926.

Müller, G., Irion, G., and Förstner, U. (1972). Formation and diagenesis of inorganic CaMg carbonates in the lacustrine environment. *Naturwissenschaften* **59,** 158-164.

Mullineaux, D. R. (1986). Summary of pre-1980 tephra-fall deposits erupted from Mount St. Helens, Washington State, USA. *Bulletin of Volcanology* **48,** 17-26.
Namais, J. (1983). Some Causes of United States Drought. *Journal of Climate and Applied Meteorology* **22,** 30-39.
Ostrom, N. E., Long, D. T., Bell, E. M., and Beals, T. (1998). The origin and cycling of particulate and sedimentary organic matter and nitrate in Lake Superior. *Chemical Geology* **152,** 13-28.
Palmer, W. C. (1965). Meteorological Drought. *In* "Weather Bureau Research Paper 45." pp. 58. U.S. Department of Commerce, Washington, D.C.
Piechota, T., Timilsena, J., and Tootle, G. (2004). The Western U.S. Drought: How Bad Is It? *Eos, Transactions* **85,** 301-304.
Quay, P. D., Emerson, S. R., Quay, B. M., and Devol, A. H. (1986). The carbon cycle for Lake Washington - A stable isotope study. *Limnology and Oceanography* **31,** 596-611.
Rosenberg, S. M., Walker, I. R., Mathewes, R. W., and Hallett, D. J. (2004). Midge-inferred Holocene climate history of two subalpine lakes in southern British Columbia, Canada. *The Holocene* **14,** 258-271.
Rosenmeier, M. F., Hodell, D. A., Brenner, M., Curtis, J. H., Martin, J. B., Anselmetti, F. S., Ariztegui, D., and Guilderson, T. P. (2002). Influence of vegetation change on watershed hydrology: implications for paleoclimatic interpretation of lacustrine d18O records. *Journal of Paleolimnology* **27,** 117-131.
Rozanski, K., Araguás-Araguás, L., and Gonfiantini, R. (1992). Relation Between Long-Term Trends of Oxygen-18 Isotope Composition of Precipitation and Climate. *Science* **258,** 981-985.
Ryder, J. M., and Thomson, B. (1986). Neoglaciation in the southern Coast Mountains of British Columbia: chronology prior to the late Neoglacial maximum. *Canadian Journal of Earth Sciences* **23,** 273-287.
Stine, S. (1990). Late Holocene fluctuations of Mono Lake, eastern California. *Palaeogeography, Palaeoclimatology, Palaeoecology* **78,** 333-381.
Stuiver, M., and Reimer, P. J. (1993). Radiocarbon calibration program. *Radiocarbon* **35,** 215-230.
Stuiver, M., Reimer, P. J., and Braziunas, T. F. (1998). High-precision radiocarbon age calibration for terrestrial and marine samples. *Radiocarbon* **40,** 1127-1151.
Talbot, M. R. (1990). A review of the paleohydrological interpretation of carbon and oxygen isotopic ratios in primary lacustrine carbonates. *Chemical Geology (Isotope Geoscience Section)* **80,** 261-279.
Talbot, M. R. (2001). Nitrogen Isotopes in Paleolimnology. *In* "Tracking Environmental Change Using Lake Sediments." (W. M. Last, and J. P. Smol, Eds.), pp. 239-269. Developments in Paleoenvironmental Research. Kluwer Academic Publishers, Dordrecht, The Netherlands.
Talbot, M. R., and Johannessen, T. (1992). A high resolution paleoclimate record for the last 27,500 years in tropical West Africa from the carbon and nitrogen isotopic composition of lacustrine organic matter. *Earth and Planetary Science Letters* **110,** 23-37.
Telford, R. J., Barker, P., Metcalfe, S., and Newton, A. (2004). Lacustrine responses to tephra deposition: examples from Mexico. *Quaternary Science Reviews* **23,** 2337-2353.
Thomas, P. A., Easterbrook, D. J., and Clark, P. U. (2000). Early Holocene glaciation on Mount Baker, Washington State, USA. *Quaternary Science Reviews* **19,** 1043-1046.

Valero-Garcés, B. L., Laird, K. R., Fritz, S. C., Kelts, K. K., Ito, E., and Grimm, E. C. (1997). Holocene Climate in the Northern Great Plains Inferred from Sediment Stratigraphy, Stable Isotopes, Carbonate Geochemistry, Diatoms, and Pollen at Moon Lake, North Dakota. *Quaternary Research* **48,** 359-369.

Waitt, R. B., Yount, J. C., and Thompson Davis, P. (1982). Regional Significance of an Early Holocene Moraine in Enchantment Lakes Basin, North Cascade Range, Washington. *The Northwest Environmental Journal* **8,** 5-28.

Waitt, R. B. J., and Thorson, R. M. (1983). The Cordilleran Ice Sheet in Washington, Idaho, and Montana. *In* "The Late Pleistocene." (S. C. Porter, Ed.), pp. 53-70. Late-Quaternary Environments of the United States. University of Minnesota Press, Minneapolis.

Whitlock, C. (1992). Vegetational and Climatic History of the Pacific Northwest during the Last 20,000 Years: Implications for Understanding Present-day Biodiversity. *The Northwest Environmental Journal* **8,** 5-28.

Whitlock, C., and Bartlein, P. J. (1993). Spatial variations of Holocene climatic change in the Yellowstone region. *Quaternary Research* **39,** 231-238.

Wiles, G. C., D'Arrigo, R. D., and Jacoby, G. C. (1996). Temperature changes along the Gulf of Alaska and the Pacific Northwest coast modeled from coastal tree-rings. *Canadian Journal of Forest Research* **26,** 474-481.

Woodhouse, C. A., Lukas, J. J., and Brown, P. M. (2002). Drought in the Western Great Plains, 1845-56: Impacts and Implications. *Bulletin of the American Meteorological Society* **83,** 1485-1493.

Wright, H. E., Mann, D. H., and Glaser, P. H. (1984). Piston corers for peat and lake sediments. *Ecology* **65,** 657-659.

Zdanowicz, C. M., Zielinski, G. A., and Germani, M. S. (1999). Mount Mazama eruption: Calendrical age verified and atmospheric impact assessed. *Geology* **27,** 621-624.